



684
2015

Berichte

zur Polar- und Meeresforschung

Reports on Polar and Marine Research

Russian-German Cooperation SYSTEM LAPTEV SEA: The expedition Lena 2012

Edited by

Thomas Opel

with contributions of the participants

Die Berichte zur Polar- und Meeresforschung werden vom Alfred-Wegener-Institut, Helmholtz-Zentrum für Polar- und Meeresforschung (AWI) in Bremerhaven, Deutschland, in Fortsetzung der vormaligen Berichte zur Polarforschung herausgegeben. Sie erscheinen in unregelmäßiger Abfolge.

Die Berichte zur Polar- und Meeresforschung enthalten Darstellungen und Ergebnisse der vom AWI selbst oder mit seiner Unterstützung durchgeführten Forschungsarbeiten in den Polargebieten und in den Meeren.

Die Publikationen umfassen Expeditionsberichte der vom AWI betriebenen Schiffe, Flugzeuge und Stationen, Forschungsergebnisse (inkl. Dissertationen) des Instituts und des Archivs für deutsche Polarforschung, sowie Abstracts und Proceedings von nationalen und internationalen Tagungen und Workshops des AWI.

Die Beiträge geben nicht notwendigerweise die Auffassung des AWI wider.

Herausgeber

Dr. Horst Bornemann

Redaktionelle Bearbeitung und Layout

Birgit Chiaventone

Alfred-Wegener-Institut
Helmholtz-Zentrum für Polar- und Meeresforschung
Am Handeshafen 12
27570 Bremerhaven
Germany

www.awi.de

www.reports.awi.de

Der Erstautor bzw. herausgebende Autor eines Bandes der Berichte zur Polar- und Meeresforschung versichert, dass er über alle Rechte am Werk verfügt und überträgt sämtliche Rechte auch im Namen seiner Koautoren an das AWI. Ein einfaches Nutzungsrecht verbleibt, wenn nicht anders angegeben, beim Autor (bei den Autoren). Das AWI beansprucht die Publikation der eingereichten Manuskripte über sein Repositorium ePIC (electronic Publication Information Center, s. Innenseite am Rückdeckel) mit optionalem print-on-demand.

The Reports on Polar and Marine Research are issued by the Alfred Wegener Institute, Helmholtz Centre for Polar and Marine Research (AWI) in Bremerhaven, Germany, succeeding the former Reports on Polar Research. They are published at irregular intervals.

The Reports on Polar and Marine Research contain presentations and results of research activities in polar regions and in the seas either carried out by the AWI or with its support.

Publications comprise expedition reports of the ships, aircrafts, and stations operated by the AWI, research results (incl. dissertations) of the Institute and the Archiv für deutsche Polarforschung, as well as abstracts and proceedings of national and international conferences and workshops of the AWI.

The papers contained in the Reports do not necessarily reflect the opinion of the AWI.

Editor

Dr. Horst Bornemann

Editorial editing and layout

Birgit Chiaventone

Alfred-Wegener-Institut
Helmholtz-Zentrum für Polar- und Meeresforschung
Am Handeshafen 12
27570 Bremerhaven
Germany

www.awi.de

www.reports.awi.de

The first or editing author of an issue of Reports on Polar and Marine Research ensures that he possesses all rights of the opus, and transfers all rights to the AWI, including those associated with the co-authors. The non-exclusive right of use (einfaches Nutzungsrecht) remains with the author unless stated otherwise. The AWI reserves the right to publish the submitted articles in its repository ePIC (electronic Publication Information Center, see inside page of verso) with the option to "print-on-demand".

Titel: Geländebegehung der Permafrostaufschlüsse an der Ostküste der Insel Muostakh in der südlichen Laptevsee (Foto von Thomas Opel, Alfred-Wegener-Institut, 09. August 2012).

Cover: Survey of the permafrost outcrops at the east coast of Muostakh Island in the southern Laptev Sea (picture taken by Thomas Opel, Alfred Wegener Institute, 9th of August 2012).

Russian-German Cooperation SYSTEM LAPTEV SEA: The expedition Lena 2012

Edited by

Thomas Opel

with contributions of the participants

Please cite or link this publication using the identifiers

hdl:10013/epic.44856 or <http://hdl.handle.net/10013/epic.44856> and

doi:10.2312/BzPM_0684_2015 or http://doi.org/10.2312/BzPM_0684_2015

ISSN 1866-3192

The Expedition Lena 2012

4 July 2012 – 05 September 2012

Central Lena River Delta and Muostakh Island



Coordinators

H.-W. Hubberten, D. Yu. Bolshiyarov, M.N. Grigoriev

TABLE OF CONTENTS

1	INTRODUCTION.....	2
2	EXPEDITION ITINERARY AND PARTICIPANTS	4
3	STUDIES IN THE LENA DELTA.....	8
3.1	Heat and water budget of permafrost landscapes on spatial and temporal scales - Instrumentation of a new long-term permafrost soil thermal site	9
3.2	Summertime carbon-cycle and hydrological flux observations, Samoylov Island	27
3.3	Airborne measurements of energy and carbon fluxes	33
3.4	Do microbes feed on old carbon in permafrost?	38
3.5	Soil heterotrophic microbial biomass and potential basal respiration rate of a typical ice-wedge polygon of Samoylov Island	40
3.6	Methane distribution and methane oxidation (MOX) rates in the water bodies of Samoylov Island and in the Lena River	43
3.7	Hydrological and geochemical studies in the Lena River Delta	46
3.8	Biological investigations in summer 2012	56
3.9	Botanical studies in polygonal structures	60
3.10	Spore-pollen studies	66
3.11	Ground ice studies on Samoylov Island	67
4	STUDIES ON MUOSTAKH ISLAND.....	71
4.1	Scientific background, objectives and methods	72
4.2	History of investigations and general geographical and geological characteristics	75
4.3	Stratigraphic and sedimentological studies	79
4.4	Studies of Holocene ice wedges	83
4.5	Studies of Late Pleistocene ice wedges	87
4.6	Studies of soils and flora of Muostakh Island	92
4.7	Studies of dissolved organic matter	96
4.8	Repeated tacheometric survey of Ice Complex coast	99

1 INTRODUCTION

Thomas Opel

This report summarizes the field work and first results of the joint Russian-German expedition Lena 2012. This expedition was the 15th expedition to the Lena River Delta and the surrounding Laptev Sea region since 1998 and was an expression of the vital Russian German science cooperation between several Russian and German research institutions. During the expedition the long-term investigations of permafrost and the periglacial environment at and around Samoylov Island in the Central Lena River Delta had been continued. Consequently, the Samoylov Research Station was the logistical and scientific base for the main part of the expedition (Figure 1-1). Additionally, a small field camp was established at Muostakh Island in the Buor Khaya Gulf east of the Lena Delta, the second study region during the expedition (Figure 1-1).

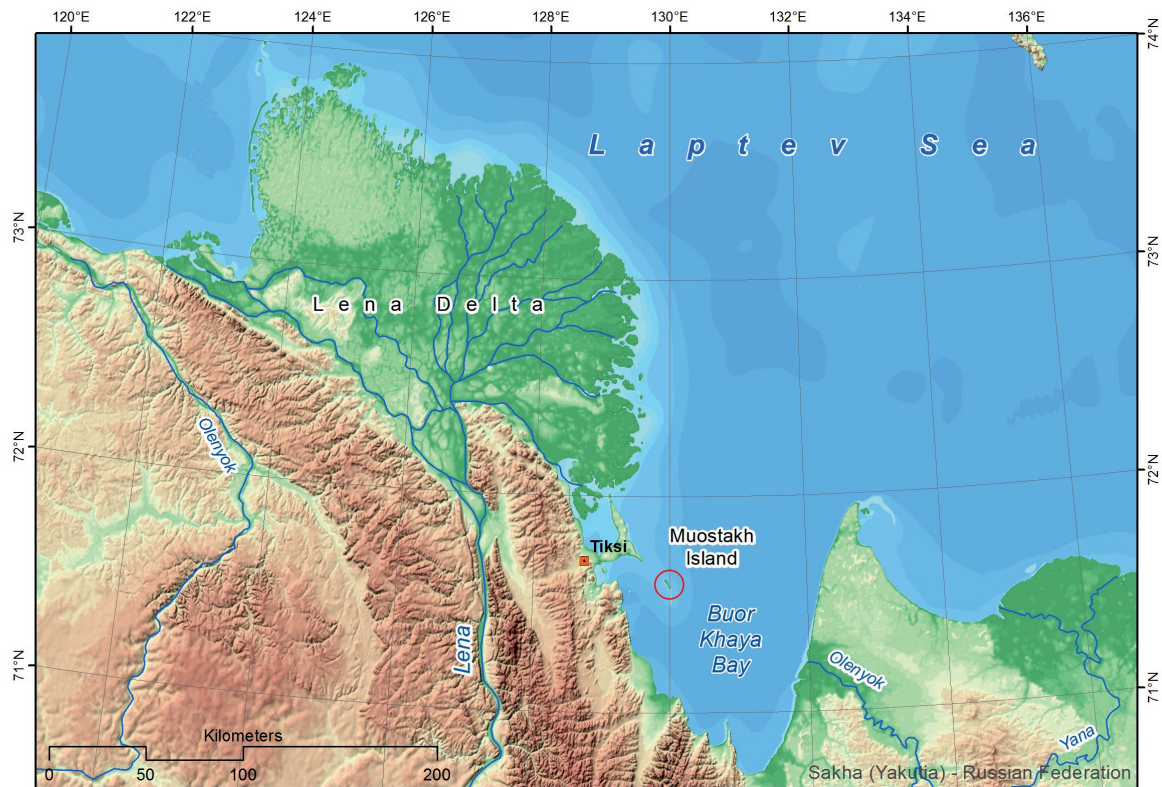


Figure 1-1 Overview map with the two main study regions: (1) The central Lena River Delta and (2) Muostakh Island. Map compiled by Frank Günther.

1 Introduction

The expedition focused on the following research topics:

- Heat and water budgets of permafrost landscapes
- Observations of carbon cycle and hydrological fluxes
- Airborne measurements of energy and carbon fluxes
- Studies of soil, water, carbon and microbiology
- Hydrological and geochemical conditions of the Lena River Delta
- Modern environmental dynamics of aquatic ecosystems and vegetation
- Paleoclimate, permafrost and environmental dynamics since the Late Pleistocene
- Coastal erosion of permafrost coasts

The scientific work during the expedition Lena 2012 was carried out by 31 participants from 13 German and Russian research institutions (Table 2-1, Table 2-2, Figure 2-1, Figure 2-2, Figure 2-3, Figure 2-4). The expedition took place in the period July 04 to September 05, 2012.

The expedition Lena 2012 was coordinated by Prof. Dr. H.-W. Hubberten (AWI, Potsdam), Prof. Dr. D. Yu. Bolshiyarov (AARI, St. Petersburg) and Dr. M.N. Grigoriev (PIY, Yakutsk).

This report contains short contributions of the participants. The authors are responsible for content and correctness.

Acknowledgements

The success of the expedition “Lena 2012” would not have been possible without the support by several Russian, Yakutian, and German institutions and authorities.

In particular, we would like to express our appreciation to the Lena Delta Reserve and the Tiksi Hydrobase, especially to A. Gukov and D. Melnichenko.

2 EXPEDITION ITINERARY AND PARTICIPANTS

Table 2-1 List of participants

Name	Email	Institute	Time	Field site
Abramova, Ekaterina	abramova-katya@mail.ru	LDR	04.07.-05.09.	LD
Bobrova, Olga	helga.castor@gmail.com	USP	31.07.-05.09.	LD
Boike, Julia	julia.boike@awi.de	AWI P	31.07.-22.08.	LD
Bolshiyarov, Dmitry	bolshiyarov@aari.nw.ru	AARI	15.08.-05.09.	LD
Chetverova, Antonina	antoshka4@mail.ru	USP	31.07.-05.09.	LD
Dereviagin, Alexander	dereviag@gmail.com	MSU	31.07.-28.08.	MUO
Dubinenkov, Ivan	ivan.dubinenkov@awi.de	AWI B	31.07.-05.09.	MUO, LD
Evgrafova, Svetlana	esj@yandex.ru	SIF	31.07.-05.09.	LD
Fülöp, Reka	rfueloep@uni-koeln.de	UC	31.07.-22.08.	LD
Grigoriev, Mikhail	grigoriev@mpi.ysn.ru	PIY	several	LD, MUO
Heikenfeld, Max	max.heikenfeld@awi.de	AWI P	04.07.-05.09.	LD
Helbig, Manuel	manuel.helbig@yahoo.com	UHH	04.07.-01.08.	LD
Kutzbach, Lars	lars.kutzbach@zmaw.de	UHH	31.07.-22.08.	LD
Langer, Moritz	moritz.langer@awi.de	AWI P	04.07.-01.08.	LD
Larmanou, Eric	eric.larmanou@gfz-potsdam.de	GFZ	31.07.-22.08.	LD
Makarov, Alexander	makarov@aari.nw.ru	AARI	04.07.-05.09.	LD
Meyer, Hanno	hanno.meyer@awi.de	AWI P	31.07.-28.08.	MUO
Münchberger, Wiebke	w.muenchberger@yahoo.de	UHH	31.07.-05.09.	LD
Opel, Thomas	thomas.opel@awi.de	AWI P	31.07.-05.09.	MUO, LD
Osudar, Roman	roman.osudar@awi.de	AWI P	04.07.-01.08.	LD
Runkle, Benjamin	benjamin.runkle@zmaw.de	UHH	04.07.-05.09.	LD
Sabrekov, Alexander	misternickel@mail.ru	MSU	04.07.-01.08.	LD
Sachs, Torsten	torsten.sachs@gfz-potsdam.de	GFZ	31.07.-22.08.	LD
Schneider, Waldemar	waldemar.schneider@awi.de	AWI P	04.07.-05.09.	LD
Soloviev, Grigoriy	greansa@gmail.com	HSP	31.07.-05.09.	LD
Stoof, Günter	guenter.stoof@awi.de	AWI P	04.07.-05.09.	LD
Spiridonova, Irina	spirdirina@mail.ru	NEFU	04.07.-01.08.	LD
Titova, Darya	tit-dacha@yandex.ru	USP	04.07.-01.08.	LD
Wischnewski, Karoline	karoline.wischnewski@gmail.com	AWI P	04.07.-05.09.	LD
Yakshina, Irina	i_yakshina@rambler.ru	LDR	31.07.-28.08.	MUO
Zibulski, Romy	romy.zibulski@awi.de	AWI P	04.07.-01.08.	LD

2 Expedition Itinerary and participants

Table 2-2 Institutions of the participants

Abbreviation	Institution
AARI	Arctic and Antarctic Research Institute, Bering St. 38, 199397 St. Petersburg, Russia
AWI B	Alfred Wegener Institute Helmholtz Centre for Polar and Marine Research, Department of Ecological Chemistry, Am Handelshafen 12, 27570 Bremerhaven, Germany
AWI P	Alfred Wegener Institute Helmholtz Centre for Polar and Marine Research, Department of Periglacial Research, Telegrafenberg A43, 14473 Potsdam, Germany
GFZ	Helmholtz Centre Potsdam – GFZ German Research Centre for Geosciences, Telegrafenberg, 14473 Potsdam, Germany
HSP	Herzen State Pedagogical University of Russia, Kazanskaya (Plekhanova) St. 6, 191186 St. Petersburg, Russian Federation
LDR	Lena Delta Reserve, Academician Fyodorov St. 28, 678400 Tiksi, Russian Federation
MSU	Lomonosov Moscow State University, GSP-1, Leninskie Gory, 119991 Moscow, Russian Federation
NEFU	Northeastern Federal University in Yakutsk, Belinskiy str, 58, 677980, Yakutsk, Russian Federation
PIY	Melnikov Permafrost Institute, Siberian Branch of Russian Academy of Science, Merzlotnaya St. 36, 677010 Yakutsk, Russian Federation
SIF	Sukachev Institute of Forest, Siberian Branch of Russian Academy of Sciences, Akademgorodok, 660036 Krasnojarsk, Russian Federation
UC	University of Cologne, Institute of Geology and Mineralogy, Zùlpicher Str. 49a, 50674 Cologne, Germany
UHH	University of Hamburg, Institute of Soil Science, Allende-Platz 2, 20146 Hamburg, Germany
USP	Saint Petersburg State University, Institute of Earth Science, Department of Land Hydrology. Vasilievskij Island, 10th line, 199178 St. Petersburg, Russian Federation

Table 2-3 Field sites

Abbreviation	Field Site
LD	Lena Delta, based on Samoylov Island
MUO	Muostakh Island



Figure 2-1 Team Lena Delta, 13.07.2012



Figure 2-2 Team Lena Delta, 21.08.2012

2 Expedition Itinerary and participants



Figure 2-3 Team Lena Delta, 30.08.2012



Figure 2-4 Team Muostakh Island, 27.08.2012

3 STUDIES IN THE LENA DELTA



Figure 3-1 Overview map of the central Lena River Delta with the main study sites Samoylov Island and Kurungnakh Island. Background: RapidEye satellite image acquired on 27 July 2014, kindly provided by BlackBridge and German Aerospace Center (DLR) through RapidEye Science Archive. Map compiled by Frank Günther.

3.1 HEAT AND WATER BUDGET OF PERMAFROST LANDSCAPES ON SPATIAL AND TEMPORAL SCALES - INSTRUMENTATION OF A NEW LONG-TERM PERMAFROST SOIL THERMAL SITE

Julia Boike, Karoline Wischnewski, Max Heikenfeld, Moritz Langer, Wiebke Müncheberger, Steffen Frey, Christian Juncher Jørgensen, and Lars Kutzbach

Fieldwork period: July 04 to September 03, 2012; Samoylov Island

3.1.1 Introduction

Monitoring of climate, active layer and permafrost thermal regime has been ongoing on the island of Samoylov since 1998 (Boike et al., 2013). In August 2012, a new long term permafrost monitoring site was established potentially replacing the old site that has been operating since 2002. The new site was chosen in close proximity to the eddy covariance site in the center part of the island (Figure 3-2, Figure 3-3). Two sub-sites were chosen in close proximity, but with strong hydrologic gradients (wet center, dry rim) (Figure 3-4).

3.1.2 Methods

Two soil pits were excavated: one in the wet polygonal center and the other one in the drier rim. Prior to the installation in the wet polygonal center, the water was removed using a pump. Excavation was done between 9-13 August, 2012 using a spade (thawed soil) and a gas-powered hammer for the frozen soil (down to 1 m depth). Care was taken to remove the soil layer by layer and to refill this material after instrumentation to its original state. The soil profile was described and classified according to the World Reference Base for Soil Recourses (FAO, 2007). Thawed and frozen samples were taken of the soil profile for later analysis of soil texture, density and for extraction of water samples. Sensors for measuring soil temperature, volumetric moisture content, soil thermal properties and heat flux were placed in the undisturbed soil face in the subsurface, and depths were recorded. For the installation in the frozen ground, a powered drill was used to create access holes. After installation, the original soil was carefully filled back, and the surface was reconstructed using the organic surface layer. All cables were put underneath the ground to minimize the impact of animals and other disturbances. After the installation was completed, the polygon center was irrigated to reestablish the original water level.

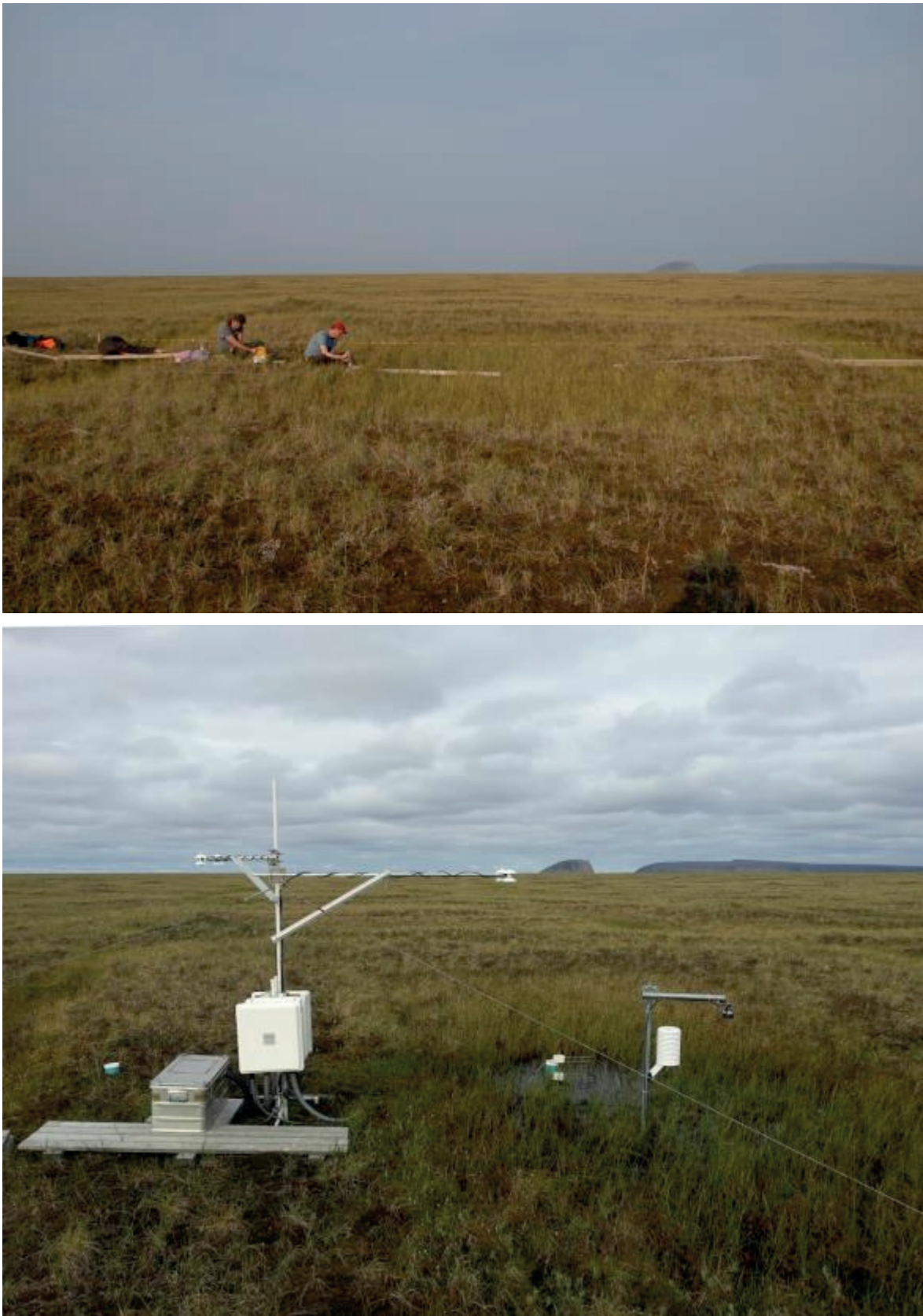


Figure 3-2 Top: The new soil site in August 2012 before instrumentation of sensors. The yellow band stretching across the polygon indicates where the profiles were installed and vegetation was recorded. Bottom: View of instrumented polygonal site in August 2013.

3.1 Heat and water budget of permafrost landscapes

A figure of the installed sensors, as well as a complete list of all climate and soil sensors can be seen in Figure 3-5 and Table 3-1.



Figure 3-3 Aerial view of the new soil site (person with yellow jacket for scale) during installation of sensors. Picture was taken on August 13, 2012 from the automated camera at 10 m height on the nearby eddy flux tower. Also shown is the snow monitoring site (snow pack analyser) on the left. Location of new soil site: 72°22.451, 126°29.753.

3.1 Heat and water budget of permafrost landscapes

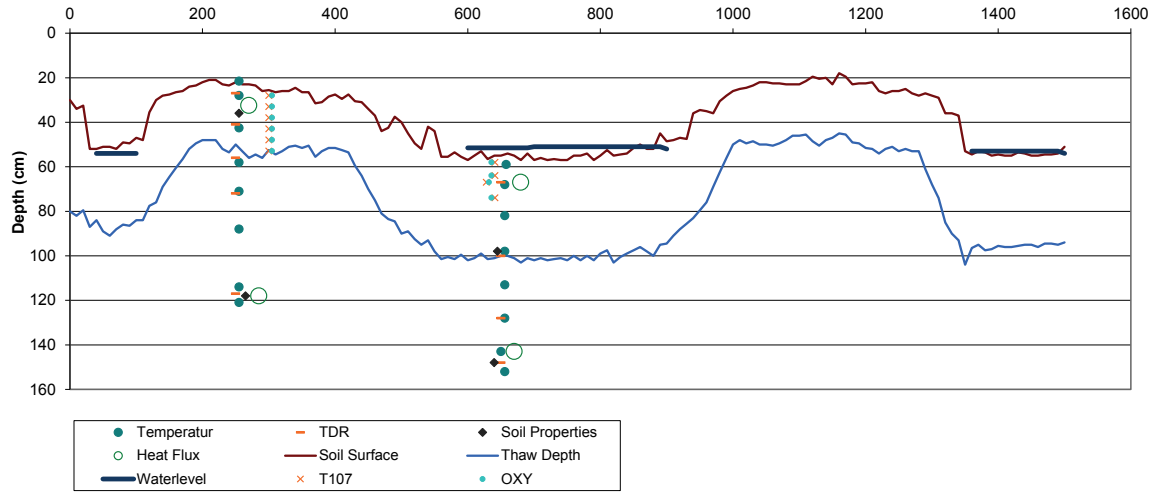


Figure 3-4 Surface topography, water level and location of two profiles of new soil monitoring station.

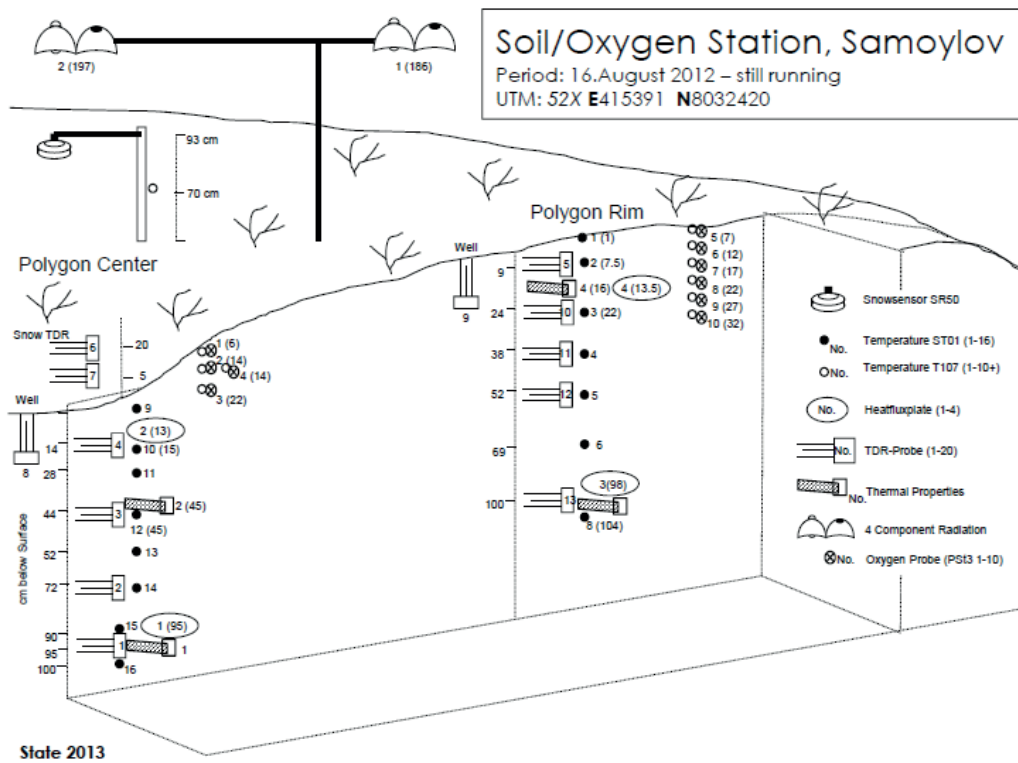


Figure 3-5 Installation depths and sensor types for the two instrumented profiles in the center (left) and rim (right). Two vertical TDR sensors are installed in wells for monitoring ground water levels.

3.1 Heat and water budget of permafrost landscapes

Table 3-1 List of installed sensors in the ground and above the surface.

Parameter	Sensor Type	Distance from Soilsurface (cm)	Range	Precision
Rim				
Ground Heatflux	HFP01 (Huxeflux)		-98 -30 - 70 °C	±15%
Ground Heatflux	HFP01 (Huxeflux)		-13.5 -30 - 70 °C	±15%
Thermal Properties	TP01 (Huxeflux)		-99 -30 - 80 °C	±5% (conductivity)
(conductivity, diffusivity, capacity)	TP01 (Huxeflux)		-16 -30 - 80 °C	±20%(diffusivity)
Volumetric Water Content	CS605 (Campbell Sci.)		-9 -40 - 55°C	±0.02 V/V
Water Level	CS605 (Campbell Sci.)	Well		
Volumetric Water Content	CS605 (Campbell Sci.)		-24 -40 - 55°C	±0.02 V/V
Volumetric Water Content	CS605 (Campbell Sci.)		-38 -40 - 55°C	±0.02 V/V
Volumetric Water Content	CS605 (Campbell Sci.)		-52 -40 - 55°C	±0.02 V/V
Volumetric Water Content	CS605 (Campbell Sci.)		-100 -40 - 55°C	±0.02 V/V
Soil Temperature	ST01 (Huxeflux)		-1 -60 - 150°C	±0.15°C
Soil Temperature	ST01 (Huxeflux)		-7.5 -60 - 150°C	±0.15°C
Soil Temperature	ST01 (Huxeflux)		-22 -60 - 150°C	±0.15°C
Soil Temperature	ST01 (Huxeflux)		-38 -60 - 150°C	±0.15°C
Soil Temperature	ST01 (Huxeflux)		-52 -60 - 150°C	±0.15°C
Soil Temperature	ST01 (Huxeflux)		-69 -60 - 150°C	±0.15°C
Soil Temperature	ST01 (Huxeflux)		-95 -60 - 150°C	±0.15°C
Soil Temperature	ST01 (Huxeflux)		-104 -60 - 150°C	±0.15°C
Soil Temperature	T107 (Campbell Sci.)		-7 -55 - 70°C	±0.3°C
Soil Temperature	T107 (Campbell Sci.)		-12 -55 - 70°C	±0.3°C
Soil Temperature	T107 (Campbell Sci.)		-17 -55 - 70°C	±0.3°C
Soil Temperature	T107 (Campbell Sci.)		-22 -55 - 70°C	±0.3°C
Soil Temperature	T107 (Campbell Sci.)		-27 -55 - 70°C	±0.3°C
Soil Temperature	T107 (Campbell Sci.)		-32 -55 - 70°C	±0.3°C
Oxygen Content	PSt3 (PreSens)		-7 0 - 50°C	±0.4% at 20.9% oxygen
Oxygen Content	PSt3 (PreSens)		-12 0 - 50°C	±0.4% at 20.9% oxygen
Oxygen Content	PSt3 (PreSens)		-17 0 - 50°C	±0.4% at 20.9% oxygen
Oxygen Content	PSt3 (PreSens)		-22 0 - 50°C	±0.4% at 20.9% oxygen
Oxygen Content	PSt3 (PreSens)		-27 0 - 50°C	±0.4% at 20.9% oxygen
Oxygen Content	PSt3 (PreSens)		-32 0 - 50°C	±0.4% at 20.9% oxygen
4 Component Radiation	NR01 (Huxeflux)	186		±15W/m ² at 1000W/m ² SW _{in} ±8W/m ² at -100W/m ² LW _{net}
Center				
Ground Heatflux	HFP01 (Huxeflux)		-90 -30 - 70 °C	±15%
Ground Heatflux	HFP01 (Huxeflux)		-13 -30 - 70 °C	±15%
Thermal Properties	TP01 (Huxeflux)		-95 -30 - 80 °C	±5% (conductivity)
(conductivity, diffusivity, capacity)	TP01 (Huxeflux)		-45 -30 - 80 °C	±20%(diffusivity)
Volumetric Water Content	CS605 (Campbell Sci.)		-95 -40 - 55°C	±0.02 V/V
Volumetric Water Content	CS605 (Campbell Sci.)		-72 -40 - 55°C	±0.02 V/V
Volumetric Water Content	CS605 (Campbell Sci.)		-44 -40 - 55°C	±0.02 V/V
Volumetric Water Content	CS605 (Campbell Sci.)		-14 -40 - 55°C	±0.02 V/V
Volumetric Water Content (Snow)	CS605 (Campbell Sci.)		20 -40 - 55°C	±0.02 V/V
Volumetric Water Content (Snow)	CS605 (Campbell Sci.)		5 -40 - 55°C	±0.02 V/V
Water Level	CS605 (Campbell Sci.)	Well		
Soil Temperature	ST01 (Huxeflux)		-5 -60 - 150°C	±0.15°C
Soil Temperature	ST01 (Huxeflux)		-15 -60 - 150°C	±0.15°C
Soil Temperature	ST01 (Huxeflux)		-28 -60 - 150°C	±0.15°C
Soil Temperature	ST01 (Huxeflux)		-45 -60 - 150°C	±0.15°C
Soil Temperature	ST01 (Huxeflux)		-60 -60 - 150°C	±0.15°C
Soil Temperature	ST01 (Huxeflux)		-72 -60 - 150°C	±0.15°C
Soil Temperature	ST01 (Huxeflux)		-90 -60 - 150°C	±0.15°C
Soil Temperature	ST01 (Huxeflux)		-100 -60 - 150°C	±0.15°C
Soil Temperature	T107 (Campbell Sci.)		-4 -55 - 70°C	±0.3°C
Soil Temperature	T107 (Campbell Sci.)		-12 -55 - 70°C	±0.3°C
Soil Temperature	T107 (Campbell Sci.)		-21 -55 - 70°C	±0.3°C
Soil Temperature	T107 (Campbell Sci.)		-14 -55 - 70°C	±0.3°C
Oxygen Content	PSt3 (PreSens)		-6 0 - 50°C	±0.4% at 20.9% oxygen
Oxygen Content	PSt3 (PreSens)		-14 0 - 50°C	±0.4% at 20.9% oxygen
Oxygen Content	PSt3 (PreSens)		-22 0 - 50°C	±0.4% at 20.9% oxygen
Oxygen Content	PSt3 (PreSens)		-14 0 - 50°C	±0.4% at 20.9% oxygen
4 Component Radiation	NR01 (Huxeflux)	197		±15W/m ² at 1000W/m ² SW _{in} ±8W/m ² at -100W/m ² LW _{net}
Snow Depth	SR50a (Campbell Sci.)		93 -45 - 50°C	±1 cm
Air Temperature	T107 (Campbell Sci.)		70 -55 - 70°C	±0.3°C

3.1.3 Preliminary data

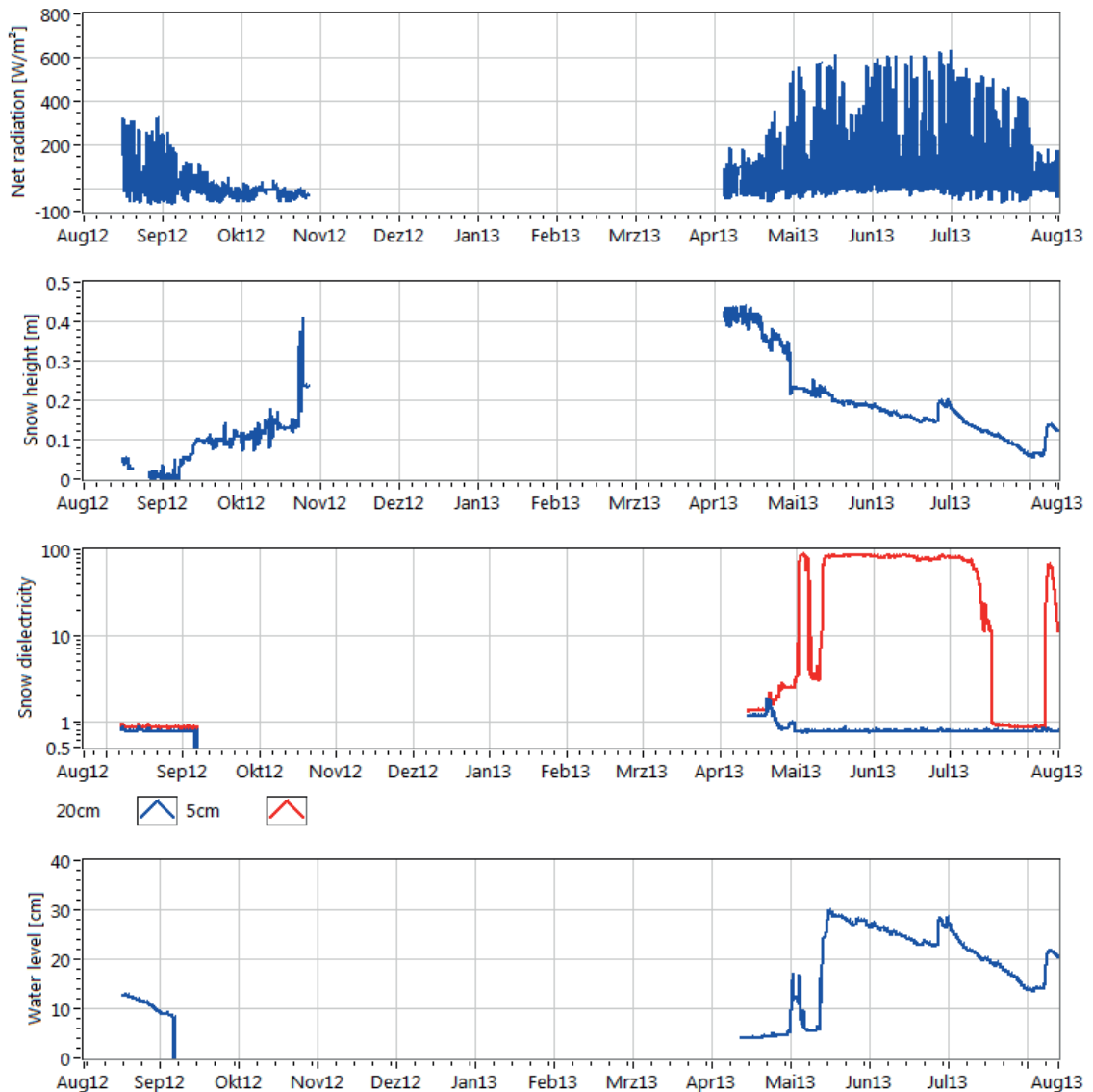


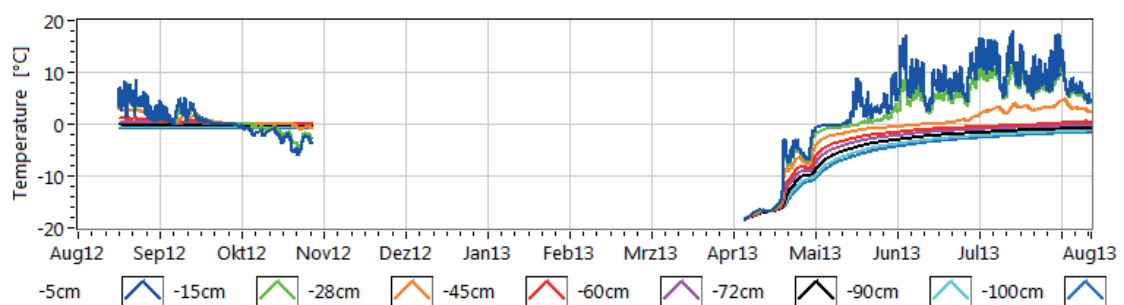
Figure 3-6 Data record from the polygon center August 2012 to 2013. From top to bottom: net radiation, distance to surface (snow/water), dielectric constant from horizontally installed TDR probes above the surface (log scale), water level in ground using well and vertically installed TDR probe.

Figure 3-6 shows raw data of net radiation, snow/water height installed over the polygon center, as well as the dielectric constant measured above the ground surface at 5 and 20 cm height (August 2012-August 2013). Due to interruption of the power supply, a large data gap exists between November 2012 and April 2013. Net radiation increases mid-April with ripening of the snow and subsequent melt. The snow height is measured with a sonic sensor, thus only data of distance to the object are collected. The sharp decrease of the distance signal in May indicates snow thaw. After the beginning of May, the sonic sensor potentially records the height of the water level in the polygon center. This is also confirmed by the horizontally installed TDR probes 5 cm height above the ground surface.

3.1 Heat and water budget of permafrost landscapes

Both probes (5 and 20 cm height) show an increase in dielectric constant (i.e. snow liquid water content) in mid-April, indicating an early snow ripening event. Continuous increase of snow liquid water content (probe at 5 cm height) indicates further ripening and ageing of the snowpack, with progressing into snow melt the beginning of May (dielectric constant changes from < 4 for dry snow to ~ 80 for water). After the melt, water ponds inside the polygon, i.e. the water table is at least 5 cm above ground surface. Starting in July, the water table slowly drops below the 5 cm TDR probe, indicated by the decreasing dielectric constant, reaching air values ~ 1) in mid-July. Additional measurements of the water level height are carried out using a vertical installed TDR probe in a 50 cm deep well installed in the subsurface. A continuous decreasing water level after the snowmelt in mid-May and a drop of 5 cm in July are confirmed by these measurements. Due to rain fall in August, the water level rises again to 5 cm above surface, indicated by both (vertical and horizontal) installed TDR sensors. These first results show that TDR is a promising method for the longer term monitoring of water levels where freezing/thawing limits the use of groundwater pressure sensors in water.

The preliminary data of the ground thermal processes is shown in Figure 3-7. Sensors were installed up to 1 meter depth, thus far below the seasonally thawed active layer. At the time of power failure in mid-October, only the ground's surface down to 25 cm had been frozen. The data record starts again in mid April 2013. In mid-April, the soil warms and the water content in frozen soil increases, potentially induced by warm days and snow warming, ripening and potential thawing processes, as indicated by the increase of snow liquid water content (increase of snow dielectric constant, see figure 5). The volumetric water content in frozen soil lies below 8 %, which is expected for the silty sand soil. The surface of the polygon starts to thaw at the beginning of May after snowmelt. Thawing is indicated by passing the 0°C temperature, as well as a sharp increase in volumetric water content. For example, the sensor at 14/15 cm soil depth thaws during mid-May, after which the temperature variations follow the daily air temperature signal. The volumetric water content ($\sim 80\%$ at 14 cm depth and $\sim 60\%$ at 44 cm depth) under saturated conditions also represents the porosity of the ground, which is expected to be high for the peat. Heat flux in the ground was recorded using heat flux plates. Data in 2012 will be removed; due to the installation, the ground was still unfrozen at 1 m depth until mid-October prior to power failure and data loss. In 2013, the ground heat flux at 1 m depth (continuously frozen ground) was very small ($\sim 10\text{ W/m}^2$) with no daily cycle compared to the surface at 13 cm depth. The small but noticeable soil heat input induced by the ablation/thawing of the snow cover in mid-April is also visible at 1 meter depth.



3.1 Heat and water budget of permafrost landscapes

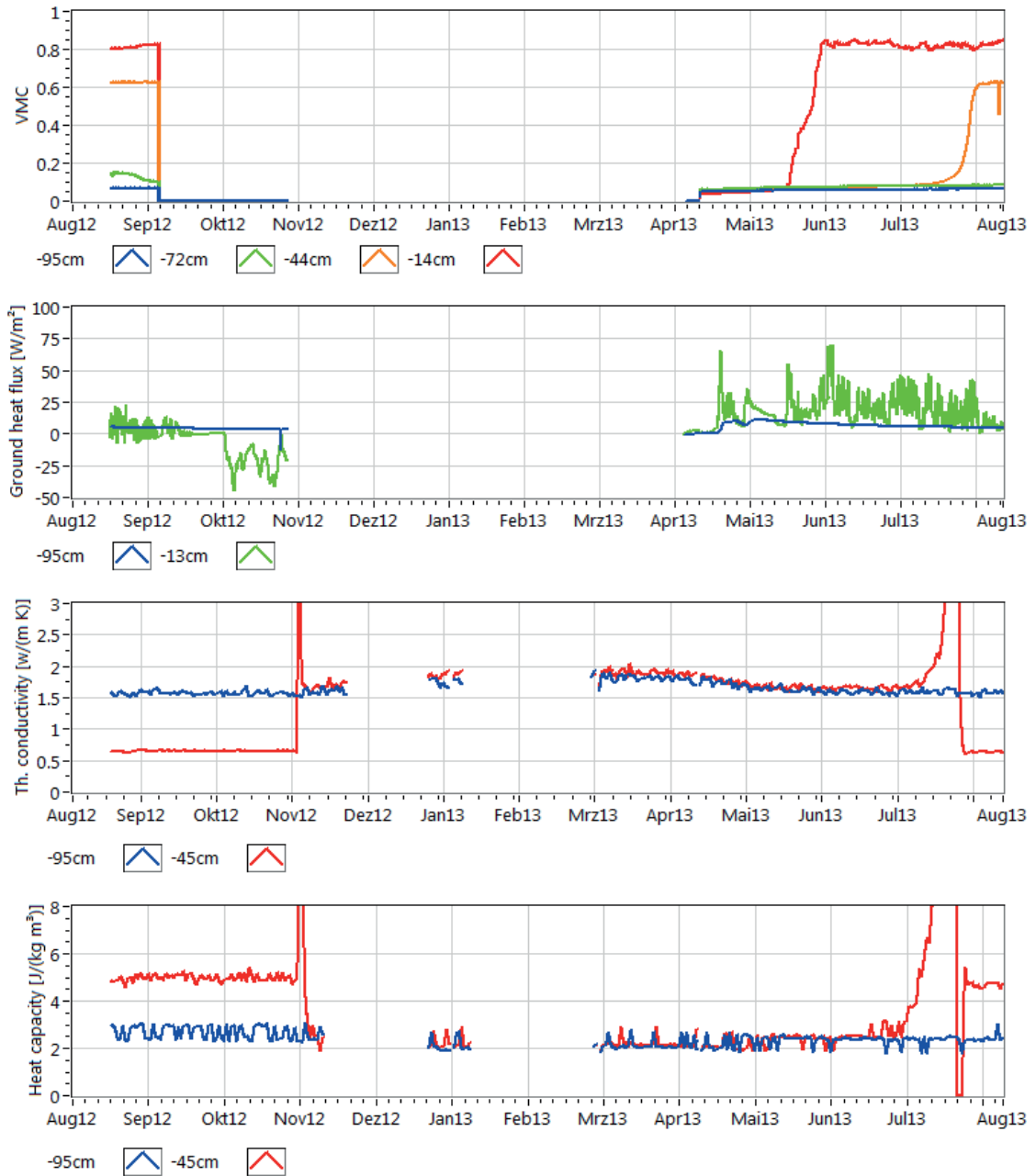


Figure 3-7 Data record from the sensors installed in the subsurface of the polygon center August 2012 to 2013. From top to bottom: temperature, volumetric water content, ground heat flux, thermal conductivity, heat capacity.

Thermal property sensors were used to monitor soil thermal conductivity and thermal capacity *in situ*. Thermal conductivity values in the frozen soil at 45 and 95 cm depth in 2013 range between 1.5 to 2 (W/m K) and for the thawed soil at 45 cm depth (peat) around 0.7. This is in agreement with the ranges given by previous model estimates from various methods. The heat capacity shows a difference between the two soil depths, but no seasonal signal. The heat capacity ranges between 2-3 (MJ/m³ K¹) at 95 cm depth (always frozen) and 5 (MJ/m³ K¹) at 45 cm depth in the thawed state. Strong changes in the thermal properties occur during the seasonal phase change during summer thaw.

3.1 Heat and water budget of permafrost landscapes

Previous estimates for the heat capacity of the wet tundra soil are 3.4 ± 0.5 (thawed) and 1.8 ± 0.3 (frozen; Boike et al., 2013; Langer et al., 2013).

3.1.4 Soil profile description

In the polygon centre, the soil was classified as *Glacic Cryosol (Eutric, Reductaquic)* (Table 3-2). It is characterized by water-saturation in the whole soil profile for most of the year, which leads to reducing conditions and soil organic matter accumulation. However, the gravimetric soil organic carbon contents in all horizons were below 12 %, thus not qualifying them as organic material. Below the topsoil Ah horizon, alternating layers of organic and mineral materials were found. The edge of an ice-wedge was cut by the left part of the soil profile from a depth of 89 cm.

At the polygon rim, the soil was classified as *Turbic Cryosol (Eutric, Reductaquic)* (Table 3-3). It is characterized by irregular horizon and sediment layer boundaries due to cryoturbation. Due to its relative higher position in the microtopography, the soil is not water-saturated for the whole year. However, reducing conditions were identified below 23 cm. Like in the soil of the center, alternating layers of organic and mineral materials were found below the topsoil Ah horizon. Organic carbon contents in the Ah horizon were lower than in the soil of the polygon center; however, a frozen buried peat horizon was found below 80 cm.

3.1 Heat and water budget of permafrost landscapes

Table 3-2 Soil profile description of the Glacic Cryosol (Eutric, Reductaquic) in the polygon center

Location: Samoylov Island, Lena River Delta, date of description: 11 August 2012		
Geographic coordinates: 72°22.451 N, 126°29.753 E		
Situation within microrelief: Center of low-center ice wedge polygon (depression)		
Mean annual air temperature: -12,5 °C		
Thaw depth on date of description: 41 cm		
Water level above moss surface before drainage: 3 cm		
Remarks: no signs of cryoturbation, drained during description		
Depth below moss surface (cm)	Horizon	Description
0...6	living moss	Dark reddish grey (2.5YR 3/1), living to dead moss layer, green moss <i>Scorpidium</i> sp., no roots, bulk density very low
6...13	Ah1	Dark reddish grey (2.5 YR 3/1), extremely high content of organic matter (15-30%), green moss peat, very many roots, <i>Carex</i> root mat, no soil aggregates visible, bulk density very low
13...23	Ah2	Very dark grey (5 YR 3/1), extremely high content of organic matter (15-30%), green moss peat, many roots, no soil aggregates visible, bulk density very low
23...41	Arhb/Cr	Very dark brown (10 YR 2/2), loam, very high content of organic matter (8-15%), alternating layers of green moss peat (with loam) and loamy sand, few roots, single corn matrix, bulk density very low, alpha-alpha-Dipyridyl reaction positive
41...89	Arhfb/Crf	Very dark brown (10 YR 2/2), silt loam, very high content of organic matter (8-15%), alternating layers of green moss peat (with loam) and silt loam, no roots, frozen, ice-cemented, alpha-alpha-Dipyridyl reaction positive
89...110...	I + Arhfb/Crf	Left side of profile clear ice, probably part of ice-wedge, right side as horizon above
Soil classification		
World Reference Base for Soil Recourses: <i>Glacic Cryosol (Eutric, Reductaquic)</i>		
US Soil Taxonomy: <i>Glacic Aquorthel</i>		

3.1 Heat and water budget of permafrost landscapes

Table 3-3 Soil profile description of the Turbic Cryosol (Eutric, Reductaquic) at the polygon rim

Location: Samoylov Island, Lena River Delta, date of description: 11 August 2012		
Geographic coordinates: 72°22.451 N, 126°29.753 E		
Situation within microrelief: Summit of elevated rim of low-center ice wedge polygon		
Mean annual air temperature: -12,5 °C		
Thaw depth on date of description: 30 cm		
Water level above moss surface before drainage: -30 cm		
Remarks: Irregular horizon and sediment layer boundaries due to cryoturbation		
Depth below moss surface (cm)	Horizon	Description
0...3	living moss	Very dark grey (5YR 3/1), living moss layer, green moss <i>Hylocomium</i> sp., no roots, bulk density very low
3...8	Ah1	Very dark grey (5 YR 3/1), sandy loam, very high content of organic matter (8-15%), many roots, bulk density very low
8...13	Ah2	Very dark grey (5 YR 3/1), loam, high content of organic matter (5-8%), many roots, bulk density very low
13...26	Ah1b@/Cl@	Dark reddish-grey and brown (2.5 YR 3/1 and 7.5 YR 3/1), silt loam, very high content of organic matter (8-15%), alternating layers of green moss peat and mineral material, bulk density very low, alpha-alpha-Dipyridyl reaction negative
26...30	Arhb@/Cr	Dark reddish-grey (2.5 YR 3/1), silt loam, extremely high content of organic matter (15-30%), alternating layers of green moss peat and mineral material, few roots, bulk density very low, alpha-alpha-Dipyridyl reaction positive
30...80	Arhfb@/Crf@	black (10YR 2/1), silt loam, very high content of organic matter (8-15%), no roots, frozen, ice-cemented
80...105...	Hrfb@1	black (10YR 2/1), organic material (>30% organic matter), silt loam (Ut4), no roots, ice-cemented
Soil classification		
World Reference Base for Soil Recourses: <i>Turbic Cryosol (Eutric, Reductaquic)</i>		
US Soil Taxonomy: <i>Turbic Aquorthel</i>		



Figure 3-8 Soil profile in the center of the polygon: Glacic Cryosol (Eutric, Reductaquic). Note the massive ice in lower left corner at about 1 m depth.

3.1 Heat and water budget of permafrost landscapes



Figure 3-9 Fully installed center profile. Frozen ground was encountered at about 41 cm below ground surface corresponding to the second TDR sensor (from top down).



Figure 3-10 Instrumentation in upper soil of center profile. From left to right: oxygen probes, white “box” TDR probes (white boxes), PT100 temp probes (white cables), heat flux plate.

3.1 Heat and water budget of permafrost landscapes

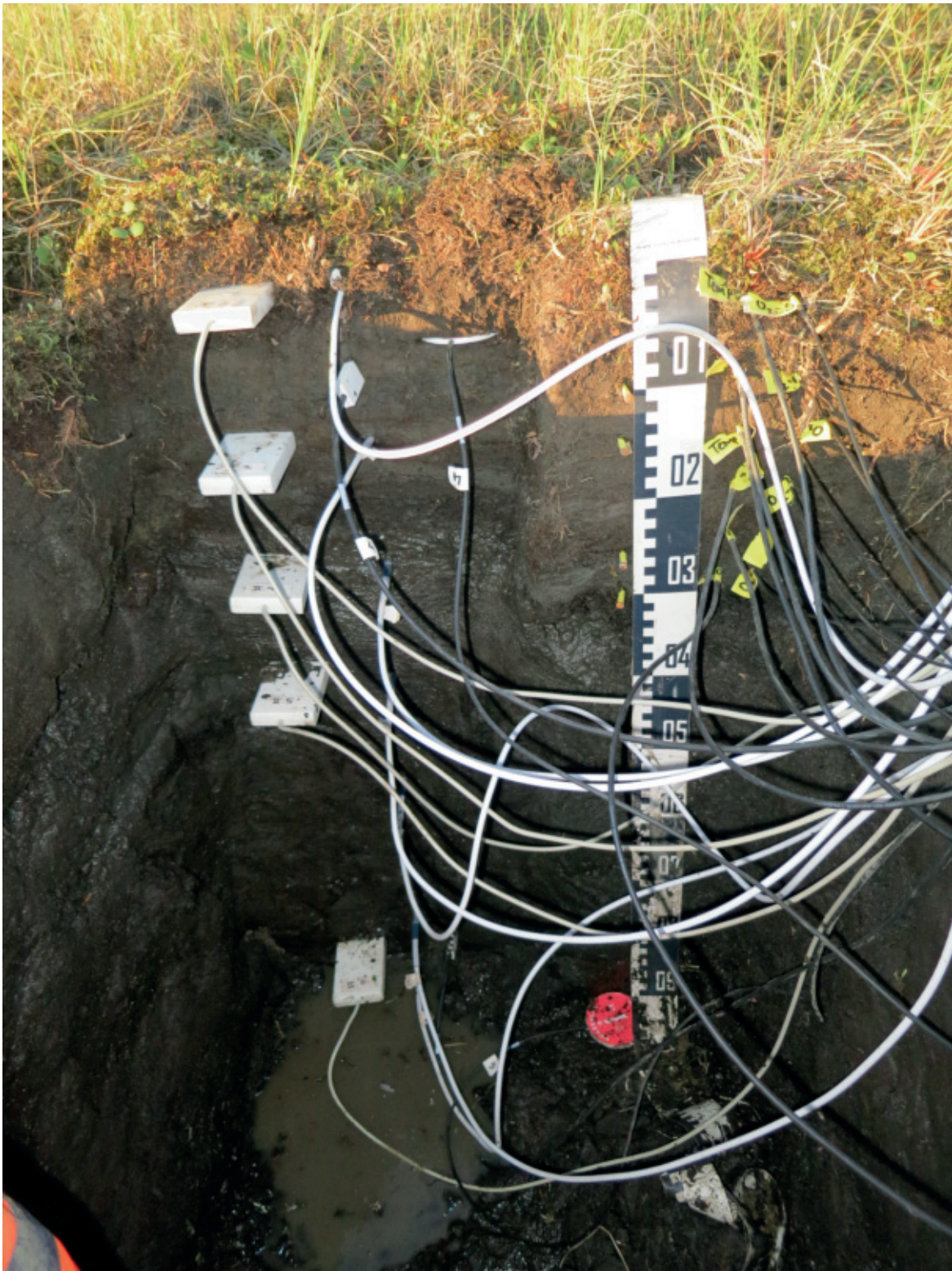


Figure 3-11 Installed rim profile. Thaw depth at about 30 cm (between 2nd and 3rd TDR probe from top)

3.1.5 Snow monitoring site

3.1.5.1 Introduction

The thermal state of permafrost is strongly controlled by the snow cover at the study site (e.g. Langer et al., 2013). Due to its low thermal conductivity, the snow cover effectively limits the cooling of the ground during the long lasting winter period. This is especially true at the study site where a shallow snow cover (of usually less than 0.5 m) exists which usually features a distinct layer composition. The characteristics of the snow layers such as density, grain size, and grain shape can be strongly different. Often, a layer of depth hoar exists at the bottom of the snow cover while the top is mostly characterized by a wind compacted ice crust. Especially for a shallow snow cover the effective insulation strongly depends on the layer composition and already small changes can strongly affect the thermal state of the ground underneath. Hence, knowledge about the snow cover characteristics including spatial and temporal variations is essential for investigating the thermal dynamics and stability of permafrost.

In order to ensure a continuous observation of the snow cover and its physical properties (density and thermal diffusivity) a comprehensive snow monitoring station was installed during the field campaign in 2012.

3.1.5.2 Snow monitoring system

The snow monitoring station consists of a 15 m aluminium rack which spans across the rims of two adjacent ice wedged polygons (Figure 3-12, Figure 3-13). The rack is fixed on four steel poles about 1.5 m above the surface. The poles are fixed in the permafrost down to a depth of about 1.5 m. This ensures a steady position of the rack despite the freeze-thaw dynamics of the active layer. The rack is equipped with four infrared surface temperature sensors (2x IRTS-P, 2x SI-111), ten ultrasonic snow depth sensors (SR50A) directed towards the ground, and one air temperature sensor (T107). This setup allows to detect spatial differences in snow depths due to the polygonal micro topography. In addition, two ultrasonic ranging sensors are mounted in horizontal orientation. The sensors point against metal targets which are fixed on poles in about 1 m distance to the sensors (Figure 3-12). This installation allows to measure lateral movements of the ground. Furthermore, a snow pack analyzer (SPA) is installed underneath the rack which measures the snow water equivalent (SWE) in different snow depths. The sensor bands (wave guides) are located about 10, 20, and 30 cm above the surface. In order to measure the temperature gradient within the snow cover 12 thermocouples are installed in different depth above the ground at the SPA (Figure 3-13). Moreover, a shallow soil temperature profile down to a depth of about 1 m is installed close to the snow monitoring systems.

3.1 Heat and water budget of permafrost landscapes

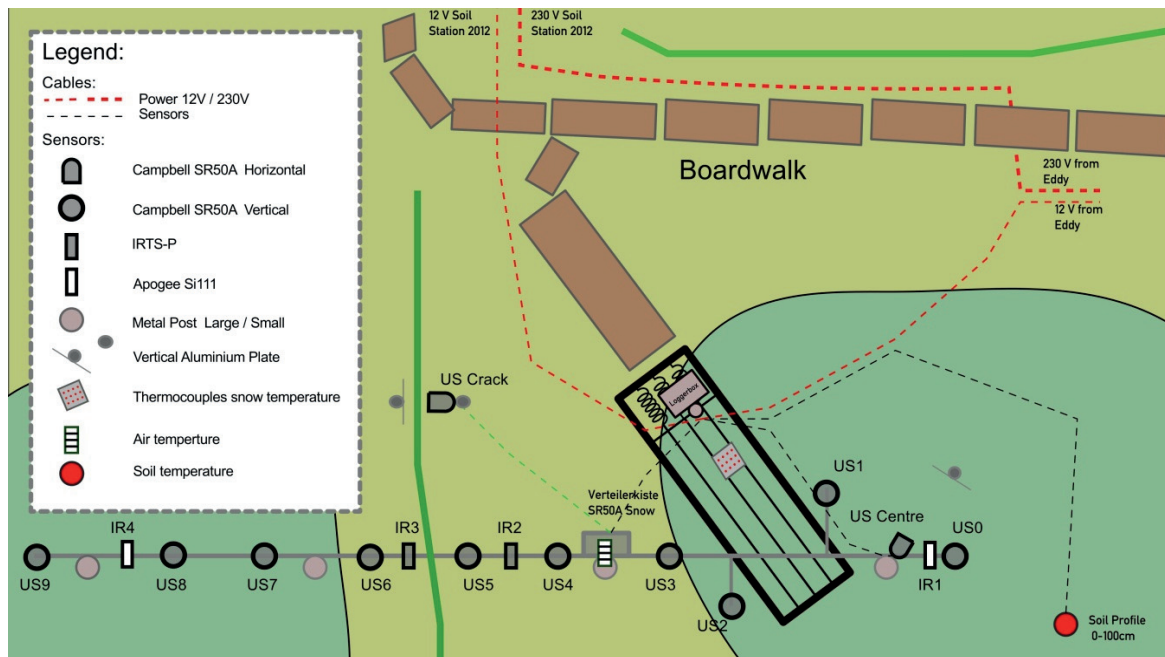


Figure 3-12 Schematic overview of the new snow motoring station including the 15 m rack for snow depth measurements, the snow pack analyser, and the cover temperature sensors.

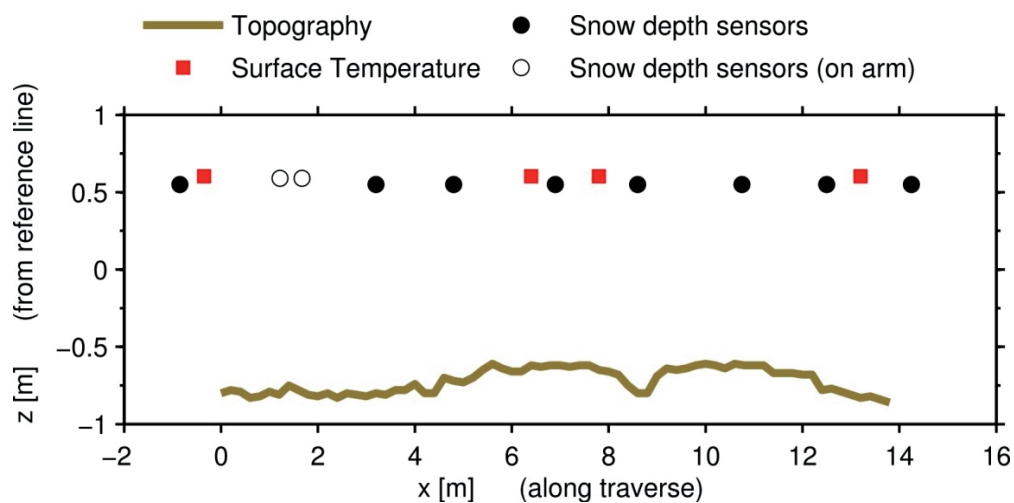


Figure 3-13 Sensor locations along 15 m rack for snow depth measurements including a profile of the surface topography.

References

Boike, J., Kattenstroth, B., Abramova, K., Bornemann, N., Chetverova, A., Fedorova, I., Fröb, K., Grigoriev, M., Grüber, M., Kutzbach, L., Langer, M., Minke, M., Muster, S., Piel, K., Pfeiffer, E.-M., Stoof, G., Westermann, S., Wischnewski, K., Wille, C., Hubberten, H.-W. (2013) Baseline characteristics of climate, permafrost and land cover from a new permafrost observatory in the Lena River Delta, Siberia (1998–2011). *Biogeosciences*, 10, 2105-2128, doi:10.5194/bg-10-2105-2013.

3.1 Heat and water budget of permafrost landscapes

FAO – Food and Agriculture Organization (2007) WRB - World reference base for soil resources 2006. First update, FAO, Rom, 128 p.

Langer, M., Westermann, S., Heikenfeld, M., Dorn, W., Boike, J. (2013) Satellite-based modeling of permafrost temperatures in a tundra lowland landscape. *Remote Sensing of Environment* 135, 12-24, doi: 10.1016/j.rse.2013.03.011.

3.2 SUMMERTIME CARBON-CYCLE AND HYDROLOGICAL FLUX OBSERVATIONS, SAMOYLOV ISLAND

Benjamin R.K. Runkle, Manuel Helbig, Alexander Sabrekov, Wiebke Münchberger, and Lars Kutzbach

Fieldwork period: July 04 to September 03, 2012; Samoylov Island

3.2.1 Objectives

3.2.1.1 Vertical fluxes

This research goal was to provide a continuation of long-term eddy covariance (EC) measurements of CH₄, CO₂, H₂O and energy exchange from the land surface to the atmosphere at Samoylov Island. This work included careful maintenance of long-term meteorological and gas flux monitoring instruments. A continuation of this data series is important for analyzing the high intra- and inter-annual variability of these fluxes. Only with long-term measurements is it possible to give generalized conclusions about the carbon balance of this tundra environment as well as climatic influences on the vertical carbon fluxes.

3.2.1.2 Lateral fluxes

Additionally, in this year we installed more durable and permanent weirs on three outflow channels from Samoylov's ice wedge network. These installations provide estimates of water discharge. When coupled with water samples to be measured for dissolved organic carbon content (DOC), they help provide the lateral flux of carbon from this catchment. Water samples have also been analyzed for their stable isotope ratios and nutrient contents; together these can be used to test hypotheses regarding hydrological flow through this complex landscape. Supporting instrumentation such as radiation sensors and soil temperature profiles were installed to provide an understanding of connections between thermal thaw and deeper sub-surface flow pathways.

3.2.1.3 Microsite scale fluxes

To develop a finer understanding of spatial variations in landscape-atmosphere gas fluxes, we initiated two surveys at different microsite scales. The first was a closed chamber study to provide estimates of CH₄ and N₂O flux at different micro-topographical zones on Samoylov. These measurements were conducted in a set of polygon types, along the outflow channel from the ice-wedge network, and in the modern floodplain.

Second, initial studies on leaf-level photosynthesis were conducted. These measurements are supported by studying the leaf area index of *Carex aquatilis*, the dominant sedge species. This research is contextualized by an ecologically-oriented description of the vegetation cover.

3.2.2 Methods

3.2.2.1 Vertical fluxes

We installed several new eddy covariance instruments at the main tower. On arrival, we placed an open-path Li-7500A sensor from the SPARC group to measure CO₂ and H₂O concentrations. We also re-installed an open-path Li-7700 sensor to measure CH₄ concentrations.

3.2.2.2 Lateral fluxes

We installed three weirs to measure discharge from the ice wedge network and an adjacent watershed composed more predominantly of intact polygons. These weirs are made from steel and are calibrated with a bucket-filling method to test the stage-discharge relationship. Grab samples of water for stable isotope analysis from each weir were conducted near daily; additional samples from other water bodies were also collected sporadically. Samples of soil matric water were also taken in profiles in different polygon and microsite locations for measuring stable isotopes and dissolved organic carbon concentration.

3.2.2.3 Microsite scale fluxes

Closed chamber study

The closed chamber measurements were performed using collars with dimensions 50 x 50 cm at sites. For the first part of the measurement period, syringe samples of gas were collected in regular intervals into vials filled with KCl salt solution. For the second part of the measurement period, syringe samples were analyzed for their CH₄ concentration using the gas chromatograph installed at the station. Salted vials were used to store and transport duplicate samples for analysis of N₂O concentration at Moscow State University.

Photosynthesis of *Carex aquatilis* and *Arctophila fulva*

Leaf-level photosynthesis measurements were performed with the Li-6400 gas analyzer.

- Light response curves were done with 3 x 5 *C. aquatilis* samples chosen from wet tundra, dry tundra and overgrown water
- *A. fulva* light response curves were also done with five samples (only found in overgrown land cover class)

Supplemental information such as leaf nutrient content and green area index were also determined.

3.2 Summertime carbon-cycle and hydrological flux observations

3.2.3 Results

Summertime exchange of water (Figure 3-14) and carbon (composed of CO₂, CH₄, and DOC; Figure 3-15) on the landscape scale were determined using a mixture of eddy covariance and lateral flux measurements. The water budget demonstrates the dominance of evaporation on the landscape during this period, though discharge is a non-negligible component of the balance (approximately 15%). The carbon budget is dominated by net uptake of CO₂ during this most vegetatively-active period. Fluxes of CH₄ and DOC were considerably lower (each more than one order of magnitude less than the other).

The closed-chamber measurements reveal microsite methane fluxes of similar magnitude to those previously reported for polygons on Samoylov (Sachs et al., 2010). They also show that saturated sites in the margins of the outflow channel (“TR2”) emit more CH₄ than saturated sites in the center of the outflow channel (TR3, TR4). A brief test of measurements from the modern floodplain part of the island demonstrated significantly lower fluxes there than in the Holocene polygonal terrace. In this site a vegetated (grassy) site emitted more CH₄ than an adjacent sandy location.

The photosynthesis work was organized by the land cover class within which each *Carex* plant was situated. The results of this study (shown in Table 3-4) demonstrate lower maximal photosynthetic capacity (*P*_{max}) in wet polygons, lower leaf nitrogen in overgrown polygons, and generally low respiration rates (*R*_d). *A. fulva* did not have significantly different photosynthetic properties from *C. aquatilis* but did have higher leaf N content.

3.2 Summertime carbon-cycle and hydrological flux observations

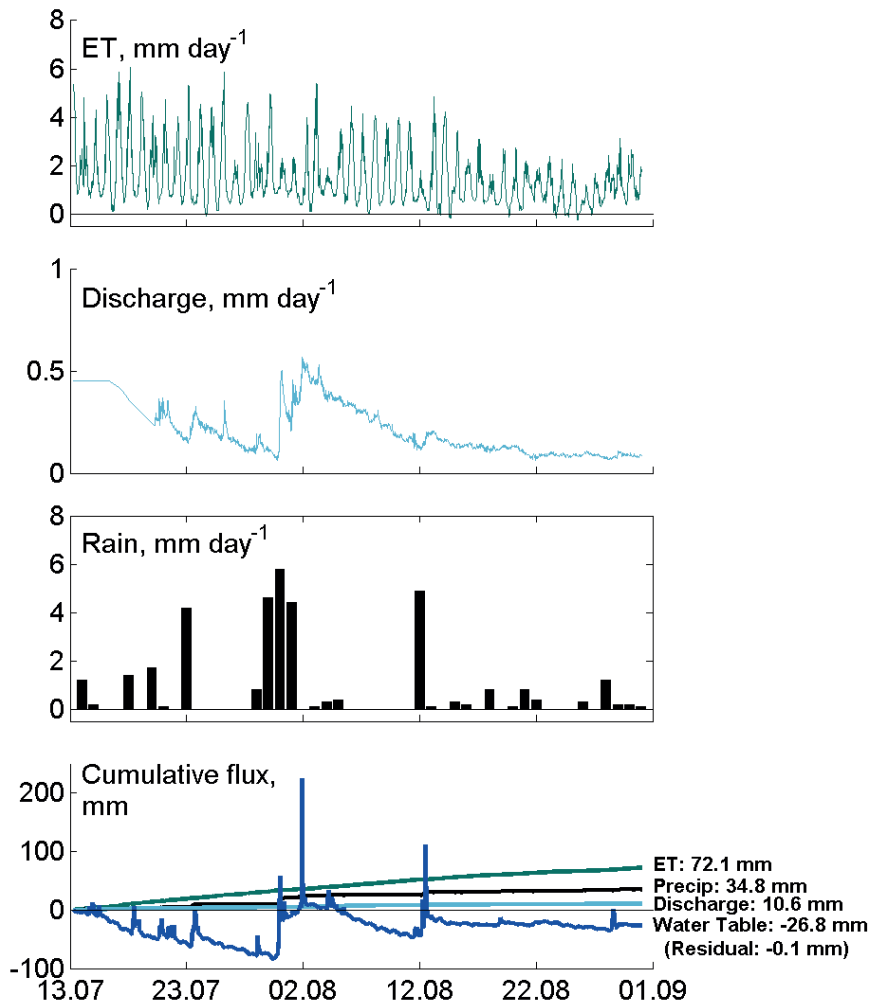


Figure 3-14 Site water fluxes during the summer period, 2012.

Table 3-4 Leaf photosynthesis parameters, classified by land cover type and determined through modeling a light response curve to measurements taken on the Li-6400 leaf photosynthesis system.

land cover class	sample size	Pmax, $\mu\text{mol CO}_2 \text{ m}^{-2}\text{s}^{-1}$	Rd, $\mu\text{mol CO}_2 \text{ m}^{-2}\text{s}^{-1}$	mixed samples for each class!		
				C/N ratio	N content (%)	total phosphorus (mg/kg)
dry	5	7.18 ± 1.04	0.42 ± 0.08	26.87	1.76	2305.93
wet	5	4.35 ± 2.22	0.47 ± 0.13	27.15	1.76	1062.99
overgrown	5	6.04 ± 0.80	-0.93 ± 2.50	32.00	1.47	1020.37
<i>A. fulva</i>	5	4.66 ± 1.72	0.33 ± 0.18	25.73	1.79	6826.33

3.2 Summertime carbon-cycle and hydrological flux observations

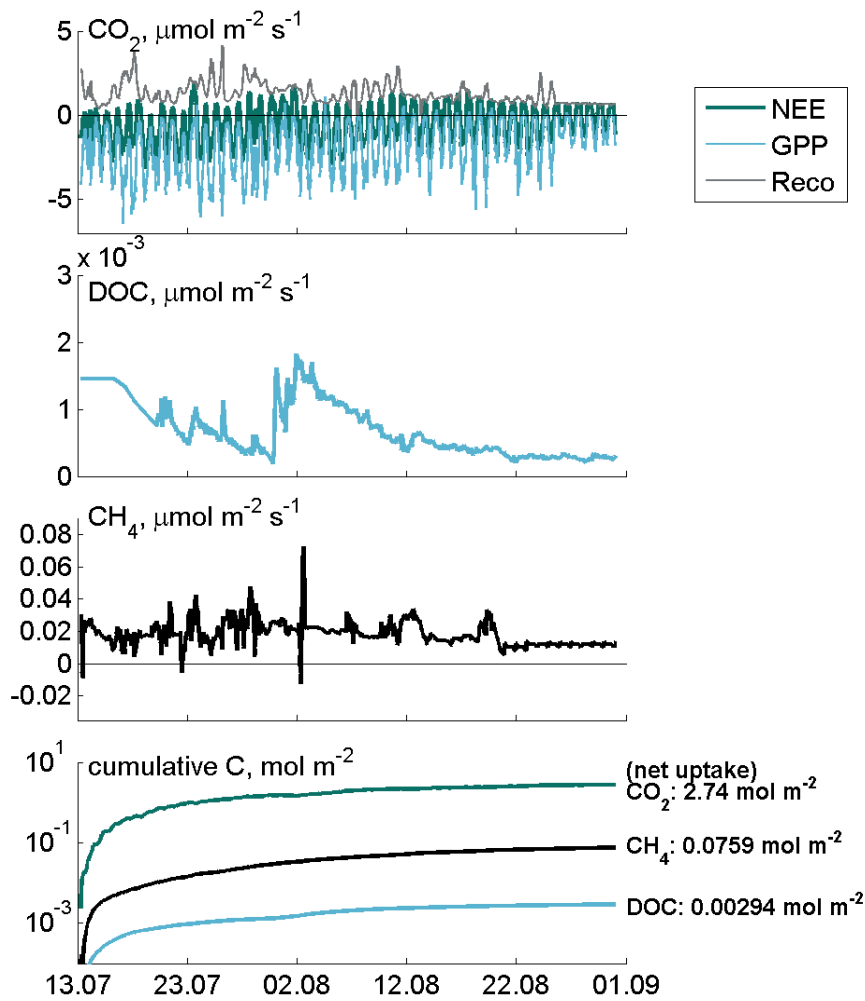


Figure 3-15 Site carbon fluxes during the summer period, 2012.

3.2 Summertime carbon-cycle and hydrological flux observations

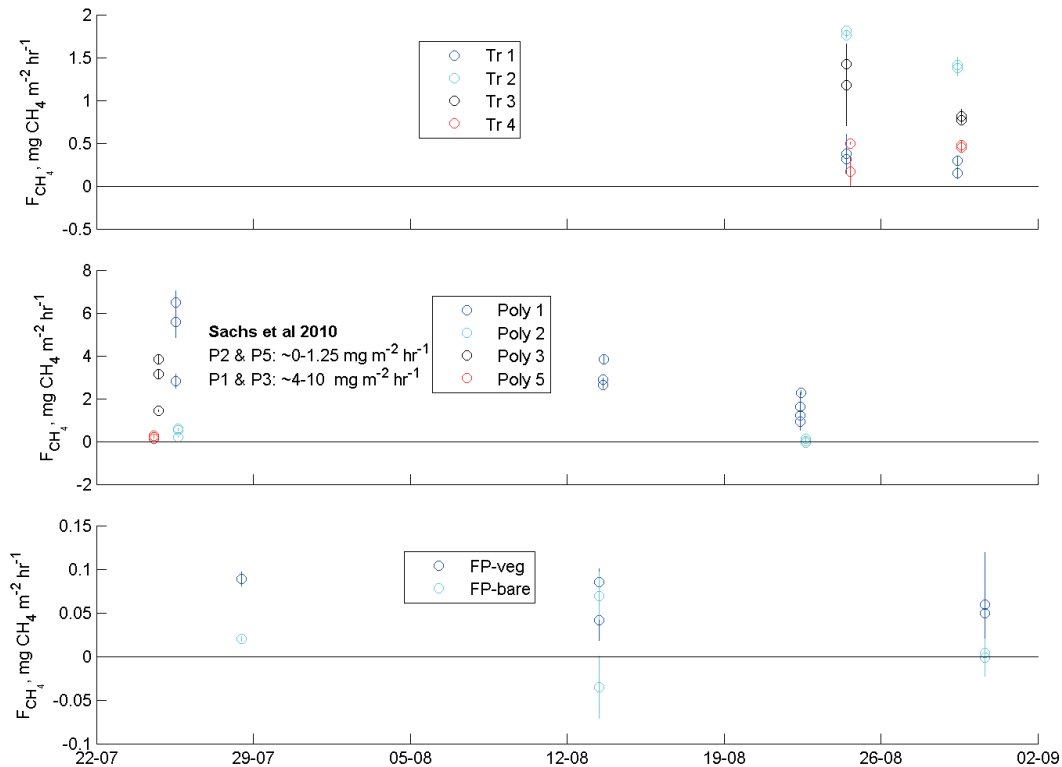


Figure 3-16 CH_4 fluxes derived from the closed-chamber experiment, compared to the values of Sachs et al. 2010. Poly 1 and 3 are wet polygon centers, polygons 2 and 5 are dryer polygon centers. The sites Tr 1-4 are aligned in a transect from driest to wettest along the outflow pathway discharging water from the ice flow network. In the lowest panel, two sites on the modern floodplain are plotted; one with vegetation and the other with bare sand cover. Note that the y-axis scaling changes between plots.

References

Sachs, T., Giebels, M., Boike, J., Kutzbach, L. (2010) Environmental controls on CH_4 emission from polygonal tundra on the microsite scale in the Lena river delta, Siberia. *Global Change Biology* 16, 3096-3110, doi: 10.1111/j.1365-2486.2010.02232.x.

3.3 AIRBORNE MEASUREMENTS OF ENERGY AND CARBON FLUXES

Torsten Sachs and Eric Larmanou

Fieldwork period: August 2012; Lena River Delta

3.3.1 Background

One of the most pressing questions with regard to climate feedback processes in a warming Arctic is the regional-scale carbon dioxide (CO₂) and methane (CH₄) release from Arctic permafrost areas. Ground-based eddy covariance (EC) measurements provide continuous in-situ observations of the surface-atmosphere exchange of these greenhouse gases. However, these observations are still quite rare in the Arctic and site selection is usually bound by logistical constraints, among others. Consequently, these observations cover only small areas that are not necessarily representative of the region of interest. Airborne measurements can overcome this limitation by covering distances of hundreds of kilometers over time periods of a few hours.

3.3.2 Objectives

The objectives of our work were to

- test the feasibility of deploying the helicopter-carried micrometeorological sensor package “Helipod” in the Lena Delta to measure eddy covariance fluxes of latent and sensible heat as well as carbon dioxide
- determine the atmospheric boundary layer (ABL) height at different locations within the delta
- put the continuous but very localized eddy covariance measurements on Samoylov Island and Kurungnakh into a regional context
- study the variability of energy and trace gas fluxes in relation to the different land surface and vegetation characteristics in the delta

3.3.3 Methods

We used the Helipod system owned by the Technische Universität Braunschweig to conduct our regional scale flux measurements. Helipod (Figure 3-17) is a 5 m long high resolution meteorological measurement system for monitoring turbulence properties of the ABL. It was carried by a MI-8 on a 30 m rope at an airspeed of 40 m s⁻¹ and is designed for in situ measurements of small scale turbulent fluctuations of wind, temperature, humidity, carbon dioxide and the associated turbulent fluxes, as well as the infrared surface temperature. Each meteorological variable is measured with two complementary sensors, one with a short response time but low absolute accuracy, the other with longer

3.3 Airborne measurements of energy and carbon fluxes

response time but high accuracy and long-term stability. The two datasets are combined by complementary filter.

Helipod is equipped with a five-hole probe, an inertial reference system (IRS) and two GPS systems, which are used to determine the static pressure, the true air speed, the position, the attitude and finally the wind vector. Temperature is measured with a Rosemount resistance thermometer and a fast open wire element. Humidity is measured by a Lyman Alpha hygrometer, a capacitive sensor (Humicap) and a dew point mirror. CO₂ and water vapor are recorded with a fast response open path infrared gas analyzer (LI-COR 7500).

Flight patterns include a wind calibration square after take-off, vertical profiles at the beginning and end of each transect to determine the boundary layer height, and long (100 km) low altitude transects for flux measurements.

3.3.4 Preliminary Results

We were able to conduct two flights on 9 August and 15 August totaling 4.5 hours of measurements and four vertical profiles. The first transect was flown in NW direction from Samoylov across the third terrace towards the coast. Weather conditions were fair and all systems worked well. The second transect was flown in NNW direction across the first and second terrace. Weather conditions were not favorable and preliminary results suggest that a thin boundary layer and occasional rain during the transect render data analysis and interpretation difficult. In addition, the Helipod GPS antennas were damaged during a failed take off and were not adjusted correctly during the flight. Navigation was impaired by the helicopter pilots' lack of a functioning GPS unit.

Table 3-5 Flight catalogue

Flight leg	Start	End	Turning point	Length (km)	Altitude (m)	T (°C)	Wind direction	CO ₂ (ppm)
20120809 outbound	12:48	13:33	72°56'42"N 123°35'35"E	109	100	22	220°	370
20120809 inbound	13:46	14:26		109	200	22	220°	370
20120815 outbound	12:13	12:59	73°32'33"N 125°13'33"E	134	100	11.5	90°	371
20120815 inbound	13:10	14:07		134	200	10.5	90°	369

3.3 Airborne measurements of energy and carbon fluxes



Figure 3-17 Helipod during first take off on Samoylov Island



Figure 3-18 CO₂ concentration (ppm) along the first flight track (9 Aug 2012)

3.3 Airborne measurements of energy and carbon fluxes

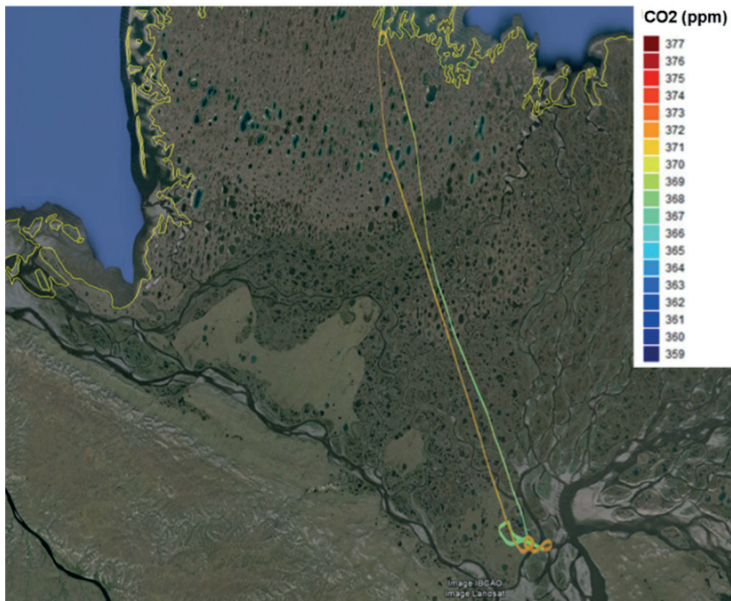


Figure 3-19 CO₂ concentration (ppm) along the second flight track (15 Aug 2012)

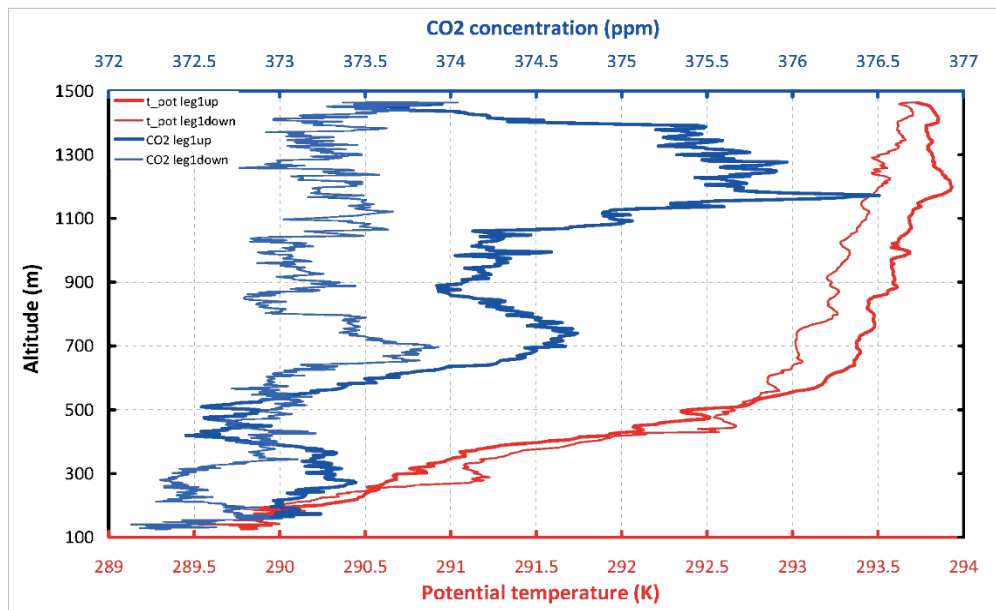


Figure 3-20 Vertical profiles of potential temperature and CO₂ concentration (ppm) near the coast on 9 Aug 2012

3.3 Airborne measurements of energy and carbon fluxes

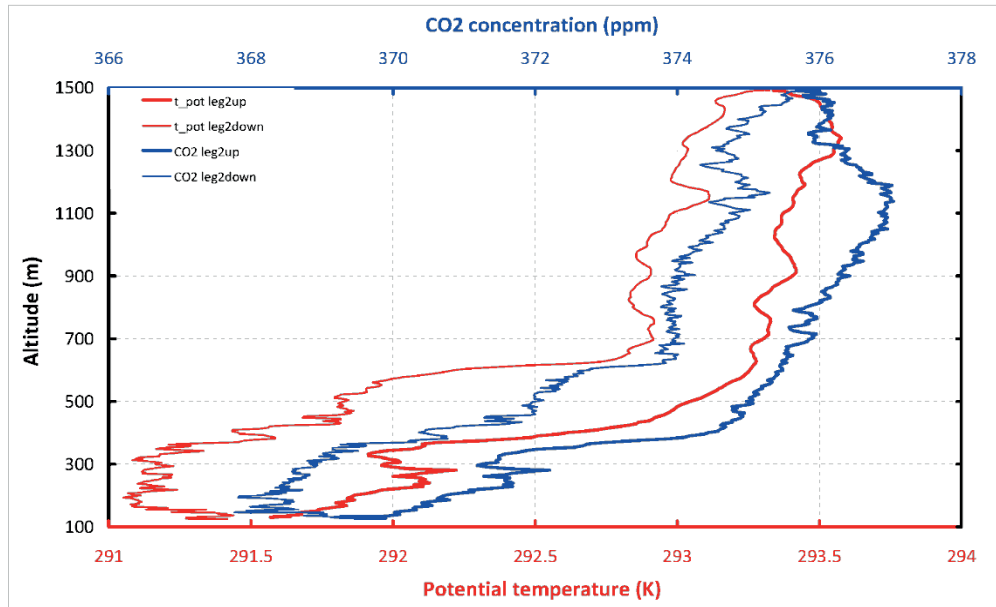


Figure 3-21 Vertical profiles of potential temperature and CO₂ concentration (ppm) near Samoylov on 9 Aug 2012

3.4 DO MICROBES FEED ON OLD CARBON IN PERMAFROST?

Réka-Hajnalka Fülöp, Silke Höfle, Lukas Wacker, Julia Boike, Lars Kutzbach, and Janet Rethemeyer

Fieldwork period: July to August 2012; Samoylov Island

3.4.1 Objective

The objective of the field campaign was to continue our investigation on the permafrost thawing depth in the Lena Delta, in order to identify and characterise the interactions between gas, water, organic material turnover and microbial activity. Our previous work in the Lena Delta's Samoylov Island has focused on determining the composition and age of the organic material in the active layer and on potential stabilisation processes preventing or reducing microbial degradation (e.g., Höfle et al., 2013). During the 2012 field season we collected several soil gas samples from different parts of the polygonal tundra (i.e. polygon rim, center and also from cracks between polygons). The main goal of the field campaign was to sample CO₂ and CH₄ released from the soil for ¹⁴C AMS determinations using molecular sieves without trapping substantial unwanted contaminants. The sampled gases are currently separated and their ¹⁴C ages are determined so that we are able to establish whether CH₄ and CO₂ are released from microbial degradation of relatively fresh or old organic matter sources in the permafrost soil. In parallel work, we have also collected water samples that will be analyzed in the recently established ¹⁴C-dating laboratory of the University of Cologne (Rethemeyer et al., 2013) with the aim of investigating the origin and transport of soil water in permafrost soil.

3.4.2 Methods

Soil gases were allowed to accumulate under self-made soil respiration chambers, from where these were transferred using diaphragm pumps to two different zeolite traps connected together using quick couplings. Two different types of zeolites were used, which were heated at 500°C for 1 hour before usage and flushed with helium gas to protect them from atmospheric exposure. The collected gas samples were shipped back to Cologne and the gases were desorbed from the molecular sieves following specialized procedures and will be sent to ETH-Zürich for AMS gas measurements.

Water samples were collected in septum capped bottles containing saturated salty solution to prevent bacterial growth using a gastight syringe. These samples are aimed at dating primary the dissolved inorganic carbon.

3.4.3 Preliminary results

Only two soil gas samples had been completely processed and analyzed to date. The two samples, collected from both a polygon rim and a polygon center, yielded different ¹⁴C ages for CO₂ and CH₄ gases. The trapped CO₂ had ¹⁴C ages of around 19,000 years BP,

3.4 Do microbes feed on old carbon in permafrost?

whereas the CH₄ separated from the same samples yielded ages only around 2,500 and 500 years BP, respectively. The age difference – if contamination can be excluded in on-going analyses – suggests that CO₂ and CH₄ are released from different depths or from different substrates.

References

Höfle, S., Rethemeyer, J., Mueller, C. W., John, S. (2013) Organic matter composition and stabilization in a polygonal tundra soil of the Lena Delta. *Biogeosciences* 10, 3145–3158, doi: 10.5194/bg-10-3145-2013.

Rethemeyer, J., Fülöp, R.-H., Höfle, S., Wacker, L., Heinze, S., Hajdas, I., Patt, U., König, S., Stapper, B., Dewald, A. (2013) Status report on sample preparation facilities for ¹⁴C analysis at the new CologneAMS center. *NIMB* 294, 168-172, doi:10.1016/j.nimb.2012.02.012.

3.5 SOIL HETEROTROPHIC MICROBIAL BIOMASS AND POTENTIAL BASAL RESPIRATION RATE OF A TYPICAL ICE-WEDGE POLYGON OF SAMOYLOV ISLAND

Svetlana Evgrafova

Fieldwork period: August 2012; Samoylov Island

Soil sampling was done at August 10, from active layer of rim and center of ice-wedge polygon of Samoylov Island. Heterotrophic microbial biomass (MB) was measured by addition into substrate excess of D(+)glucose and $(\text{NH}_4)_2\text{SO}_4$. CO_2 released during first two hours was converting to microbial carbon: $\mu\text{g CO}_2 - \text{C g soil}^{-1} \text{ h}^{-1}$ (Anderson and Domch, 1978; Sparling, 1995). Basal soil respiration rate was estimated from CO_2 emission from soil samples incubated at 23°C and ambient moisture content during 80 hours (incubation experiment). In addition, organic carbon and nitrogen content in soil samples was determined (Figure 3-22).

Soil MB both polygon rim and polygon center strong positively correlated with C_{org} content ($r = 0.81$). Within active layer profiles, a distribution of MB differed between polygon rim and polygon center. The main pool of MB content in organic layers and above permafrost table in polygon rim was observed. MB distribution within polygon center soil profile was nearly uniform (Figure 3-23).

In incubation experiment, all soil samples placed in a temperature exceeded ambient into 1.2-20 times showed exponential basal heterotrophic respiration (HR) rate (Figure 3-23). Initial HR rate depended on MB content in soil ($r=0.95$ for polygon rim active layer profile and $r=0.99$ for polygon center samples after 8 hours of incubation). During incubation period significance of initial microbial pool declined whereas C_{org} content and C/N ratio in soil showed increase in correlations with HR rate. Besides after 80 hours of incubation C_{org} content was more significant for polygon rim samples HR ($r=0.95$) than C/N ratio ($r=0.87$), whereas for polygon center samples HR C/N ratio was more important ($r_{\text{Corg}}=0.93$; $r_{\text{C/N}}=0.86$).

Thus, aboriginal heterotrophic microorganisms of permafrost soil of Samoylov Island are psychro-tolerant. To predict their ability to fully organic matter decomposing in case of temperature increasing longer incubation experiments are needed.

Acknowledgements

The author would like to thank Lars Kutzbach, Günter Stoof (Molo) and Benjamin Runkle for their assistance with all technical problems as well as all members of the joint Russian–German expeditions LENA 2012 for friendly and unselfish support in whatever situation.

3.5 Soil biomass and respiration studies

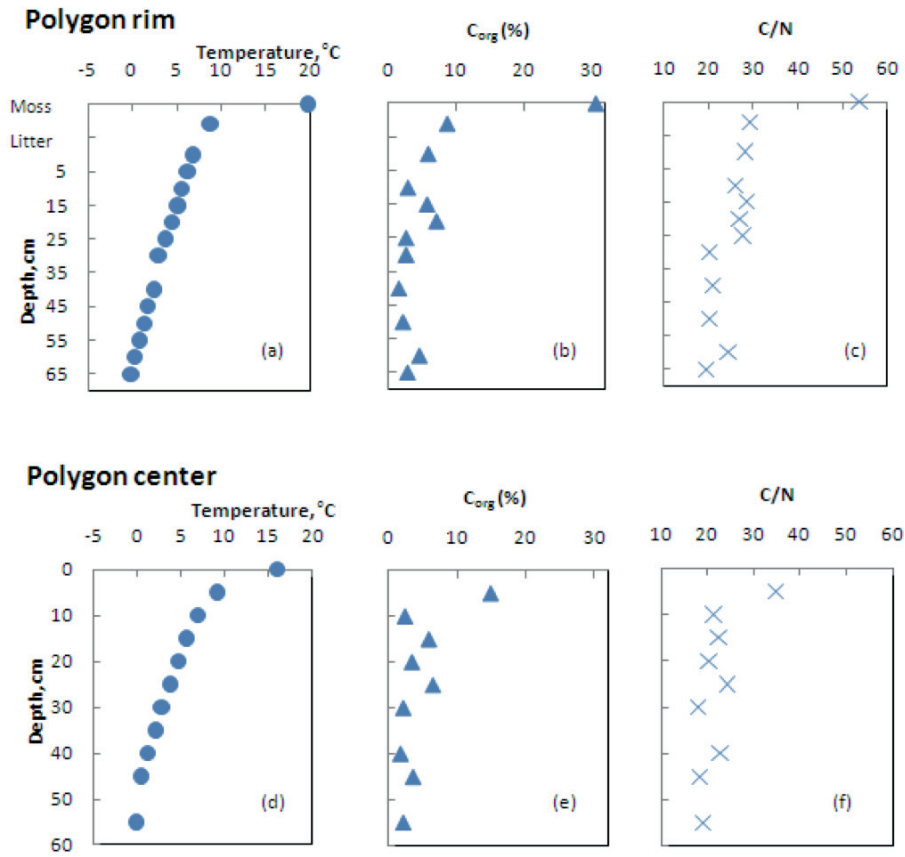


Figure 3-22 Vertical profiles of temperature measured at soil sampling (a, d), organic carbon (b, e), and C/N ratios (c, f) of active layer of ice-wedge polygon

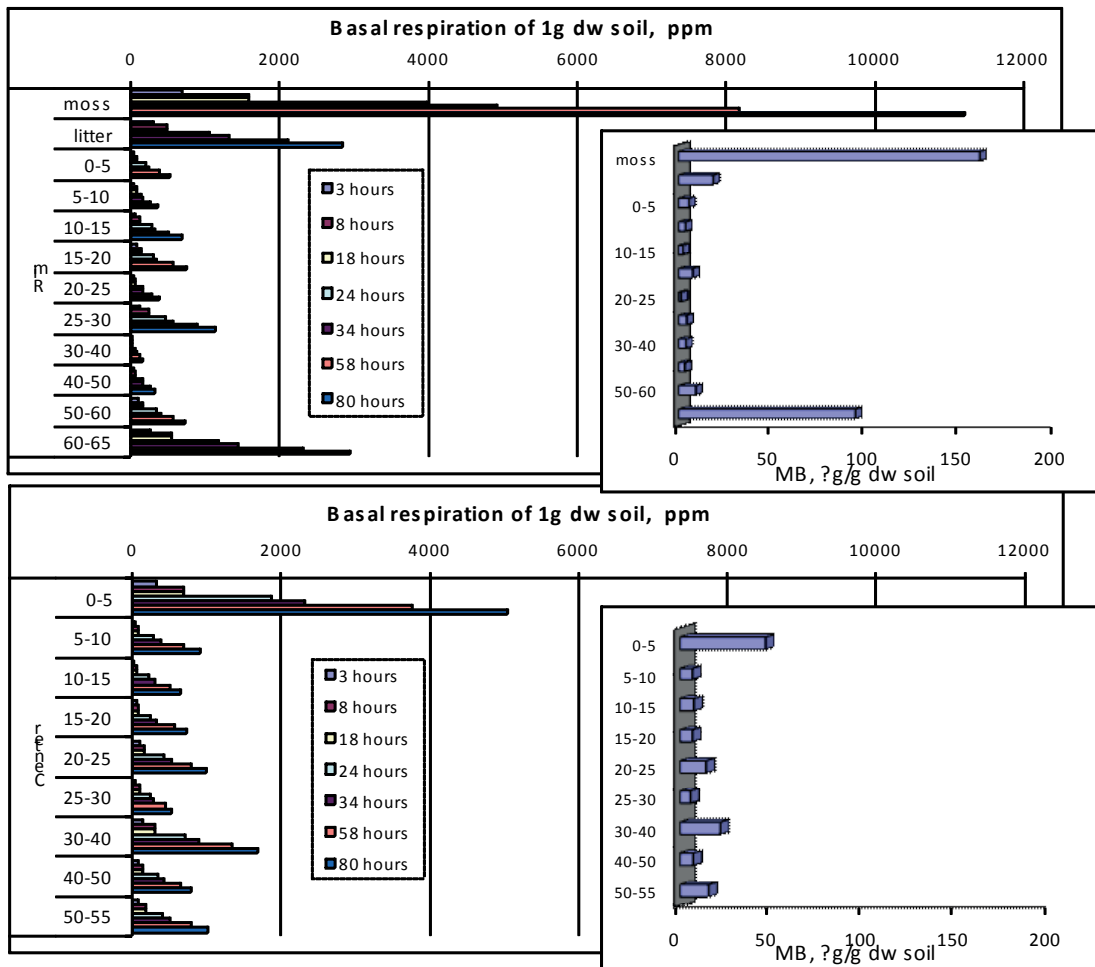


Figure 3-23 Basal respiration rate measured at 23°C and microbial biomass (MB) of active layer of ice-wedge polygon.

References

- Anderson, J.P.E., Domsch K.H. (1978) A physiological method for the quantitative measurement of microbial biomass in soil. *Soil biology and biochemistry* 10, 215-221.
- Sparling G.T. (1995) The substrate-induced respiration method. In: Alef, K., Nannipieri, P.(eds). *Methods in applied soil microbiology and biochemistry*. Academic Press, 397-404.

3.6 METHANE DISTRIBUTION AND METHANE OXIDATION (MOX) RATES IN THE WATER BODIES OF SAMOYLOV ISLAND AND IN THE LENA RIVER

Roman Osudar

Fieldwork period: July 10 to July 30, 2012; Samoylov Island

3.6.1 Objectives

Great amounts of methane, a very potent greenhouse gas, are produced via anaerobic decomposition of organic carbon in permafrost-affected soils and aquatic sediments of the Lena Delta area, Northeast Siberia. With predicted global climate change permafrost thaws and more methane will escape to the atmosphere through soils and water bodies. Methanotrophic bacteria can act as counterpart of these processes and as important sink of methane in these ecosystems.

The main objective of this research is to investigate the distribution of methane and to determine methane oxidation (MOX) rates in lakes and streams of the Lena Delta and in the Lena River itself as well as to analyze the physico-chemical parameters which can affect methanotrophy in changing environments (suspended particulate matter, light, salinity).

3.6.2 Methods

The water samples were collected from the five lakes along the coastline of Samoylov Island, streams, which connected these lakes with the Lena River and from the river itself (Figure 3-24). Additionally water samples were collected along the Bykovsky Channel, one of the largest Lena River channels (Figure 3-25). Then the samples were processed and incubated under different conditions for the further methane concentration and MOX rate measurements, which took place in the Institute of Microbiology, Moscow, Russia. Methane concentrations were determined using gas chromatography, methane oxidation rates were counted following radiotracer (tritiated methane) technique using liquid scintillation counter.

3.6 Methane distribution and methane oxidation (MOX) rates

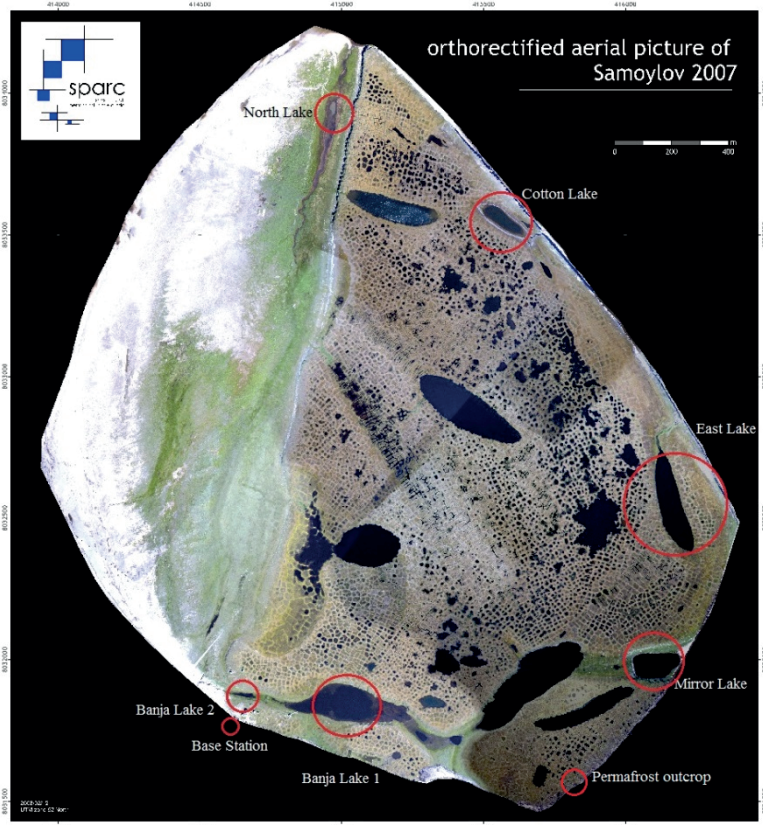


Figure 3-24 Sampling sites, Samoylov Island.

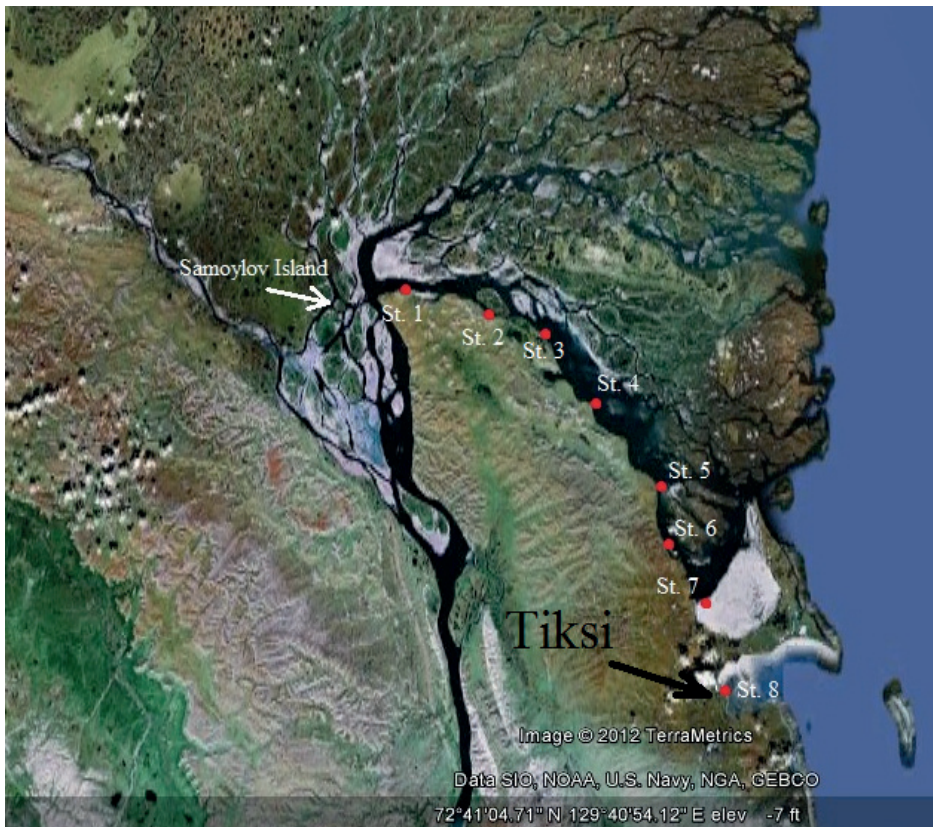


Figure 3-25 Sampling sites, transect Bykovsky Channel.

3.6 Methane distribution and methane oxidation (MOX) rates

3.6.3 Preliminary results

Investigation revealed that methane concentrations in lakes and streams varied from relatively low (200 nM) to extremely high (20 μ M). MOX rates varied from 0.2 to 360 nM/h in lakes and from 0.6 to 480 nM/h in streams. Methane concentrations along the lake-river systems indicated a terrestrial input of methane into the river. MOX rates were also decreasing towards the river showing positive correlation with methane concentrations. Turbidity (suspended particulate matter) and salinity but not light influenced the MOX rates. Salt concentration of 1 g/L decreased MOX rate on 70%, at the same time salt concentration of 30 g/L did not inhibit methane oxidation completely. Methane concentration in the Lena River was significantly changing during the whole period of measuring and varied from 0.3 to 0.75 μ M. No daily regularity was detected.

3.7 HYDROLOGICAL AND GEOCHEMICAL STUDIES IN THE LENA RIVER DELTA

Antonina Chetverova and Olga Bobrova

Fieldwork period: August 2012; Lena River Delta

3.7.1 Introduction

Hydrological and geochemical investigations took place on Samoylov Island and on other small islands around and on big and small channels of the Delta in August 2012.

The main objective of the expedition study is prolongation of annual (from 2003 y.) hydrological and geochemical regime observation of water objects of the Lena River Delta. There are big and small channels, lakes of the 1st and 3rd terraces of the Delta. The special part of the work has concerned of carbon cycle elements study. Hydrological work was organized in different parts of the Delta such as the area adjacent to the Head of the Delta: Samoylov Island, Kurungkakh Island and some other islands around, gauging lines of the big channels and some of the small channels; Olenekskaya channel; and the mouth part of Olenekskaya channel.

The program included following types of work:

Hydrology:

- Water level and temperature measurements on Olenekskaya channel (from Samoylov Island) and on the Fish lake (Samoylov Island);
- Morphometric characteristics and water velocity measurements on the big channels and then water discharge calculation;
- Hydrological measurements in the tidal (wind-surges) zone – a mouth of Olenekskaya channel.

Geochemistry (Sampling):

- Water sampling for main and trace elements and nutrients contents, TOC & DOC content on big and small channels and on lakes of the Delta;
- Suspended particular matter (SPM) sampling for turbidity determination and following geochemistry analyzes (main, trace and organic elements) on big and small channels of the Delta;
- Bottom sediments sampling and sediment cores taking from lakes of the Delta.

Special measurements for Carbon cycle components study (Fish Lake drainage area):

- Active layer depth;
- Active layer humidity;
- Air samples for CO₂ emission determination;
- Pore water sample from drainage of the Fish Lake for nutrients, TOC & DOC content.

3.7.2 Methods

Hydrology

Hydrological measurements (water level, water discharge) occurred on standard water gauging lines on big channels of the Delta using methods of field measurements described in Fedorova et al., 2013. Along and on the mouth of Olenekskaya channel measurements were supported by the group of geomorphologists.

Water level measurements were organized on Olenekskaya channel on Samoylov Island for recalculation of water discharges measured on different dates. Water level gauging post near Samoylov Island consisted of 4 measuring marked piles due to high differences in values of water level during the period from August 4 to September 1. Relative marker with "0" m of a ground level on the island have been used for binding of piles to one level. Water level and water temperature were measured 2 times per day (8 am and 8 pm) according to Roshydromet rules.

Water level and water temperature measurements were also organized on the Fish Lake on Samoylov Island. The top of the pile was used as marker of "0" m.

Water level and water temperature in outlet of Olenekskaya channel were measured every hour during all the day on August 20 to find out tidal cyclicity.

Echo sounder Garmin 421s and GPS Garmin GPSmap 76CSx were used for depth profile measurements. Water velocity was measured using CTD probe (FSI) on several points and on several depths (Fedorova et al., 2013).

Geochemistry

Geochemical work during expedition consisted of sampling and water conductivity measurements by portable sensor. Water samples for main and trace elements were collected in 60 ml plastic bottles pre-cleaned by nitric acid (a.g.) (1:1 diluted HNO₃) and the samples held in cool. Water samples for nutrients were collected in pre-cleaned by pure water 40 ml plastic bottles and frozen. Suspended particular matter were collected to prepared filters (paper filters, GF/F and PC) using for following lab analysis of turbidity, contents of organic and mineral elements correspondingly. Bottom sediments and cores were taken using UVITECH sampling tube and frozen. All samples were transported to St. Petersburg for processing in OSL laboratory (Fedorova et al., 2013).

Carbon cycle

To study the formation of carbon sinks of arctic water objects drainage areas and carbon cycle measurements were carried out on the drainage of Fish Lake (N 72°22'23,5" E 122°29'9,9") of Samoylov Island. The following samples were taken to study the components of the carbon cycle: pore water (from a depth of seasonal thawing) for analysis of DOC and TOC content for the calculation of carbon sinks to the lake; surface samples from the Fish Lake for DOC and TOC content; air samples to calculate CO₂ emissions. Measurements of DOC concentration were made in the pore water of active layer at 21 points in the drainage (catchment) area of the lake. The depth and humidity of active layer were also measured in the same points. The points were selected in different parts of the polygons to account for the heterogeneity of the landscape in the catchment area. Samples were taken at a depth of seasonal thawing using a special device, which is

a thin metal tube with holes at the bottom and a valve at the top. Samples were collected in 120 ml plastic bottles and stored at a 0°C till the analysis. Muddy samples were filtered before analysis.

Samples were analyzed in the field using a Spectrolyser probe. The measure is based on the water absorption of radiation at wavelengths from 220 to 790 nm at 2.5 nm intervals. The soil moisture was measured at the same points where the samples were collected for DOC to calculate the income of DOC to the Fish Lake from the catchment area with groundwater flow. The Some samples were transported to Saint-Petersburg for analysis of permanganate oxidation (PO).

3.7.3 Results

3.7.3.1 Hydrology

Water level

Water level of Olenekskaya channel on the gauging post near Samoylov Island increased gradually two times for the period until August 13 and from August 25 that is probably connected to precipitations. From August 13 to August 25 water level is dropped down which is more typical for this period. Water temperature declined slightly during the period (Figure 3-26).

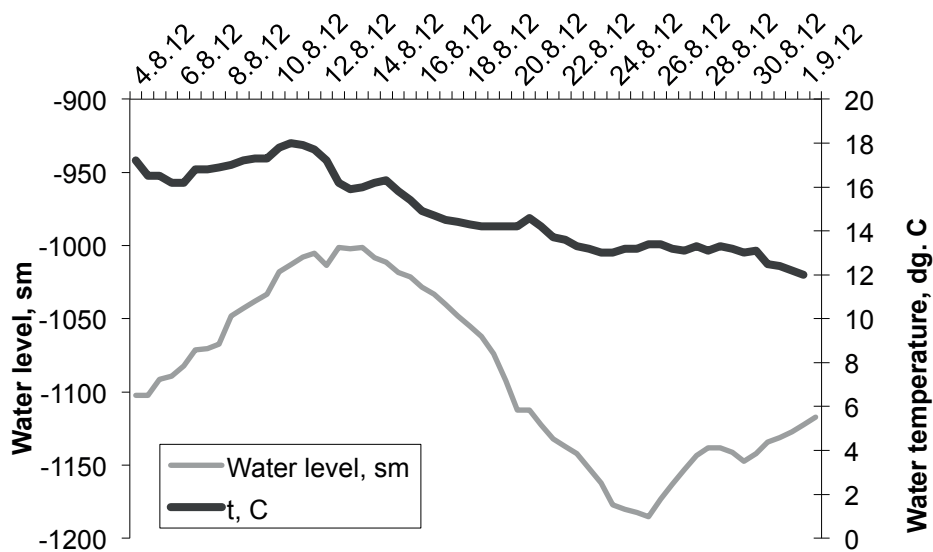


Figure 3-26 Water level and temperature of Olenekskaya channel (Samoylov Island) in August 2012.

Water level and temperature in the outlet of Olenekskaya channel characterized by semidiurnal fluctuations and changed simultaneously on sinusoidal way due to tidal influenced regime of channel mouths (Figure 3-27).

3.7 Hydrological and geochemical studies in the Lena River Delta

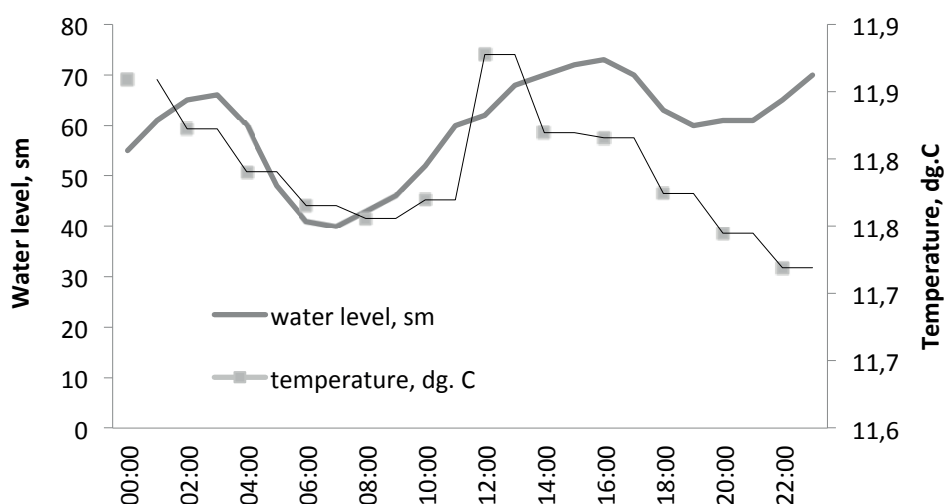


Figure 3-27 Water level of Oleneskaya channel (mouth) on daily station August 20, 2012.

Water discharges

Measurements were organized on 12 profiles, including big channels around the delta head: Main channel, Trophimovskaya, Bykovskaya, Oleneskaya, Tumaskaya and Bulkurskaya channels; and along the Oleneskaya channel and on small channels: Krekhskaya, Arynskaya, Angardam (Table 3-6). The values of water discharges will be adapted afterwards using binding to one date and to one water level.

Table 3-6 Water discharges and profile areas of the Lena River Delta channels, August 2012. * High probability of errors during measurements

№	Channel name	Date	Channel profile area, m ³	Water discharge, m ³ /sec	Comments
1	Main channel	14.08.	31,563	24,865	Near Tit-Ary isl.
2	Bykovskaya	15.08.	6,107*	2,948*	Standart water gauging line (SWGL)
3	Trophimovskaya	24.08.	23,067	14,839	SWGL
4	Main channel	29.08.	33,993	25,380	SWGL, 4.7 km from Stolb isl.
5	Oleneskaya	25.08.	3,041	1,439	SWGL
6	Tumatskaya	26.08.	4,316	610	SWGL
7	Oleneskaya	23.08.	2,500	1,609	Near Gusinka riv.
8	Angardam	23.08.	5,026	726	In 2 km from Oleneskaya ch.

3.7 Hydrological and geochemical studies in the Lena River Delta

9	Oleneskaya	23.08.	1917	460	Near Nagym vil.
10	Krestyakhskaya	22.08	3,086	849	Near Oleneskaya ch.
11	Oleneskaya	20.08.	Figure 3-28	Figure 3-28	Daily station near Petrushka isl.
12	Bulkurskaya	25.08.	2,474.1	0	2 km downstream from Oleneskaya channel

Water discharge and water velocity rates during „daily-station“ (20.08.2012) in the mouth of Oleneskaya channel is demonstrated on Figure 3-28. The graph demonstrates that water discharges strongly depends on water velocity. The reason is inhibition of river water masses by sea backwaters. However inflow of salt water at the site was not observed, that can be seen in the values of conductivity whose were 54-58 ppm during all measured period.

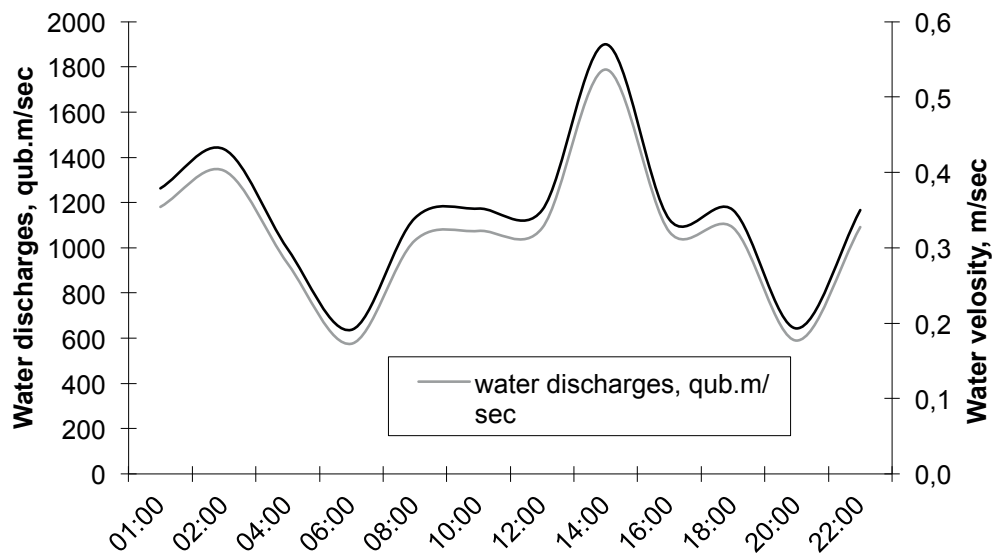


Figure 3-28 Water discharge and water velocity of Oleneskaya channel (mouth) during “daily-station”, August 20, 2012.

3.7.3.2 Geochemistry

Water, SPM and bottom sediment samples were taken from all the big and some small channels and from 22 lakes of the Delta. Some data measured by portable sensors in a field are presented in Table 3-7.

3.7 Hydrological and geochemical studies in the Lena River Delta

Table 3-7 Table of samples, August 2012.

No	Water object	Coordinates	Date	Water (planned analysis)	SPM (sample type)	Bottom sediment	Conductivity, ppm	Water temp, °C
1	Main channel (Tit-Ary isl)	72°0'9.19" 127°4'20.20"	14.08.	Main + trace elements, nutrients	Paper filter, GF/F, PC	-	-	14.5
2	Bykovskaya	72°24'28,0" 126°54'47,9"	15.08.	Main + trace elements, nutrients	Paper filter, GF/F, PC	-	-	-
3	Trophimovskaya	72°25'36.96" 126°37'58.7"	24.08.	Main + trace elements, nutrients, isotopes	Paper filter, GF/F, PC	Upper layer	-	-
4	Main channel	72°22'13.98" 126°43'48.3"	29.08.	Main + trace elements, nutrients, isotopes	Paper filter, GF/F, PC	-	-	-
5	Olenekskaya	72°17'46,1" 126°05'40,0"	25.08.	Main + trace elements, nutrients, isotopes	Paper filter, GF/F, PC	Upper layer	-	-
6	Tumatskaya	72°25'06,4" 126°27'23,6"	26.08.	Main + trace elements, nutrients, isotopes	Paper filter, GF/F, PC	Upper layer	-	-
7	Olenekskaya	72°30'20,9" 125°17'10,4"	23.08.	Main + trace elements, nutrients, isotopes	Paper filter, GF/F, PC	Upper layer	-	-
8	Angardam	72°45'25,4" 123°38'54,1"	23.08.	Main + trace elements, nutrients, isotopes	Paper filter, GF/F, PC	Upper layer	-	-
9	Olenekskaya	72°46'35,3" 123°42'18,0"	23.08.	Main + trace elements, nutrients, isotopes	Paper filter, GF/F, PC	-	53	-
10	Krestyakhskaya	72°51'14,6" 123°25'37,6"	22.08.	Main + trace elements, nutrients, isotopes	Paper filter, GF/F, PC	Upper layer	56	-
11	Olenekskaya	73°00'00,0" 122°30'25,0"	20.08.	Main + trace elements, nutrients, isotopes	Paper filter, GF/F, PC	Upper layer	54-58	11.7
12	Bulkurskaya	72°13'57,7" 126°06'18,5"	07.08.	Main + trace elements, nutrients, isotopes	Paper filter, GF/F, PC	Upper layer	62	12.2
13	Lake 1 (Samoylov isl.)	72°23'13.32" 126°28'55.73"	04.08., 27.08.	Main + trace elements, nutrients	-	-	110	-
14	Lake 2 (Samoylov isl.)	72°22'11.9" 126°31'00.8"	4.08., 27.08.	Main + trace elements, nutrients	-	-	63 49	-

3.7 Hydrological and geochemical studies in the Lena River Delta

15	Lake 3 (Samoylov isl.)	72°22'05.4" 126°29'14.4"	4.08., 27.08.	Main + trace elements, nutrients	-	-	39 40	-
16	Lake 4 (Samoylov isl.)	72°22'05.3" 126°29'57.3"	4.08., 27.08.	Main + trace elements, nutrients	-	-	48 38	-
17	Lake 5 (Samoylov isl.)	72°22'06.0" 126°30'19.0"	4.08., 27.08.	Main + trace elements, nutrients	-	-	53 42	-
18	Lake 6 (Samoylov isl.)	72°22'07.9" 126°29'36.1"	4.08., 27.08.	Main + trace elements, nutrients	-	-	48 49	-
19	Lake 7 (Samoylov isl.)	72°22'23.5" 126°29'10.0"	4.08., 27.08.	Main + trace elements, nutrients	-	-	39	-
20	Lake 8 (Samoylov isl.)	72°23'03.3" 126°30'01.8"	4.08., 27.08.	Main + trace elements, nutrients	-	-	35	-
21	Lake 9 (Samoylov isl.)	72°22'38.1" 126°30'03.1"	4.08., 27.08.	Main + trace elements, nutrients	-	-	28 28	-
22	Lake 10 (Samoylov isl.)	72°23'04.2" 126°29'33.8"	4.08., 27.08.	Main + trace elements, nutrients	-	-	28	-
23	Lake 11 (Samoylov isl.)	72°22'27.2" 126°31'09.9"	4.08., 27.08.	Main + trace elements, nutrients	-	-	24 25	-
24	Lake 12 (Samoylov isl.)	72°22'28.6" 126°30'48.1"	4.08., 27.08.	Main + trace elements, nutrients	-	-	28 20	-
25	Lake 13 (Petrushka isl.)	72°53'24.60" 122°43'45.90"	20.08.	Main + trace elements, nutrients	-	-	-	-
26	Lake 14 (Matvey isl.)	72°26'45.96" 126°25'08.16"	28.08.	Main + trace elements, nutrients	-	-	33	-
27	Lake 15 (Matvey isl.)	72°26'35.15" 126°27'50.07"	28.08.	Main + trace elements, nutrients	-	Upper layer	107	-
28	Lake 16 (Belir isl.)	72°17'58.98" 126°27'56.05"	13.08.	Main + trace elements, nutrients	-	A core	46	13.2
29	Lake 17 (Belir isl.)	72°17'54.47" 126°27'04.14"	13.08.	Main + trace elements, nutrients	-	A core	48	12.4
30	Small channel near Belir isl.	72°18'15.52" 126°27'16.50"	13.08.	Main + trace elements, nutrients	-	-	53	-
31	Stream 1 (Kurungnakh)	72°17.601' 126°04.258'	08.08.	Main + trace elements, nutrients, isotopes	-	Upper layer	285	-
32	Stream 2 (Kurungnakh)	72°18'8.75" 126°15'34.68"	08.08.	Main + trace elements, nutrients, isotopes	-	Upper layer	227	-
33	Small channel near Bulkurskaya	72°11'48.17" 126°03'15.36"	07.08.	Main + trace elements, nutrients	-	-	80	10.6

3.7 Hydrological and geochemical studies in the Lena River Delta

	ch.							
34	Stream 3	72°22'45.08" 126°24'04.16"	28.08.	Main + trace elements, nutrients	-	-	162	-
35	Stream 4	72°18'02.74" 126°34'38.97"	29.08.	Main + trace elements, nutrients	-	-	-	-
36	Lake 18	72°18'39.55" 126°35'13.58"	29.08.	Main + trace elements, nutrients	-	-	-	-
37	Lake 19	72°17'54.47" 126°35'11.10"	29.08.	Main + trace elements, nutrients	-	-	-	-
38	Lake 20	72°16'06.91" 126°27'48.63"	29.08.	Main + trace elements, nutrients	-	-	-	-
39	Lake 21	72°11'33.81" 126°01'55.23"	07.08.	Main + trace elements, nutrients	-	-	16	13
40	Lake 22	72°11'31.92" 126°02'58.27"	07.08.	Main + trace elements, nutrients	-	-	53	13
41	Oxbow lake on Tit-Ary isl.	71°59'58.50" 127°00'11.77"	14.08.	Main + trace elements, nutrients	-	-	-	-
42	Thermokarst lake on Tit-Ary	71°59'37.87" 127°00'37.72"	14.08.	Main + trace elements, nutrients	-	-	-	-

3.7.3.3 Carbon cycle components (Changes of the components of the carbon cycle on the watershed of the Fish Lake)

The depth of the active layer was between 20 and 60 cm: 20-30 cm on the rim of polygons and 30-60 cm in the center of polygons and near the lake. During the month when the measurements were made, the depth increased to 10-15%.

Soil moisture values were 28-72%. The wettest - 60-72% part was in the center of polygons and in whole polygons located in the lower part of the catchment near the lake.

The mean concentration of DOC for the catchment was 25 mg/l. DOC in pore water was from 8 to 51 mg/l depending on location. The highest DOC values were obtained in the dry center of polygons, which can be explained by the accumulation of DOC in those spots. DOC concentration in the water objects (polygonal ponds, Fish Lake) and in delta channels was 5-7 mg/l. Thaw depth, soil moisture of the active layer and the values of DOC concentration in pore water allow calculating the income of DOC to the lake during one month. Considering the water runoff from the catchment of Fish Lake is 32 m³ per day (Ogorodnikova, 2011), the DOC runoff to the lake is about 800 g per day (Bobrova et al., 2013)

The drainage area of the Fish Lake is 1.52 sq.km, thus preliminary flow rate for the Lena River delta ($800/1.52 = 493 \text{ g/km}^2 \cdot \text{day}$) could be evaluated. The values of the permanganate oxidation was 15-22 mg/l for the delta channels and the lakes on Samoylov Island (including Fish Lake) and 45-48 mg/l for the pore water on Fish Lake catchment

that is higher than the values for the Lena River (5-20 mg/l for August) published in Hydrological Yearbook (1960-1975).

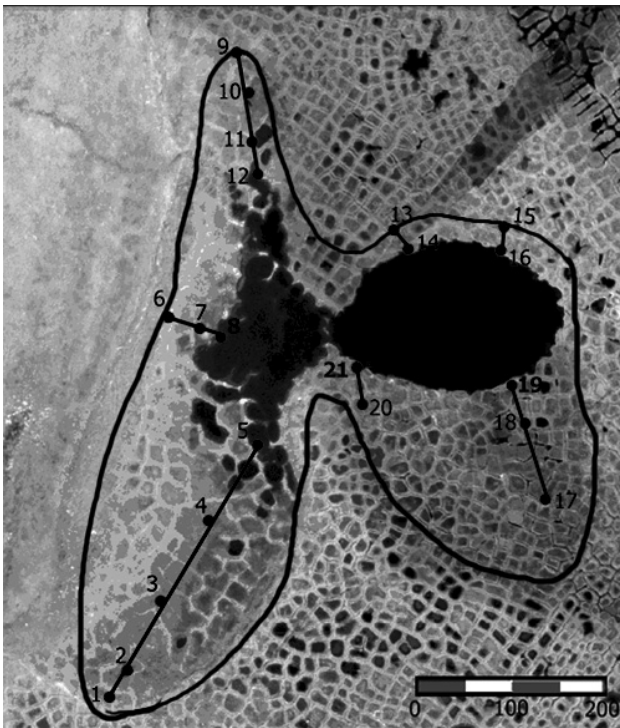


Figure 3-29 Sampling points and transects on the watershed of the Fish Lake

During August 2012 there were very small changes in the water level in the Fish Lake (Figure 3-30). The level was decreasing slowly and total decrease was 3.5 cm. These measurements could be used for the evaluation of water and carbon balance in the Fish Lake and on its drainage area as they reflect the changes of water volume in the lake during the period.

3.7 Hydrological and geochemical studies in the Lena River Delta

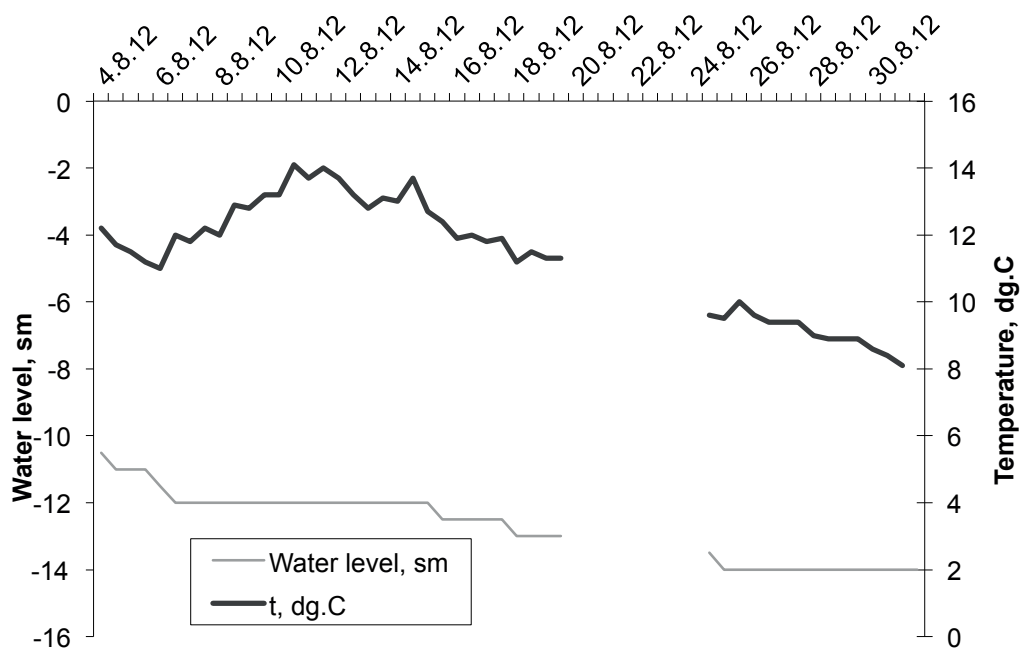


Figure 3-30 Changes of the water level and temperature in Fish Lake

References

Bobrova, O., Fedorova, I., Chetverova, A., Runkle, B., Potapova, T. (2013) Input of Dissolved Organic Carbon for Typical Lakes in Tundra Based on Field Data of the Expedition Lena – 2012. Proceedings. 19th International Northern Research Basins Symposium and Workshop, Southcentral Alaska, USA – August 11–17, 2013.

Fedorova, I., Chetverova, A., Bolshiyarov, D., Makarov, A., Boike, J., Heim, B., Morgenstern, A., Overduin, P., Wegner, C., Kashina, V., Eulenburg, A., Dobrotina, E., Sidorina, I. (2013) Lena Delta hydrology and geochemistry, Biogeosciences Discussion 10, 20179-20237, doi:10.5194/bgd-10-20179-2013.

Hydrological Yearbook (1960-1975) Volume 8, Issue 0-7. Basins of the Laptev, East Siberian and Chukchotskoye Seas, St.Petersburg, Gidrometizdat.

Ogorodnikova N.N. (2012) Calculating the depth of seasonal thawing of permafrost in the delta of the Lena river (for example Samoilovsky Island). Graduate work, St. Petersburg State University.

3.8 BIOLOGICAL INVESTIGATIONS IN SUMMER 2012

Ekaterina Abramova and Grigoriy Soloviev

Fieldwork period: July 11 to August 31, 2012; Samoylov Island, Tit-Ary Island

3.8.1 Objectives

Different lakes and ponds are a typical feature of northern ecosystems of Eastern Siberia. Undoubtedly, the numerous lakes play a significant role in the delta ecosystem provided crucial feeding conditions for the different aquatic organisms and enormous breeding populations of water birds. It is considered that these high Arctic water pools are commonly inhabited by only a few species of rotifers, cladocerans and copepods which narrowly specialized to the harsh environment (Morison et al., 2000).

During the last decade (2000-2011) 127 zooplankton taxa from Rotifera and Arthropoda phylum were determined in the oxbow lakes, thermokarst lakes, small thermokarst ponds (polygons) and flood-land water bodies on Samoylov Island, south area of the Lena Delta. The number of zooplankton collections and the amount of data considerably increased during last two decades in the Lena Delta in comparison to those of other areas of similar latitude in Russia. As a result, several crustacean species were recorded for the Lena Delta region in the first time; two calanoid copepods among them: *Eurytemora foveola* and *Eurytemora arctica* are the new species for Eurasian pelagic fauna. The data obtained demonstrate rather high species diversity, abundance and biomass of zooplankton in the tundra waters despite of the short ice-free season, low temperatures, low nutrient and food levels

The present investigation is a continuation of monitoring studies of the different freshwater ecosystems in the Lena Delta and contribution to the pelagic fauna investigations of the northern Siberia areas. The main goals of our research in summer 2012 were:

1. The detailed analysis of the modern species composition and distribution of zooplankton in the southern part of the Delta;
2. Zoogeographical and taxonomical study of the rare pelagic crustaceans inhabiting various reservoirs on Samoylov Island;
3. The observation of the seasonal/interannual variations in the population structure, abundance and biomass of the common zooplankton species in the small thermokarst ponds (polygons) which are the most numerous ponds in the area of our investigation;
4. The estimation of the river water influence upon lakes pelagic fauna formation in the Lena Delta.

3.8.2 Methods

75 quantitative zooplankton samples were collected from eleven different water bodies during summer expedition in July-August 2012 on Samoylov Island and four samples from oxbow lakes were obtained on Tit-Ary Island.

Zooplankton collections from the all big thermokarst and oxbow (Banja I-III) lakes were made by dipping small plankton net (diameter 20 and 25 cm, mesh size 100 μ) in the deepest part of the lakes from the rubber boat or by tossing net attached to a line out into a lake and then pulling the net slowly to the shore. Both vertical and horizontal samplings were done. The zooplankton from four polygons were collected by filtering 50 or 100 liters of water through plankton net (20 cm diameter, mesh size 100 and 200 μ) or by vertical drawing of net from the bottom to the surface in the middle part of polygon. Samples were preserved with 4% neutral formalin or 70% alcohol. Period of sampling have been changed from 3 days in the polygons to 10 days from another lakes.

Zooplankton samples processing and detailed taxonomic investigations were carried out using binoculars Olympus SZX9 and BX60 with Analyzing system and drawing attachment U-DA. The whole sample or its part was studied in the Bogorov's camera and the abundance of organisms was calculated. We determined species, sex and moulting stages. Naupliar stages of Cyclopida and Calanoida were counted separately, but without species identification.

For the estimation of Chl" a" concentration one liter of water was taken from the surface, filtered through glass microfibre filters (GFF) and frozen at -20°C for preservation. Chl" a" samples were analyzed on SPECORD 200 spectrometer and TD-700 fluorimeter in the Russian-German Otto Schmidt Laboratory for polar and marine research (OSL, AARI, St. Petersburg, Russia). In addition to the plankton sampling, pH and water temperature measurements were made.

3.8.3 Preliminary results

There are well-manifested differences in zooplankton community structure of different water basins depending on hydrological and hydrochemical regime.

The zooplankton species composition was clearly dominated by Rotifera and Copepoda in the big thermokarst lakes situated on the first terrace of Samoylov Island. Eurytopic *Keratella quadrata*, *Keratella cochlearis* and *Kellicottia longispina* were numerous among rotifers during period of our investigation in summer 2012. Several copepods: *Acanthocyclops vernalis* and *Cyclops abissorum* were abundant in July and *Eudiaptomus graciloides* with *Heterocope borealis* dominated among copepods in August in zooplankton community.

Different from the thermokarst lakes species diversity was recognized in the oxbow Banja lakes, where Rotifera constituted up to more than 60% of the total species richness. The representatives from genus: *Polyarthra*, *Keratella*, *Synchaeta*, *Filinia*, *Trichocerca*, *Euchlanis* and *Asplanchna* prevailed numerically in pelagic fauna of these lakes. In June *Cyclops kolensis*, *C. abysorum*, *Diacyclops bicuspidatus* and different juvenile stages of 2-3 Calanoida species were very abundant. In August *Keratella quadrata* dominated

quantitatively among Rotifera with abundance reached up 12.5 thousands ind./m³ and three calanoid copepods: *Limnocalanus johanseni*, *Eurytemora foveola* and *E. bilobata* with total abundance around 10 thousands ind./m³.

According to the species diversity Rotatoria and Copepoda constitute the dominant groups in the zooplankton associations of polygons in our material. However in term of abundance and biomass the Copepoda and Cladocera apparently predominate among other zooplankton taxa in the small thermokarst ponds. Despite high species diversity, Rotifera usually represent by singular individuals and do not contribute significantly to plankton societies of polygons.

The analysis of zooplankton total abundance and relative abundance of common species revealed a large contrast in the development of processes in the two neighboring polygons in the second half of August. In one of the polygons the average zooplankton abundance consisted of 11 thousands ind./m³. Adult stages of *Leptodiptomus angustilobus* dominated in that time (Figure 3-31). The absolute abundance maximums (44.5 thousands ind./m³) was fixed at 16th of August in this polygon.

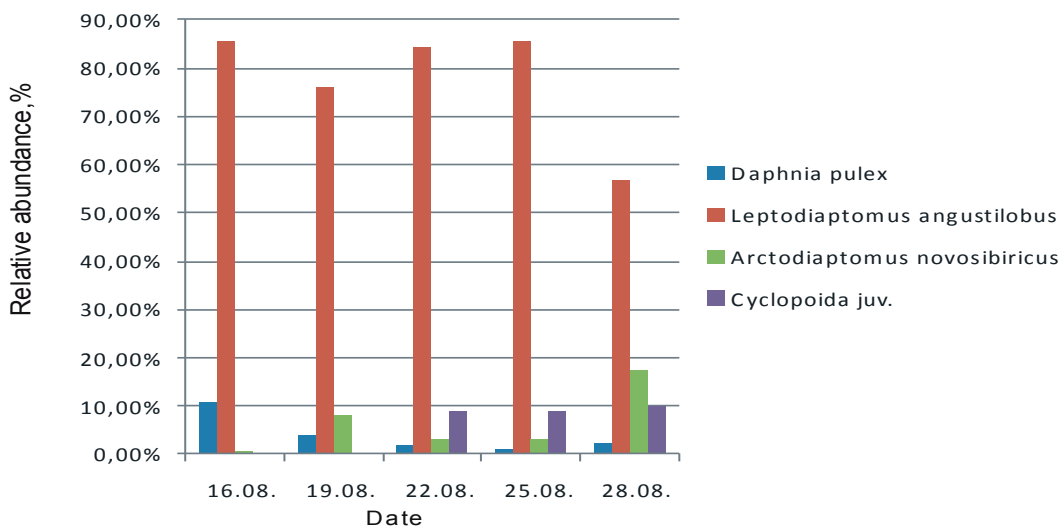


Figure 3-31 The relative abundance of the common zooplankton species in the polygon I.

Different situation was observed in the second polygon where highest zooplankton abundance was less than 100 ind./m³ and average abundance consisted of 70 ind./m³. Juvenile stages of *Cyclopoida* prevailed numerically in this water body in the second half of August.

We found very low chlorophyll "a" concentrations in the polygons indicating a low level of primary production in summer 2012. Average chlorophyll "a" concentration in July-August of 2012 in the polygons was 0.5 mg/ m³ with maximum in the middle July 1.04 mg, which is more than four times less than in oxbow lakes (4.4 mg/ m³).

3.8 Biological investigations in summer 2012

References

Morison, N.T., Aagaard, K., Steele, M. (2000) Recent environmental changes in the Arctic: review. *Arctic* 53, 359-371.

3.9 BOTANICAL STUDIES IN POLYGONAL STRUCTURES

Romy Zibulski

Fieldwork period: July 2012; Samoylov Island

3.9.1 Introduction

It is known that the recent warming is abetted by the disposal of greenhouse gases like methane, carbon dioxide or water vapour since the age of industry. The resulting continuous global warming and changes in the length of seasons favours i.e. thawing of permafrost and the decomposition of frozen biomass due to subsequently microbial activity (e.g. Koven et al., 2011). The loss of decomposition products like carbon dioxide or methane gives a positive feedback to global warming. For a better understanding of these cycles a distinct knowledge about biomass composition and the processes within these cycles are crucial. Of particular importance to carbon dioxide emissions are small ponds (Abnizova et al., 2012) which are a typical component of the arctic polygonal tundra (Minke et al., 2007). Often, these small ponds or water bodies are the inner part of low-centred polygons and show an advanced stage of polygonal succession (Meyer, 2003). These polygonal structures contain more than 15% of the world's soil carbon (Post et al., 1982) by only covering 3% of the terrestrial arctic area. Thus the aspect of increasing soil thawing, decomposition of soil carbon and subsequent emission to the atmosphere is important. Microbial organisms play significant roles in this system. Especially methanotrophic bacteria show considerable activity in polygonal ponds. They use the ascending methane from the thawing ground and metabolize it to carbon dioxide. The symbiotic relationship with mosses (Moss-associated methane oxidation – MAMO) buffers the methane and carbon emissions (Liebner et al., 2011), because mosses incorporate the metabolized CO₂ partially to build up their own biomass. Yet, the uptake depends on the moss species (70% of CO₂ assimilation capacity for *Scorpidium scorpioides* (Liebner et al., 2011), only 15% for *Sphagnum cuspidatum* (Raghoebarsing et al., 2005)). Thus it seems to be important which vascular plants and cryptogame species occur in polygons, respectively. Further the individual polygon divisions of dry to wet terrestrial or freshwater sub-biotopes are mainly formed by abiotic parameters from which the obvious botanical inventory is dependent. They gather the wide spectrum of tundra habitats.

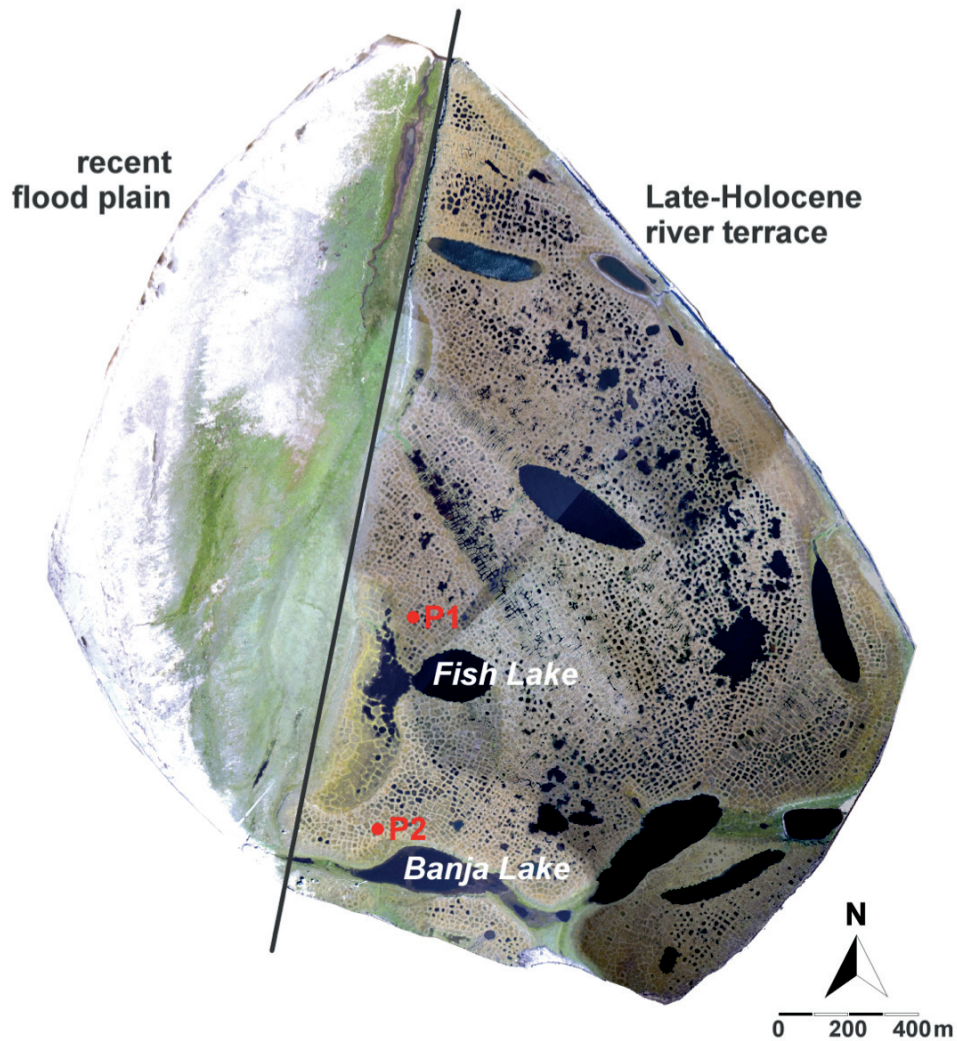


Figure 3-32 Aerial Image of Samoylov Island (Boike et al., 2012). Samoylov is divided in the recent flood plain in the East and a Late-Holocene river Terrace in the western part. The two investigated polygons are located on the Late-Holocene river terrace nearby the Fish Lake (P1) and the Banja Lake (P2).

3.9.2 Study sites – Polygons

The Island Samoylov in the Lena Delta is well-suited for investigations in polygon mires as about 12 % of the Island are covered by open-water polygons or small lakes (Sachs et al., 2008). But there is a geomorphical dichotomy on the Island (Figure 3-32). It is divided into the sandy flood plain on the Westside without polygonal mires and the eastern part with different types of polygons and thermokarst lakes on peaty sediments at the higher elevated Late-Holocene river terrace (Boike et al., 2013; Kutzbach, 2006). High and low-centred polygons occur in the North of the eastern part; towards the South typical low-centred polygons with different water levels become dominate. Derived from development stages by Meyer (2003) the low-centred polygons could be classified into four types (Figure 3-33) without relating to successional stages: with 1.) a deep intrapolygonal pond (water level of 0.3 to 1.3 m depth), 2.) a shallow intrapolygonal pond (max. 0.3 m water depth). The two other types which do not have a water-filled centre are: 3.) the boggy low

centred polygon (with only high moisture in the centre) and directly on the southern coast 4.) the leaked low-centred polygons which erode along with the coastline. Here, the eroded type provides an insight into the development of polygons on Samoylov. They have a peat body nearly 8 to 9 m thick, with a sandy, washed out layer at 3 m depth, which is only few decametre in size. But these interruptions are distributed over the whole island in different depths, thus it is rather a local flooding depending from the surface properties of the Island, than a regional event like a prolonged flood (personal communication with H. Meyer, AWI). It has not yet been clarified, whether the development of Island polygons started at the same time and polygon types are at different stages due to local disturbances or the development started at different times and these four types are caused, for instance, by local soil properties, terrain, time of origin or the position on the Island.

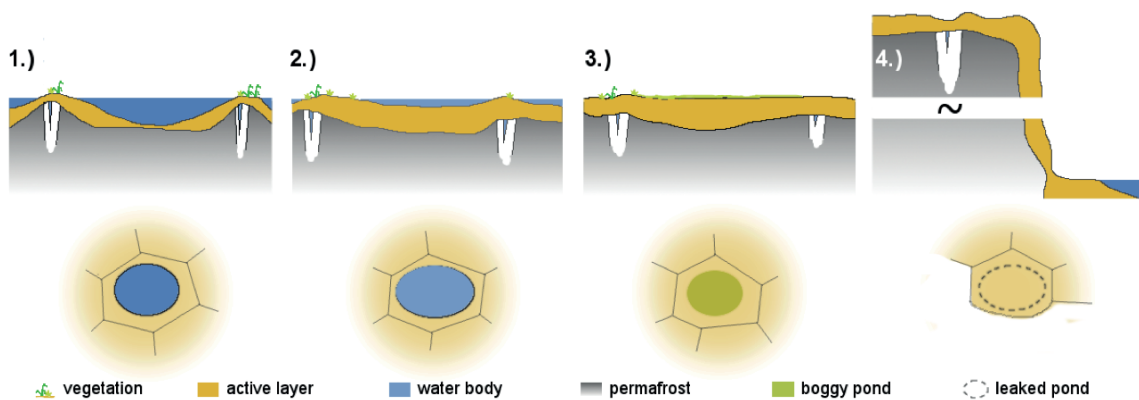


Figure 3-33 The four types of low-centred-polygons on Samoylov Island. Two types with a water-filled, centred pond, differentiated in a deep (1) or a shallow type (2) and furthermore two types which are only boggy in the centre with a thick moss mat (3) or which have a leaked centre as a result of coast erosion (4).

On this expedition we were concentrating on low-centred polygons with intrapolygonal ponds of the two different water level types. The deep water type (P1, Figure 3-34) was found in the North of Fish Lake (Figure 3-32). The maximum water depth was reached 0.68 m in the middle of the pond. The ground was moss-covered and the water surface was free of any vegetation. At the transition between the intrapolygonal pond and the elevated sites the cover of vascular plants started and proceeded up to the dry rim. The second low-centred polygon (P2, Figure 3-35) nearby Banja Lake had a shallow intrapolygonal pond (size: metre by metre) with a maximum water depth of 0.19 m. The surface of the water body was always covered by vascular plants or mosses.



Figure 3-34 The low-centred polygon P1 in the North of the Fish Lake has a deep intrapolygonal pond without a thawed layer below the central pond, whereas the rim has a thaw layer which was up to 10 cm thick. The thickest thaw layer was measured in the transition zone between the pond and the rim sites (~50 cm). The pond was vegetated by submerged living moss species like *Scorpidium scorpioides* and *Calliergon giganteum*. The rim was dominated by vascular plants with a thick moss layer.

3.9.3 Investigations in low-centred polygons

Polygons were overlaid by a grid from rim to the opposite rim and the same for the perpendicular. We used tapelines and cords to form the grid with precise metre by metre plots for our investigations. Thereby the following dimensions resulted: P1 with 17 by 19 m and P2 with 19 by 27 m.

Before estimating the vegetation pattern plot by plot, the first abiotic parameters like surface elevation, water level and the current thaw depth were surveyed with a water level gauge from a reference point and a measuring rod. This procedure was not necessary for P2, because the polygon is annually studied for these parameters and a 12 year long record already exists. Subsequently we start to estimate the coverage for vascular plants and cryptogams after the Braun-Blanquet scale (1964) modified by Reichelt and Wilmanns (1973). We studied P1 completely, whereas in view of the short time remaining, it was not possible to survey every plot in P2. Thus we utilised a chess pattern for the section from row 6 to 27 (investigated plots at P2: 301 instead of 513). We define one representative transect in our polygons in order to take sediment samples in form of a monolith (length depends on the current thaw depth) from the rim, the transition and the pond (with exception of the P1 pond site, as the permafrost table was directly situated

below the water body). These samples were taken with a saw, wrapped with cling film and placed in our cold store until the transport to Germany. Plants for the herbarium and surface water samples from the pond were taken for further analyses.

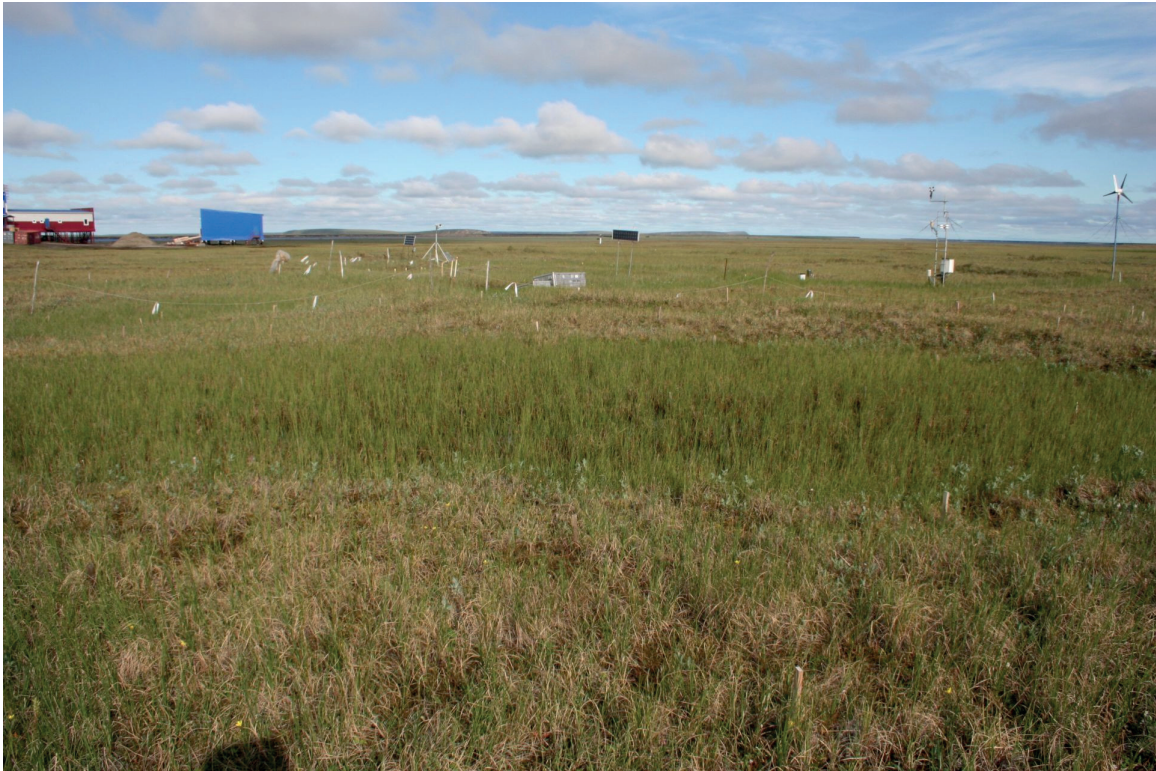


Figure 3-35 The shallow low-centred polygon P2 in the North of the Banja Lake. It does not have an open water surface. Vascular plants and bryophytes covered the pond completely. The thaw layer was similar over the complete polygon (~45 cm) with exception of higher elevated rim sites.

3.9.4 Outlook

The sediment samples will be used for analysis and measurements such as grain size, CNS, stable isotopes of carbon and nitrogen, microfossils (vascular plants/bryophytes), pollen grain or diatom analysis. Additionally to the sedimentological parameters, we want to measure the pH, HCO_3^- , anions, cations, and TOC contents of the surface water samples.

References

- Abnizova, A., Siemens, J., Lager, M., Boike, J. (2012) Small ponds with major impact: The relevance of ponds and lakes in permafrost landscapes to carbon dioxide emissions. *Global Biogeochemical Cycles* 26, 1-9.
- Boike, J., Grüber, M., Langer, M., Piel, K., Scheritz, M. (2012) Orthomosaic of Samoylov Island, Lena Delta, Siberia. Alfred Wegener Institute for Polar and Marine Research - Research Unit Potsdam, PANGAEA.

3.9 Botanical studies in polygonal structures

Boike, J., Kattenstroth, B., Abramova, K., Bornemann, N., Chetverova, A., Fedorova, I., Fröb, K., Grigoriev, M., Grüber, M., Kutzbach, L., Langer, M., Minke, M., Muster, S., Piel, K., Pfeiffer, E.-M., Stoof, G., Westermann, S., Wischnewski, K., Wille, C., Hubberten, H.-W. (2013) Baseline characteristics of climate, permafrost and land cover from a new permafrost observatory in the Lena River Delta, Siberia (1998–2011). *Biogeosciences* 10, 2105–2128.

Braun-Blanquet, J. (1964) *Pflanzensoziologie: Grundzüge der Vegetationskunde*. Springer, Wien.

Koven, C.D., Ringeval, B., Friedlingstein, P., Ciais, P., Cadule, P., Khvorostyanov, D., Krinner, G., Tarnocai, C. (2011) Permafrost carbon-climate feedbacks accelerate global warming. *Proceedings of the National Academy of Sciences* 108, 14769–14774.

Kutzbach, L., (2006) The exchange of energy, water and carbon dioxide between wet arctic tundra and the atmosphere at the Lena River Delta, Northern Siberia = Der Austausch von Energie, Wasser und Kohlendioxid zwischen arktischer Feuchtgebiets-Trundra und der Atmosphäre im nordsibirischen Lena Delta. *Berichte Zur Polar- und Meeresforschung/Reports on Polar and Marine Research* 541.

Liebner, S., Zeyer, J., Wagner, D., Schubert, C., Pfeiffer, E.-M., Knoblauch, C. (2011) Methane oxidation associated with submerged brown mosses reduces methane emissions from Siberian polygonal tundra. *Journal of Ecology* 99, 914–922.

Meyer, H., 2003. Studies on recent cryogenesis, in: *Russian-German Cooperation System Laptev Sea: The Expedition LENA 2002, Berichte zur Polarforschung und Meeresforschung/Reports on Polar and Marine Research* 466, 29–48.

Minke, M., Donner, N., Karpov, N.S., De Klerk, P., Joosten, H. (2007) Distribution, diversity, development and dynamics of polygon mires: examples from Northeast Yakutia (Siberia). *Peatlands International* 1/2007, 36-40.

Post, W.M., Emanuel, W.R., Zinke, P.J., Stangenberger, A.G. (1982) Soil carbon pools and world life zones. *Nature* 298, 156–159.

Raghoebarsing, A.A., Smolders, A.J.P., Schmid, M.C., Rijpstra, W.I.C., Wolters-Arts, M., Derksen, J., Jetten, M.S.M., Schouten, S., Sinninghe Damsté, J.S., Lamers, L.P.M., Roelofs, J.G.M., Op den Camp, H.J.M., Strous, M. (2005) Methanotrophic symbionts provide carbon for photosynthesis in peat bogs. *Nature* 436, 1153–1156.

Reichert, G., Wilmanns, O. (1973). *Vegetationsgeographie, Das Geographische Seminar*. Georg Westermann Verlag, Braunschweig.

Sachs, T., Wille, C., Boike, J., Kutzbach, L. (2008) Environmental controls on ecosystem-scale CH₄ emission from polygonal tundra in the Lena River Delta, Siberia. *Journal of Geophysical Research – Biogeosciences* 113, G00A03.

3.10 SPORE-POLLEN STUDIES

Daria Titova

Fieldwork period: July 04 to July 29, 2012; Samoylov Island, Kurungnakh Island, Stolb Island, and Amerika-Khaya Island

3.10.1 Objectives

Main objectives during this expedition for me were:

- The description of modern vegetation.
- The creation of a herbarium.
- Taking photographs of plants for the Lena River Delta region.
- The selection of air samples.

3.10.2 Methods

- Pollen and plants sampling
- Working with the pollen trap

3.10.3 Preliminary results

During this work 8 plots (1 m x 1 m) were described, which were located in different parts of Samoylov Island, Kurungnakh Island, Stolb Island and Amerika-Khaya Island. Surface samples were selected from these plots to study the sub-fossil spore-pollen spectra. The corresponding modern vegetation was described and photographed (n = 1,400).

To assess the quantitative and qualitative composition of the pollen rain in the Lena River Delta region, a pollen trap was placed at different relief levels. During eight days samples of the air were taken. The tubes were changed every twelve hours, hence, as a result, 16 samples of air were obtained.

3.11 GROUND ICE STUDIES ON SAMOYLOV ISLAND

Thomas Opel

Fieldwork period: August 28 to August 31, 2012; Samoylov Island

3.11.1 Background, objectives and methods

The ice-rich permafrost deposits of Northeast Siberia are characterized by different types of ground ice. Among them, ice wedges are the most abundant type and form by the periodic repetition of wintertime frost cracking and subsequent crack-filling by snowmelt in spring. Consequently, the oxygen and hydrogen isotopic composition of the wedge-forming ice veins can be related to winter precipitation and, therefore, to winter temperatures during the time of their formation. Organic remains of ice wedges can be dated by the ^{14}C method. In the last years progress has been made in ice-wedge-based paleoclimate reconstruction and it has been shown that ice wedges have the potential to provide up to centennial-scale climate information for the Late Glacial as well as Late Holocene periods in Alaska (Barrow) and Northeast Siberia (Dmitry Laptev Strait), respectively (Meyer et al., 2010; Opel et al., 2011).

The main objectives of the fieldwork conducted on Samoylov Island were:

1. to collect new ice-wedge samples for a) the reconstruction of the regional Mid to Late Holocene climate history and b) to provide sample material for new analysis approaches such as physical properties of wedge ice (e.g. structures, crystallography, air bubbles), analysis of air bubbles, ^{14}C dating of dissolved organic carbon or of air bubbles, analysis of cosmogenic nuclides.
2. To study and sample other types of ground ice (e.g. texture ice or massive ice) for the reconstruction of ground ice genesis.

After surveying the coastal bluffs of Samoylov Island, two outcrops were selected to be studied. After describing, photographing and sketching ice wedges and massive ice were sampled by chain saw. Texture ice was sampled by hammer and axe. All samples were transported in frozen state to Germany for further subsampling and analysis.

3.11.2 Ice wedge LD12-IW1 (N 72°22'11.2", E 126°31'6.7")

Ice wedge LD12-IW 1 belongs to the Holocene terrace of the Lena River and was sampled at the southeast coast of Samoylov Island. It was cut perpendicular to its long axis (along its growth direction) and its exposed vertical extension was 2.6 m (1.0-3.6 m b.s.) and up to 2 m wide (Figure 3-36). The lowermost part was buried. The ice wedge was characterized by marked shoulders in two height levels (1.5 m b.s. and 2.5 m b.s.) and a distinct evidence for ice wedge rejuvenation. The recent "ice wedge head" was overtopping the older part by about 0.5 m.

The surrounding sediments consisted of grey-yellowish silty sand at the bottom (below 3.2 m b.s.) covered by a thick organic-rich unit consisting of peaty silt and silty peat layers,

characterized by distinct amounts of sand (3.2-0 m b.s.) and different cryostructures. The active layer thickness was about 0.7 m.

The wedge ice was milky-white and very rich in elongated, vertically oriented air bubbles (up to 1 mm in diameter, up to 1 cm long). Sediment and organic content was low to medium. Single ice veins were very good visible and 2 mm to 2 cm wide. Also dilatation cracks from horizontal to vertical directions were observed.

Samples were taken by chain saw. Six blocks were cut in three height levels: 3.3 m b.s. (block 1), 2.6 m b.s. (blocks 2, 3) and 2 m b.s. (blocks 4 -6).

About 2 m beside the ice wedge also a vertical profile of texture ice (ice layers, pore ice) was sampled with 17 samples in a resolution of 5-20 cm from 3.6 to 0.8 m b.s.



Figure 3-36 Ice wedge LD12-IW1.

3.11.3 Massive ice LD12-MI and LD12-IW2 (N 72° 22' 6.6", E 126° 30' 55.6")

Massive ice LD12-MI was sampled at the river cliff of the southeast coast of Samoylov island. It was about 3.5 m wide and about 1 m thick with a hill slope of about 45° (Figure 3-37). Below the massive ice, separated by an ice and organic-rich sandy-silt layer with an

3.11 Ground ice studies on Samoylov Island

irregular reticulate cryostructure the top of an older truncated ice wedge was exposed. Deeper parts of massive ice and ice wedge were buried.

The massive ice was covered by partly by yellowish sand and by brown sandy-silty peat (about 70 cm thick). The active layer depth was 50 cm.

The massive ice could be divided roughly in three parts: 1. milky-white bubble-rich ice at the top and left side, 2. relative clear to clear ice with only little bubbles below and at the right side (partly with vertically elongated bubbles up to several cm long and diameters of up to 3 mm), and 3. a bubble-rich central part with a transition from milky-white to yellowish-brown to reddish ice at the bottom. The whole ice body was characterized by several cracks. It was probably formed by the complete freezing of standing water, likely a polygon pond.

A vertical profile across the massive ice was taken by chain saw in a resolution of about 10 cm. Additionally, a block was cut from the ice wedge.

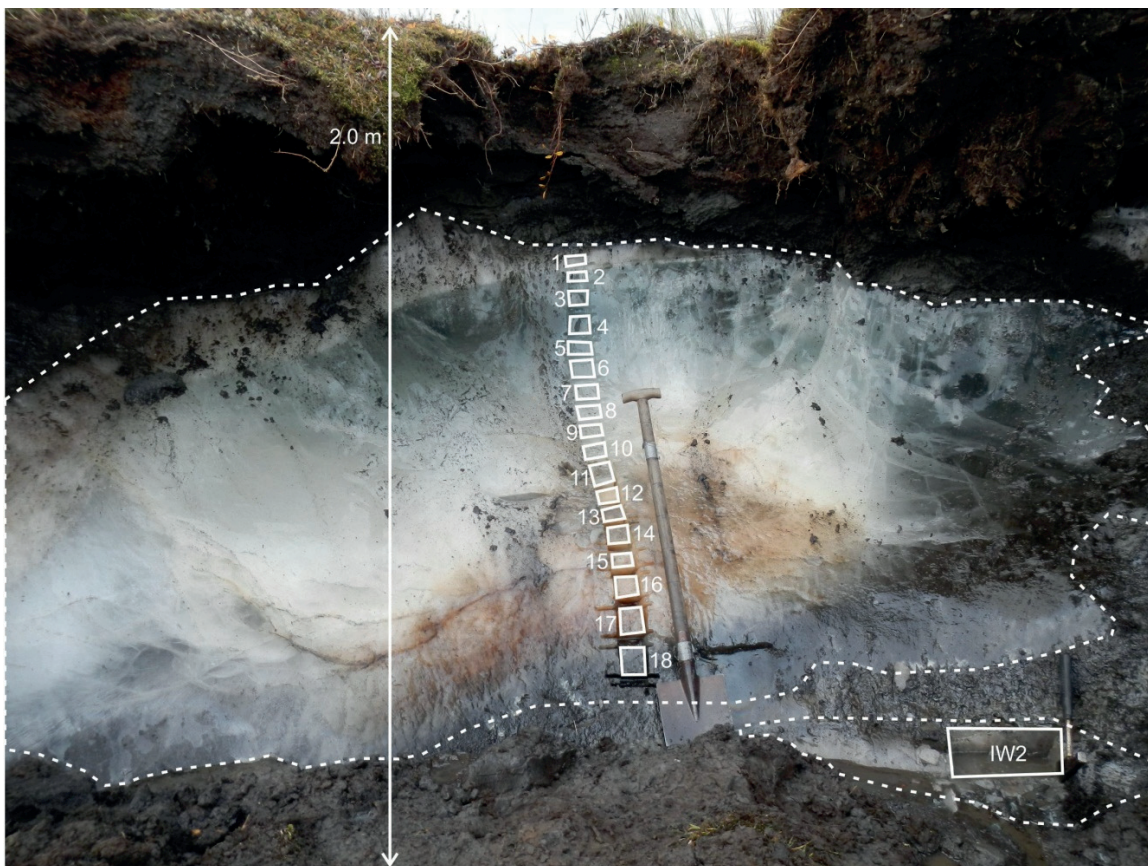


Figure 3-37 Massive Ice LD12-MI and ice wedge LD12-IW2.

References

Meyer, H., Schirmeister, L., Yoshikawa, K., Opel, T., Wetterich, S., Hubberten, H.-W., Brown, J. (2010) Permafrost evidence for severe winter cooling during the Younger Dryas in northern Alaska. *Geophysical Research Letters* 37, L03501.

3.11 Ground ice studies on Samoylov Island

Opel, T., Dereviagin, A., Meyer, H., Schirrmeister, L., & Wetterich, S. (2011) Paleoclimatic information from stable water isotopes of Holocene ice wedges at the Dmitrii Laptev Strait (Northeast Siberia). *Permafrost and Periglacial Processes* 22, 84–100.

4 STUDIES ON MUOSTAKH ISLAND



Figure 4-1 *Aerial view of Muostakh Island from the Northeast.*

4.1 SCIENTIFIC BACKGROUND, OBJECTIVES AND METHODS

Hanno Meyer

The ice-rich permafrost deposits on Muostakh Island are characterized by a peculiar sedimentological sequence including different types of ground ice. Muostakh Island is subject to heavy coastal erosion with high rates of up to 25 m/year (at the northern tip). Another key observation suggests changes in sediment supply to have major impact on the distribution and shape of ground ice and organic matter in the section.

The island has been visited by AWI scientists before: first for a day of reconnaissance in 2002 and again during the LD 2011 campaign. During both previous expeditions, lack of time or difficult outcrop conditions did not permit to sample the complete sedimentary sequence nor all types of ground ice. This is especially true for the middle part of the section, which has been barely accessible. Hence, the main objective of this campaign was to carry out detailed cryolithological and sedimentological field work i.e. sample ice wedges, segregated ice and sediments on Muostakh Island complementing the published data from Schirrmeister et al. (2011) and observations from 2011 (Opel and Wetterich, 2013) as well as the work of Russian colleagues (see chapter 4.2).

Ice wedges as the most abundant type of ground ice on Muostakh Island are climate archives and one key object of this field campaign. They are formed by repetitive frost-cracking events in winter and subsequent filling of frost cracks with snow meltwater in spring. As a consequence, we are able to use oxygen and hydrogen isotope information of ice wedges as proxies for winter temperatures during the time of their formation. The latter period is defined by radiocarbon dating of organic matter either directly enclosed in ice wedges or from the sedimentary sequence.

Hence, one focus was to retrieve ice-wedge based recent, Holocene (see chapter 4.4) and Late Pleistocene (see chapter 4.5) climate information from permafrost deposits on Muostakh Island and, thus, adding a new cryolithological dataset to the regional paleoenvironmental picture. A second focus was set on completing the sediment profile (see chapter 4.3), which up to now enclosed only the lower section (about 8-10 m) of the complete permafrost sequence (Schirrmeister et al., 2011). The ice-wedge and sediment study sites are displayed in Figure 4-2.

Furthermore, recent precipitation and surface waters (small streams, ponds) were sampled to get a broader picture of the hydrological situation of Muostakh Island.

Sedimentological and paleo-ecological work is encompassed by a detailed classification of the local soil and vegetation situation (see chapter 4.6) as well as studies on the quality of dissolved organic matter (DOM) stored in frozen deposits and transported by melt water streams to the ocean (see chapter 4.7).

Based on previous work in 2011 (Günther et al., 2013), a tacheometric coastline survey in the northern part of Muostakh Island was carried out for studies of coastal erosion (see chapter 4.8).

4.1 Scientific background, objectives and methods

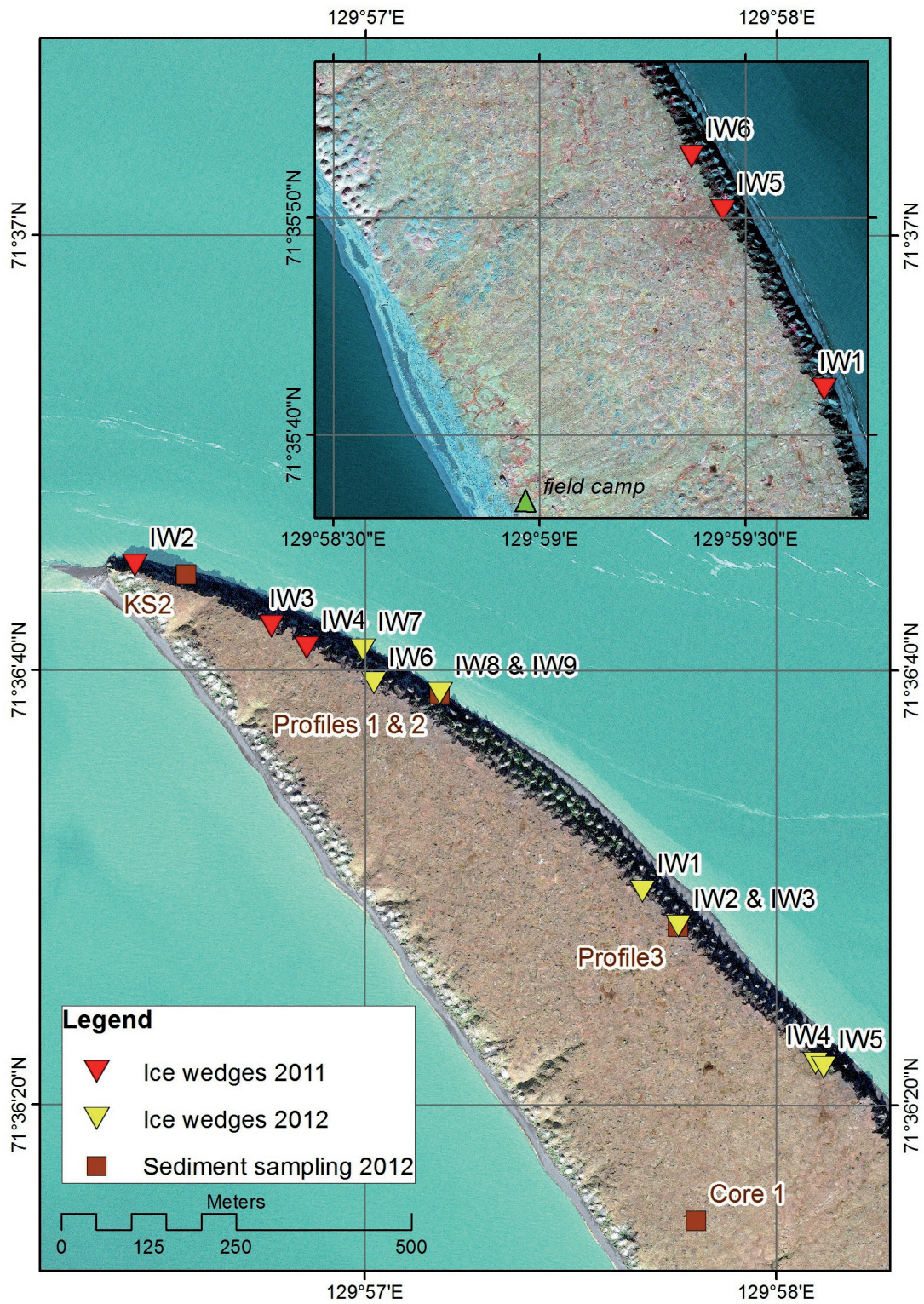


Figure 4-2 Overview map of the northern part of Muostakh Island with ice-wedge and sediment study sites. Background: Pansharpned GeoEye satellite image, acquired on 7 September 2012. Map compiled by Frank Günther.

Methods for cryolithological and hydrological studies

Ice wedges were studied according to their best exposure perpendicular to the frost cracking direction, were described, photographed and drawn. Ice-wedge samples were taken using a STIHL chain saw in horizontal profiles either by cutting thin slices of about 1.5 cm width every 10 cm, or by cutting ice blocks (about 25x15x15 cm) for detailed analyses. Additionally, recent ice wedges assemblages were sampled as being indicative for modern ice wedge growth conditions. Both ice slices and the ice blocks were stored in a freezer in the camp, and then transported in the frozen state back to Germany, where they will be further processed in a cold laboratory. In total, we studied and sampled 9 older ice wedges (4 Holocene, 5 Pleistocene) and 2 recent ice wedges.

Surface water and precipitation (as well as a few melted ground ice) samples were stored in 30 ml PE bottles, which were completely filled and tightly closed to avoid evaporation for stable isotope analyses. For hydrochemical laboratory analyses, meltwater from selected samples was filtered using a cellulose-acetate filtration set (pore size 0.45 µm) and collected in 8 ml HDPE-flasks for anion analyses by ion chromatography, and in 15 ml PP-tubes for element (cation) analyses by ICP-OES. Samples for cation analyses were acidified to pH 2 with 50 µl HNO₃. We determined electrical conductivity (EC) of the hydrochemistry samples with a WTW LF 340 conductometer, and pH by a WTW LF 340 pH meter.

Additionally, fresh precipitation (N=6) and surface water samples (N=20) were collected on Muostakh Island for stable isotopes and hydrochemistry and stored as described above.

References

- Günther, F., Sandakov, A., Baranskaya, A., and Overduin, P. (2013) Topographic survey of Ice Complex coasts, in: Günther, F. et al. (Eds.) *The Expeditions Laptev Sea Mamontov Klyk 2011 & Buor Khaya 2012. Berichte zur Polar- und Meeresforschung/Reports on Polar and Marine Research* 664, 16–54.
- Opel, T., and Wetterich, S. (2013) Studies of Holocene ice wedges. In: Günther, F. et al. (Eds.) *The Expeditions Laptev Sea Mamontov Klyk 2011 & Buor Khaya 2012. Berichte zur Polar- und Meeresforschung/Reports on Polar and Marine Research* 664, 55-63.
- Schirrmeister L., Kunitsky V.V., Grosse G., Wetterich, S, Meyer, H., Schwamborn, F. Babiy, O., Derevyagin, A. and Siegert, C. (2011) Sedimentary characteristics and origin of the Late Pleistocene Ice Complex on North-East Siberian Arctic coastal lowlands and islands - a review. *Quaternary International* 241, 3-25.

4.2 HISTORY OF INVESTIGATIONS AND GENERAL GEOGRAPHICAL AND GEOLOGICAL CHARACTERISTICS

Alexander Dereviagin

“Muostakh” is translated from Yakutian language as “with mammoth tusk”. This is most likely because of the specific island form that looks like mammoth tusk as well as of numerous findings of mammoth bones including tusks at the islands coast. At this moment this small island has a length of about 7 km and a width of not more than 400-500 m and continues to destroy actively. Muostakh Island is located at a distance of about 25 km from the mainland in the Buor Khaya Bay. It is defined as the southeastern continuation of the Bykovsky Peninsula and is located about of 15 km apart from the cape Muostakh at Bykovsky Peninsula.

Since 1936 the island is of geographical and geological interest (Gusev, 1936). In 1936 meteorological observations were started in the Polar Station Muostakh located at the southern end of the island. The Polar Station was closed in 1991. The intensive geocryological investigations of the island (including permafrost drilling transects in the shallow strait between the island and Bykovsky Peninsula) started in 1962 by scientists from Yakutian Permafrost Institute and Moscow State University (Danilova, 1965, 1966; Katasonov, 1965; Solomatin, 1965; Maslov, 1965; Grigoriev, 1966; Molochushkin, 1969; 1970; 1973; Ivanov and Katasonova, 1978; Romanov and Kunitsky, 1985; Kunitsky, 1989; Grigoriev, 1993; Nakayama and Akiyama, 1994; Slagoda, 2004). These investigations showed that Muostakh Island is the continuation of Bykovsky Peninsula and that the Ice Complex continues under the sea level to a depth of about 10 m. In 2002, Muostakh Island was shortly visited by a Russian-German ship expedition in the frame of the System Laptev Sea project. First data on the isotopic composition of Late Pleistocene ice wedges as well as new ¹⁴C data of sediments were obtained (Table 4-1; Schirrmeister et al., 2003; Schirrmeister et al., 2011). In 2011, a Russian-German expedition has continued field investigations at Muostakh Island. Investigations included geophysical and tacheometric survey of coast line, study of Holocene ice wedges isotopic composition for reconstructing the regional Late Holocene climate (Opel and Wetterich, 2013).

Table 4-1 Radiocarbon age determinations of Muostakh Island sections.

Lab. no.	Height [m asl]	Sample Description	Radiocarbon Ages [years BP]	Reference
PI-1190	20	Peat	4900 ± 300	Schirrmeister et al., 2003
PI-1189	7.5	Peat	42500 ± 5400	Schirrmeister et al., 2003
KIA 25718	0.5	Plant remains	39110 +2220/-1740	Schirrmeister et al., 2011
KIA 25720	1.0	Twigs	46780 +1270/1-100	Schirrmeister et al., 2011

4.2 History of investigations and general characteristics

KIA 25719	2.0	Twigs, moss	42800 +980/-870	Schirrmeister et al., 2011
KIA 25721	5.0	Plant remains	38620 +1310/-1120	Schirrmeister et al., 2011
KIA 25722	7.5	Carex, eriophorum	40340 +820/-740	Schirrmeister et al., 2011
KIA 25723	9.7	Twigs	19560 ± 80	Schirrmeister et al., 2011

The island mainly consists of Ice Complex deposits which are well exposed at the Northeast and East Coasts from the sea level up to the islands surface at about of 18-20 m a.s.l. The heights of the island smoothly decrease to the southern part to 5-10 m a.s.l. The surface (the top) of the island is flat with a well pronounced polygonal net and numerous small ponds (diameter of about 1-7 m and depth not more than 0.3-0.4 m). There are alas remains in the middle part of the island (around the camp). In the Northern part there is field of peat mounds (heights of 0.5-0.8 m). The steep slopes of island are characterized by numerous baydzherakhs and ovrags with small brooks. Around the island there is a narrow (10-50 m) sand beach with numerous wood remains.

The climate of the region is characterized by long severe winters and short rainy and cold summers. The available meteorological data covers the period from 1936 to 1985 (Table 4-2). The mean annual air temperature in this period is -13.1°C. Maximum (-10.6°C) was in 1943, minimum was in 1979 (-16.1°C). The warm period (with daily air temperature > 0°C starts in the first decade of June (4-5 of June) and finished in the second (or third) decade of September.

Table 4-2 Mean monthly air temperature (°C).

I	II	III	IV	V	VI	VII	VIII	IX	X	XI	XII	Year
-30.5	-30.3	-26.3	-18.6	-7.1	0.8	3.9	6.3	2.5	-8.7	-21.8	-27.6	-13.1

There are about 240 mm of annual precipitation; more than 60% is precipitated in summer. Snow begins to accumulate in the end of September and reaches a maximum depth (25-30 cm) in spring.

The mean annual ground temperature is about -9°C (Kunitsky, 1989). Mean thickness of active layer is about 50 cm (Molochushkin, 1969).

References

- Danilova N.S. (1965) Peculiarities of recent permafrost formation in Lena Delta. In: News of AN USSR, Geography, №5, 63-71 (In Russian).
- Danilova N.S. (1966) About seasonal thawing in Lena Delta. In: Seasonal thawing of ground in the Northern-East of USSR. Moscow, 29-33 (In Russian).

4.2 History of investigations and general characteristics

Grigoriev, M.N. (1993) Cryomorphogenesis of the Lena River mouth area. Yakutsk: SO AN SSSR, 176 pp. (in Russian).

Grigoriev, N.F. (1966) Perennially frozen ground of the Yakutian maritime zone. Moscow: Nauka, 180 pp. (in Russian).

Gusev, A.I. (1936). Island Muostakh. "Soviet Arctic" 1936, №2 (in Russian).

Ivanov M.S., Katasonova E.G. (1978) Peculiarities of cryolithogenic deposits of the Muostakh Island. In: Anisimova N.P., Katasonova E.G. (eds.) Geokriologicheskie i gidrogeologicheskie issledovaniya in Yakutia (Geocryologic and hydrogeologic research in Yakutia), 12-25, Permafrost Institute, SO AN SSSR, Yakutsk (In Russian).

Katasonov E.M. (1965) Permafrost-facies investigations of permafrost and questions of paleogeography of Quaternary period in Siberia. In: Main problem of Quaternary period studies. Moscow, Nauka, 286-293 (In Russian).

Kunitsky, V.V. (1989) Kriolitologiya nizo'ev Leny (Cryolithology of the Lower Lena). Permafrost Institute Press, Yakutsk, 162 pp. (In Russian).

Maslov A.D. (1965) Ice wedges in the first stage of its formation. In Ground ice Vol. II, MSU Publishing, 73-82 (In Russian).

Molochushkin E.N. (1969) Results on annual ground temperature observations at the Muostakh Island. In Problem of Yakutian Geography, Vol.5, Yakutsk, 127-137 (In Russian).

Molochushkin E.N. (1970) Sediments heating regime in the east-southern part of Laptev Sea. PhD Thesis, Moscow State University, 109 pp. (in Russian).

Molochushkin E.N. (1973) An influence of thermoabrasion on the permafrost temperature in the coastal zone of Laptev Sea. Proceedings of II International Conference on Permafrost., Vol. 2, Yakutsk, 52-58 (In Russian).

Nakayama T., Akiyama A. (1994) Measurement of methane Flux in a Tundra Wetland, Muostakh Island in 1993. Proceedings of the Second Symposium on the Joint Siberian Permafrost Studies between Japan and Russia in 1993, Tsukuba, 12.13 January 1994. Tsukuba: Printed Isebu, 37-39.

Opel, T., and Wetterich, S. (2013) Studies of Holocene ice wedges. In: Günther, F. et al. (Eds.) The Expeditions Laptev Sea Mamontov Klyk 2011 & Buor Khaya 2012. Berichte zur Polar- und Meeresforschung/Reports on Polar and Marine Research 664, 55-63.

Romanov V.P., Kunitsky V.V. (1985) Methodic of permafrost deposits genesis determination in Muostakh Island. In: Cryogidrogeological investigations. Yakutsk, 161-166 (In Russian).

Schirrmeyer L., Grosse G., Kunitsky V., Meyer H., Dereviagin A., Kuznetsova T. (2003) Permafrost, periglacial and paleo-environmental studies on New Siberian Islands. In: Grigoriev M. et al (Eds.) The Expedition Lena 2002. Berichte zur Polar- und Meeresforschung/Reports on Polar and Marine Research 466, 195-314.

Schirrmeyer L., Kunitsky V.V., Grosse G., Wetterich, S, Meyer, H., Schwamborn, F. Babiy, O., Derevyagin, A., Siegert, C. (2011) Sedimentary characteristics and origin of the Late Pleistocene Ice Complex on North-East Siberian Arctic coastal lowlands and islands - a review. Quaternary International 241, 3-25.

4.2 History of investigations and general characteristics

Slagoda, E.A. (2004). Cryolithogenic Deposits of the Laptev Sea Coastal Plain: Lithology and Micromorphology. Publishing and Printing Centre Express, Tyumen, 119 pp. (in Russian).

Solomatin V.I. (1965) About ice wedge ice structure. In Ground ice Vol. II, MSU Publishing, 46-72 (In Russian).

4.3 STRATIGRAPHIC AND SEDIMENTOLOGICAL STUDIES

Hanno Meyer, Thomas Opel and Alexander Dereviagin

Fieldwork period: August 07 to August 26, 2012; Muostakh Island

The small island Muostakh Island is boomerang-shaped and reaches about 7.5 km in the N-S extension and up to 500 m in E-W direction. Muostakh Island is dominated by Middle to Late Weichselian Ice Complex sequences characterized by large syngenetic ice wedges. These are partly covered by Holocene boggy deposits, i.e. patchy peat pockets often enclosing smaller ice wedges.

After a detailed survey of the coastal cliffs on Muostakh Island, we selected 2 key sections, where the complete sedimentological and cryolithological inventory was visible and started to describe these outcrops in detail. An about 50 m wide and 20 m high exposure (key section 2) at the northern tip of Muostakh Island (Figure 4-2) has been selected and is exemplarily displayed in Figure 4-3 and Figure 4-4.

The section comprised older, likely Pleistocene very ice-rich Ice Complex sediments: mostly silty sands intercalated by several thin peat layers enclosing the oldest generation of ground ice (below 8 m a.s.l.) on Muostakh Island covered by an about 1 m thick peat layer which can be found in all outcrops. Here ice wedges may reach up to 4-5 m in width. The top of this unit shows indications of a heavy erosional event, likely of alluvial origin. The discordance is detectable over several km.

Between ca. 8-9 m and ca. 15-17 m a.s.l., a far less ice-rich middle unit characterized by coarser grained sandy to gravelly material (often gravel layers) with low organic matter content is found, assumed to be of Late Pleistocene age. This unit is characterized by a second generation of smaller (1-3 m wide) ice wedges. Both, sediments and ice wedges indicate that the energetic level is higher than in the lower unit with more transport energy needed to accumulate these sediments. Hence, we assume that less time was necessary to deposit these about 8-9 m of sediments and, as a consequence of higher accumulation rates, ice wedges had less time of stable surfaces to develop and are, thus, smaller in width.

The top of the section (upper 4-5 m) characterized by patchy peat pockets reaching about ten meters in horizontal extension. These organic-rich and ice-rich silty sands often show signs of thermal denudation of the underlying sediments and are likely related to small lakes and ponds. These deposits enclose smaller ice wedges (less than 1 m wide), but may also comprise larger ice wedges of 3-5 m width, which may extend several meters downward into the older sediments.



Figure 4-3 Key section 2. Note: the photo has been taken in a slightly different position than the drawing of the general stratigraphic and cryolithological profile (Figure 4-4).

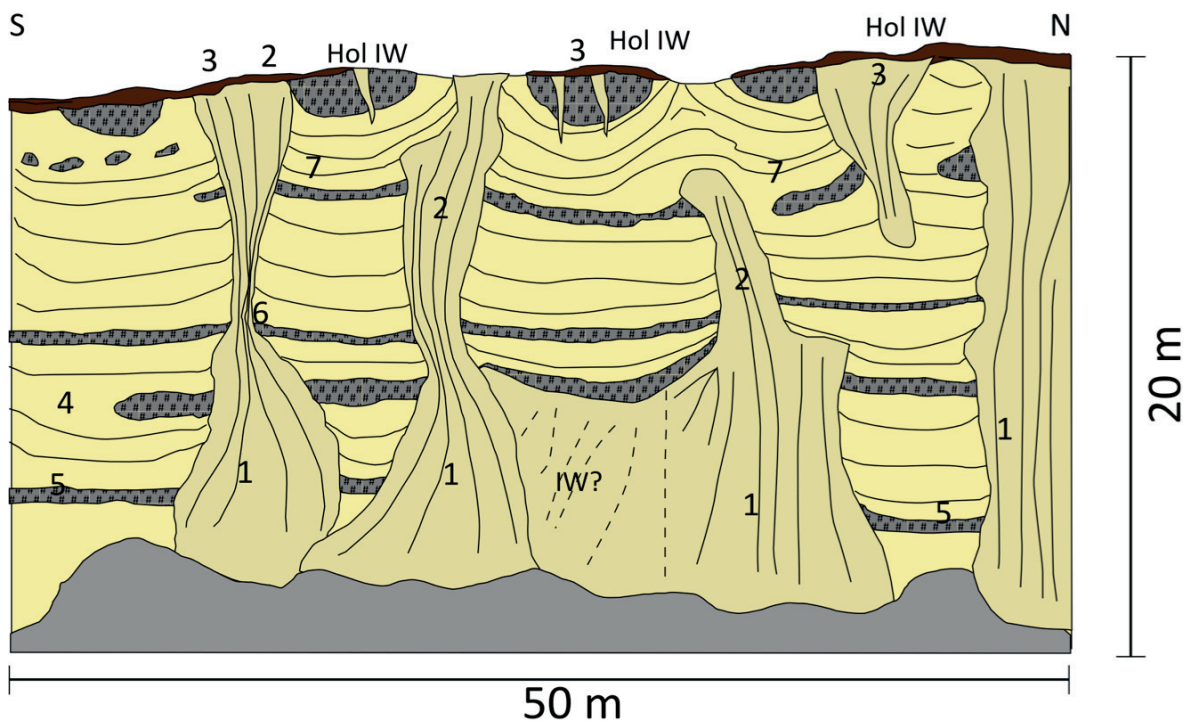


Figure 4-4 Key section 2 with general stratigraphic and cryolithological profile. (1) Pleistocene ice wedges (first generation) 3-5 m width, (2) Pleistocene ice wedges (second generation) 1-3 m width, (3) Holocene ice wedges, variable in width, (4) prominent peat layer, up to 1 m thick, ca. 8 m a.s.l., (5) to (7) peat layers, 0.5m thick. Compiled by Christoph Manthey.

We tried to sample the complete sedimentary sequence including the different peat layers as important datable horizons for stratigraphy as well as to access ice wedges of all three

4.3 Stratigraphic and sedimentological studies

generations. For sediment sampling, three profiles were sampled (in the vicinity of IW8), starting from the bottom (profile 1), to the middle part (profile 2) and then sampled from the top of the section downward (profile 3) in order to get overlap with profile 2. In total, 24 samples (SS01 to SS24) have been retrieved covering the complete sedimentary sequence from 4 m a.s.l. to the top of the section at 20 m a.s.l. (Figure 4-6).

These samples have been complemented by a 1.13 m long sediment core (Core 1, Figure 4-2) taken with a Kovacs corer in a Holocene peat mound to gather more detailed information about the Holocene and recent peat accumulation. These peat mounds are widely distributed at the surface in the northern part of Muostakh Island (Figure 4-5) and are likely related to surface subsidence due to intense thawing of ground ice.

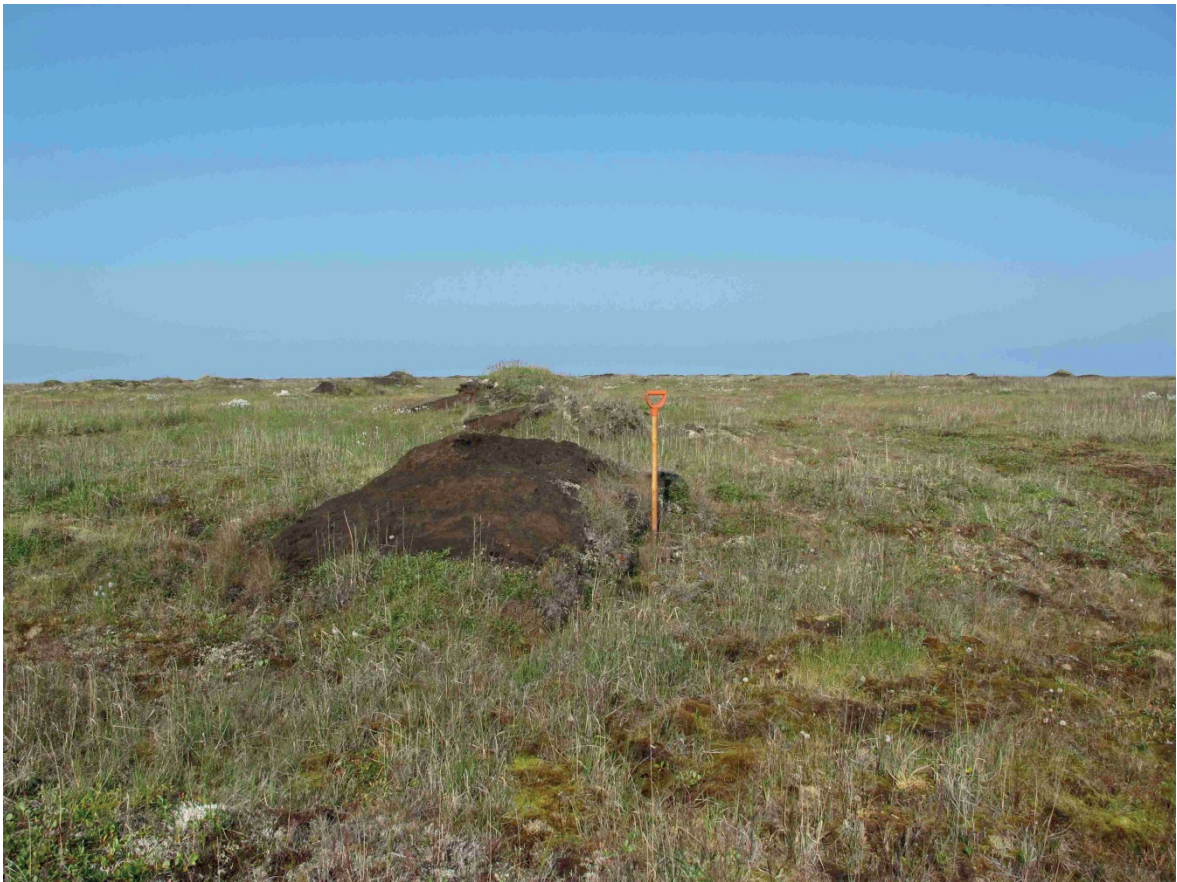


Figure 4-5 Peat mounds in the northern part of Muostakh Island.

4.4 STUDIES OF HOLOCENE ICE WEDGES

Thomas Opel, Hanno Meyer, and Alexander Dereviagin

Fieldwork period: August 07 to August 26, 2012; Muostakh Island

4.4.1 Ice wedge MUO12-IW1 (N 71°36'29.8", E 129°57'40.5")

Ice wedge MUO12-IW1 was an up to 1 m wide ice wedge at the top of Ice Complex (about 19 to 20 m a.s.l.). It was cut almost perpendicular to its long axis (= along its growth direction) and its exposed vertical extension was about 1.3 m (Figure 4-7).



Figure 4-7 Ice wedge MUO12-IW1.

The ice wedge was covered by an active layer of about 60 cm, consisting of 20 cm brown peat-like organics (grass, roots) on top and 40 cm gray soil penetrated by roots. The ice wedge was surrounded by gray to brown sandy silt with singular gravels, characterized by a (fine-) lens like reticulated cryostructure, probably Ice Complex sediments. About 1 m northwest of the ice wedge an up to 1 m thick peat mound only slightly elevated over the surface was found, probably developed on top of the polygon pond filling sediments.

The wedge ice was milky-white and very rich of small vertically oriented air bubbles. Most of them were smaller than 1 mm but some up to 5 mm long. Clear structures as e.g. single ice veins were not detectable. The content of organic or mineral inclusions was very low. The rightmost part of the ice wedge consisted of clear, darker schlieren ice of up to 10 cm width.

We sampled the ice wedge by cutting blocks. One horizontal profile of 80 cm consisting of three blocks (1-3) was cut 50 cm below the ice-wedge surface. The right block also contained some schlieren ice. Additionally we took one block (4) from the lowest part of the ice wedge about 1.20 m below the ice-wedge surface.

4.4.2 Ice wedge MUO12-IW4 (N 71°36'21.9", E 129°58'5.7")

Ice wedge MUO12-IW4 consisted of at least two ice-wedge generations at the top of the Ice Complex (about 19 to 20 m a.s.l.). The younger (Holocene) was about 40 cm wide and elevated the older (Holocene or Pleistocene?) part at its left side by about 50 cm (Figure 4-8). On top of this younger generation also some recent ice veins were exposed (width about 3 cm) elevating this wedge generation by about 20 cm and reaching the permafrost surface. In total, the ice wedge was about 2.3 m wide and the vertical wedge extension exposed in the outcrop was about 1.3 m. The younger ice-wedge generation was cut in an angle of about 45°.

The younger ice wedge generation was covered by about 50 cm of sediments. The uppermost 15 to 20 cm consisted of vegetation cover and brown peat-like organics underlain by brownish grey soil penetrated by roots. The active-layer depth was 25 to 30 cm. The sediments overlaying and surrounding the older ice-wedge generation consisted of gray, brownish sandy silt with some gravel similar and to the typical Ice Complex sediments. They were characterized by a lens-like to net-like reticulate cryostructure. Only in the uppermost frozen part also layered structures with up to 3 cm thick ice bands were detectable.

The white, milky ice of the younger generation was rich in small (<2 mm), non-oriented bubbles. Single ice veins were clearly detectable with thicknesses up to 1 cm. The content in organic material and sediment was low. The clearer, white ice of the older generation contained larger oriented bubbles up to 1 cm long. Single ice veins were only partly detectable and up to 1 cm thick. The sediment content was medium and the organic matter content also low.

We sampled this ice wedge by cutting blocks in three different height levels. One block (RIW) was taken containing the recent ice veins on top of the younger ice-wedge generation. Two blocks (1-2) were taken about 30 cm below the ice-wedge top containing a complete profile of the younger ice-wedge generation and adjacent sediments. Another

4.4 Studies of Holocene ice wedges

four blocks (3-6) were cut 0.8 m below the ice-wedge top, two of them (3-4) close to the younger ice-wedge generation and two (5-6) in the older outer part.

About 0.5 m southeast of the ice wedge we sampled also a vertical profile of texture ice: Two samples with layered cryostructure: 45 cm and 55 cm below surface and four samples with reticulate cryostructure: 72 cm, 82 cm, 98 cm, 102 cm below surface.

About 2.5 m southeast of the ice wedge we also cut a block of refrozen water from a deepened polygon crack. Single layers representing different freezing steps were clearly distinguishable.



Figure 4-8 Ice wedge MUO12-IW4 and frozen water in a polygon crack.

4.4.3 Ice wedge MUO12-IW6 (N 71°36'39.4", E 129°57'1.3")

Ice wedge MUO12-IW6 was an about 3 m wide ice wedge at the top of the Ice Complex in an altitude of about 20 m a.s.l. It was cut almost perpendicular to its long axis and the exposed vertical extension was 1.2 m (0.9 to 2.1 m b.s.). The ice wedge was characterized by twinned head: a 30 cm high and 10 to 20 cm ice-veins assemblage representing the youngest, i.e. recent growth stage of this ice wedge (Figure 4-9).

The active-layer thickness was 25 cm and the unfrozen material consisted mostly of brown peat-like organics. Below the active layer, single ice bands were detectable. The ice wedge enclosing sediments were gray silty clays with peat nests and a reticulate cryostructure, except for the upper right part of the ice wedge that showed signs of thawing (due to the development of a polygonal pond). Consequently, here the sediments consisted of Holocene polygon sediments: brownish gray peaty silts with a massive cryostructure.

The milky white wedge ice was very rich in small (mostly < 1 mm), partly oriented air bubbles. It exhibited very clear structures. Single ice veins (2 to 5 mm) were detectable as well as dilatation cracks (2 to 5 mm) cross-cutting them. Interestingly also these dilatation cracks were characterized by air bubbles. The content in organics and sediments was low.

We took samples in three levels. First the twinned head of the ice wedge (80 cm b.s., block 1), second a horizontal profile of blocks and slices (1.2 m b.s., blocks 2-5, slices 101-107) and third a complete horizontal profile in blocks (1.7 m b.s., blocks 6-18).

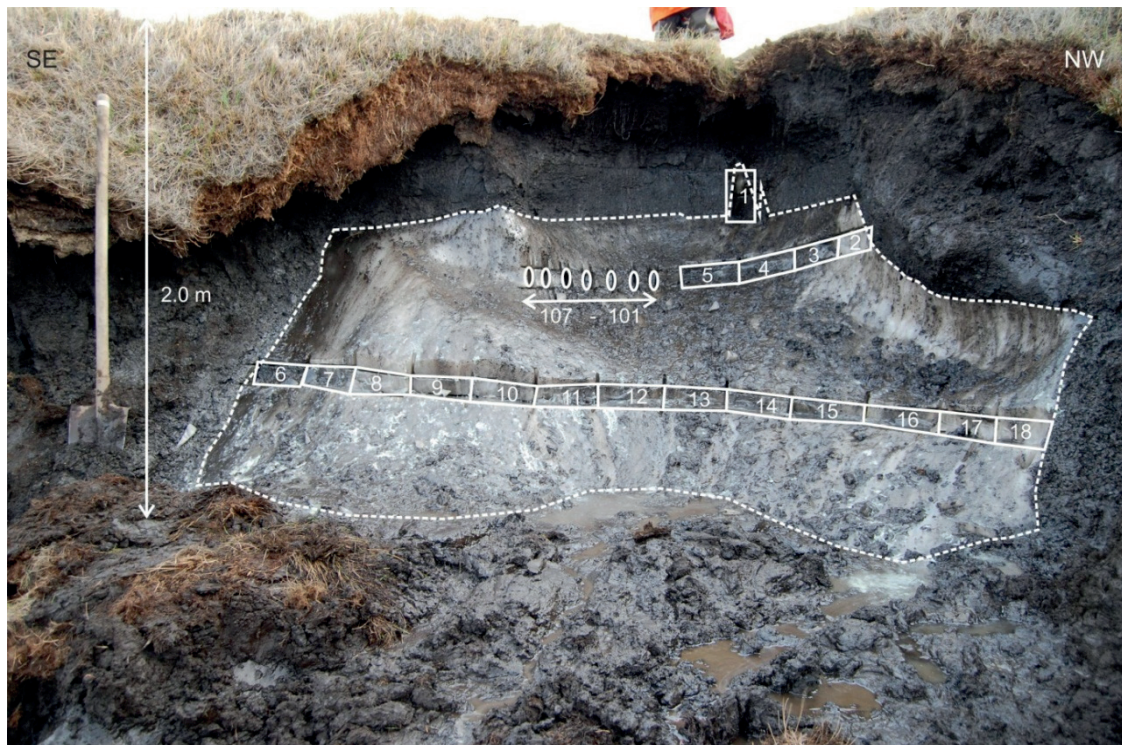


Figure 4-9 Ice wedge MUO12-IW6.

4.5 STUDIES OF LATE PLEISTOCENE ICE WEDGES

Hanno Meyer, Alexander Dereviagin, and Thomas Opel

Fieldwork period: August 07 to August 26, 2012; Muostakh Island

4.5.1 Ice wedge MUO12-IW2 (N 71°36'28.2", E 129°57'45.7")

Ice wedge MUO12-IW2 is an up to 2.3 m wide ice wedge visible from about 5 m (at about 15 m a.s.l.) to about 9.5 m (about 10.5 m a.s.l.) below the top of section. The vertical extension is more than 5 m widening upwards from 1.1 m to 2.3 m. It is cut almost along its growth direction and has been sampled in three profiles (lower: ~9.2 m b.s., middle: ~7.2 m b.s., upper: ~5 m b.s.). IW2 is considered as an ice wedge of the second oldest generation.

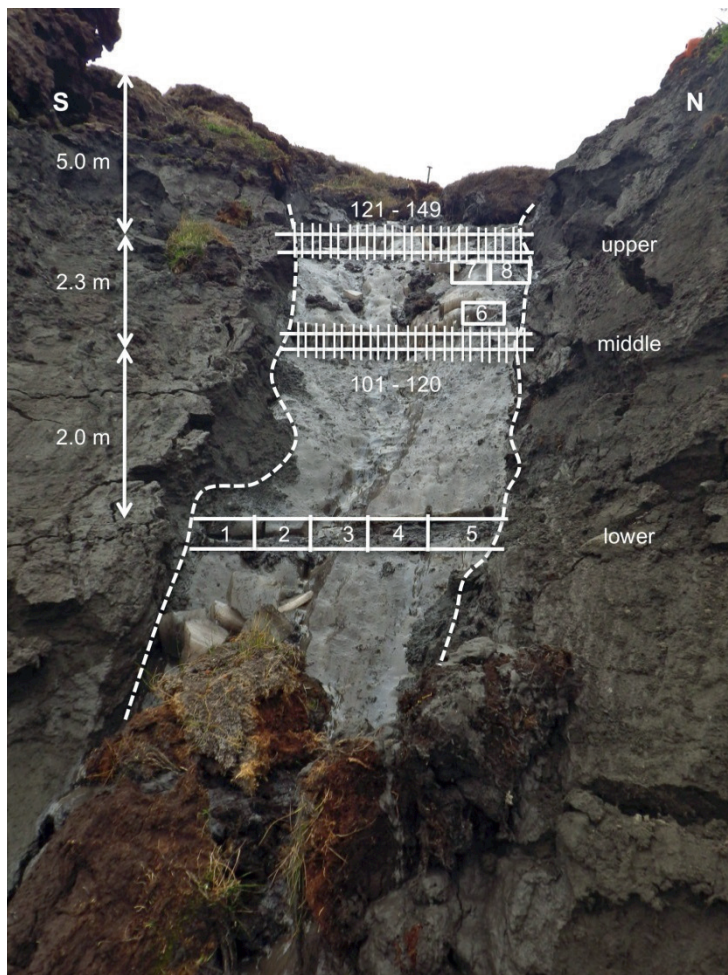


Figure 4-10 Ice wedge MUO12-IW2 with sampling strategy.

Since the ice wedge has been covered by debris, the upper contact was not visible. IW2 is embedded in greyish to brownish sandy silt with some coarser sandy interbeds,

characterized by a lens-like reticulated to massive cryostructure and relatively low ice content. The wedge ice is transparent greyish and very rich in small gas bubbles, generally < 1mm in diameter and partly elongated to 3 mm. Clear structures as e.g. single ice veins of about 2 mm were detected but are often hardly visible. Both, contents of organic or mineral (mostly sandy) inclusions, are low. The middle part of the ice wedge consisted of an about 50 cm wide meltwater channel.

We sampled the ice wedge IW2 by chain saw either by cutting defined ground ice blocks or slices in 10 cm intervals from left to right (Figure 4-10). The lower horizontal profile of 1.1 m width (~9.2 m b.s.) was sampled in blocks (samples 1 to 5). The middle profile of 1.6 m width (~7.2 m b.s.) was sampled in slices (samples 101-120) and one block (6) was taken above the profile for analyses needing more sample material. The upper horizontal profile of 2.3 m width (~5 m b.s.) was sampled in slices (121-149) and two blocks (7 and 8) were taken at the right side underneath the profile.

4.5.2 Ice wedge MUO12-IW5 (N 71°36'21.7", E 129°58'06.9")

Ice wedge MUO12-IW5 is about 3.5 m wide and extends more than 9 m in vertical direction (from about 20 to 11 m a.s.l.) As IW2, IW5 is considered as an ice wedge of the second oldest generation but has been sampled in a higher level as IW2. MUO12-IW5 consists at least of two ice-wedge generations: an older generation (second ice wedge generation; as IW2) reaching about 3.5 m of width and thinning downwards to about 1.5 m width at 11 m a.s.l. There, IW5 penetrates an older about 5 m wide ice wedge from the top. A younger ice wedge generation of up to 1 m wide buried ice wedges enters the larger part of IW5 from the top. MUO12-IW5 is embedded in grayish-brownish silty sand with lens-like to layered cryostructure with a high content of organic matter.

We sampled IW5 by cutting ice slices in two different height levels (Figure 4-11). Both profiles have been sampled in 10 cm intervals from left to right; the first profile at about 16 m a.s.l. (4 m b.s., samples 1 to 35), whereas the upper profile is a buried part of a younger ice-wedge generation was sampled at 17.5 m a.s.l. (2.5 m b.s., samples 36 to 46). The lower and upper profiles were about 3 m and 0.9 m wide, respectively. The lower sampling profile was sampled in an angle of about 45°, whereas the upper ice wedge generation was sampled along the growth direction.

The upper profile (younger generation) of MUO12-IW5 consists of colourless to grayish ice. The ground ice displays very clear vertical structures such as small, elongated gas bubbles of 1 mm in diameter, but reaching up to 5 mm in length. Single ice veins were hardly recognizable. This part of IW5 has very low sediment and low to middle content in organic matter dispersed in the ice. The lower profile of MUO12-IW5 is composed of grayish ice with very many small spherical gas bubbles. The sediment inclusions in the ice are more frequent than in the upper profile with coarse-grained sandy particles, but organic content is lower. Here, single ice veins of 3-4 mm in width are clearly visible.

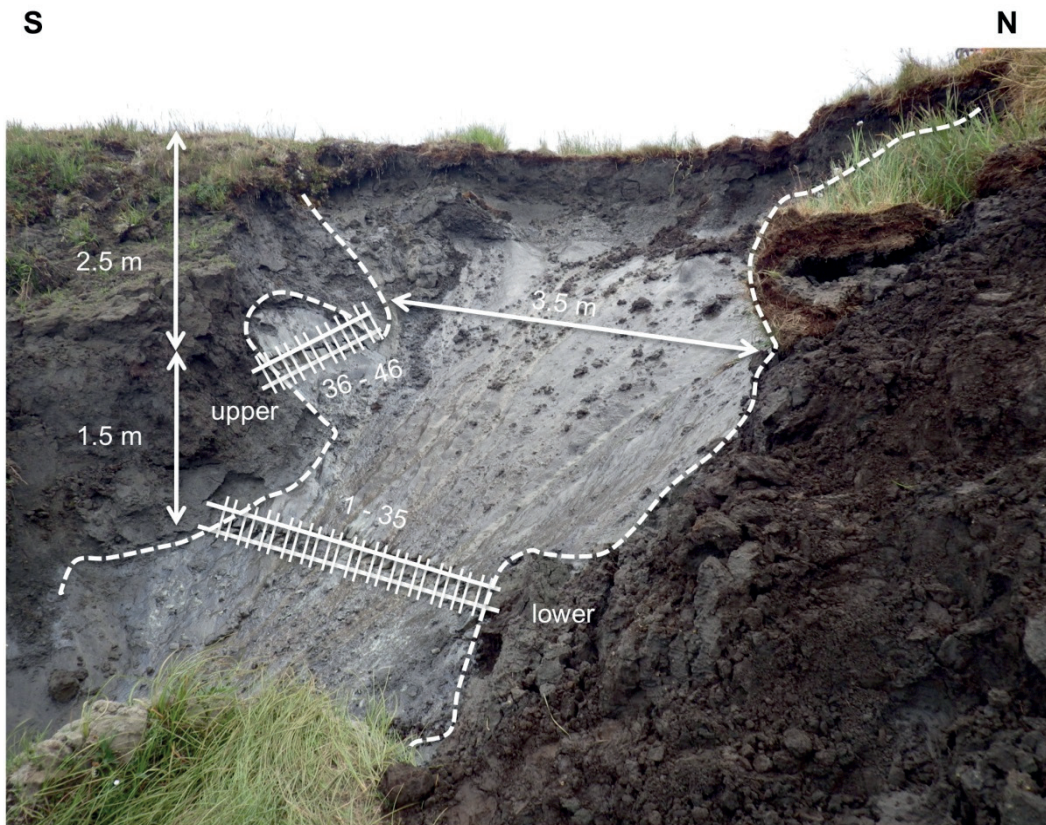


Figure 4-11 Ice wedge MUO12-IW5.

4.5.3 Ice wedge MUO12-IW7 (N 71°36'40.9", E 129°56'59.7")

Ice wedge MUO12-IW7 was an about 5 m wide Ice Complex ice wedge at the bottom part of the outcrop sampled in an altitude of about 3 to 4 m a.s.l. This is the lowest profile and likely the oldest ice wedge transect sampled during this field campaign (first ice wedge generation). The ice wedge is embedded in very ice-rich grayish-brownish silty sand with lens-like to layered cryostructure with several distinct peat horizons: at ca. 4 m a.s.l., a 0.2-0.3 m thick organic layer as well as at 8 to 9 m a.s.l., an about 1 m thick peat horizon. Hence, the vertical extension of the ice wedge was about 8 to 9 m. Above the upper peat, the ice wedge thins considerably and reaches less than 2 m width (second ice wedge generation).

The ice wedge has been sampled in two horizontal profiles in 10 cm intervals from right to left at 3 m and 4 m a.s.l (Figure 4-12). The 1st profile (right side, 3 m a.s.l.) is about 3.4 m wide (samples 1 to 33) and displays a change in the cracking direction. The rightmost 1.3 m are cut only a few degrees to the growth direction likely connected with a smaller ice wedge entering IW7 from the side. In contrast, the left 3.7 m of IW7 were cut almost perpendicular to its long axis including the central part of IW7 sampled in profile 1 and the complete 2nd profile (left side, 4 m a.s.l.). The Profile 2 is about 2 m wide (samples 34 to 48) and extends the profile 1 to the left. It had to be sampled 1 m above profile due to muddy outcrop conditions.

The turbid yellowish-greyish wedge ice at the left side of IW7 was rich in very small (mostly < 0.1 mm) air bubbles. It is characterized by very clear structures such as single

ice veins of 5-6 mm width. The sediment content in the wedge ice is low and organic matter was low to middle. At the right side the ice is more transparent and rather grey in colour, with more spherical bubbles reaching up to 1 mm.

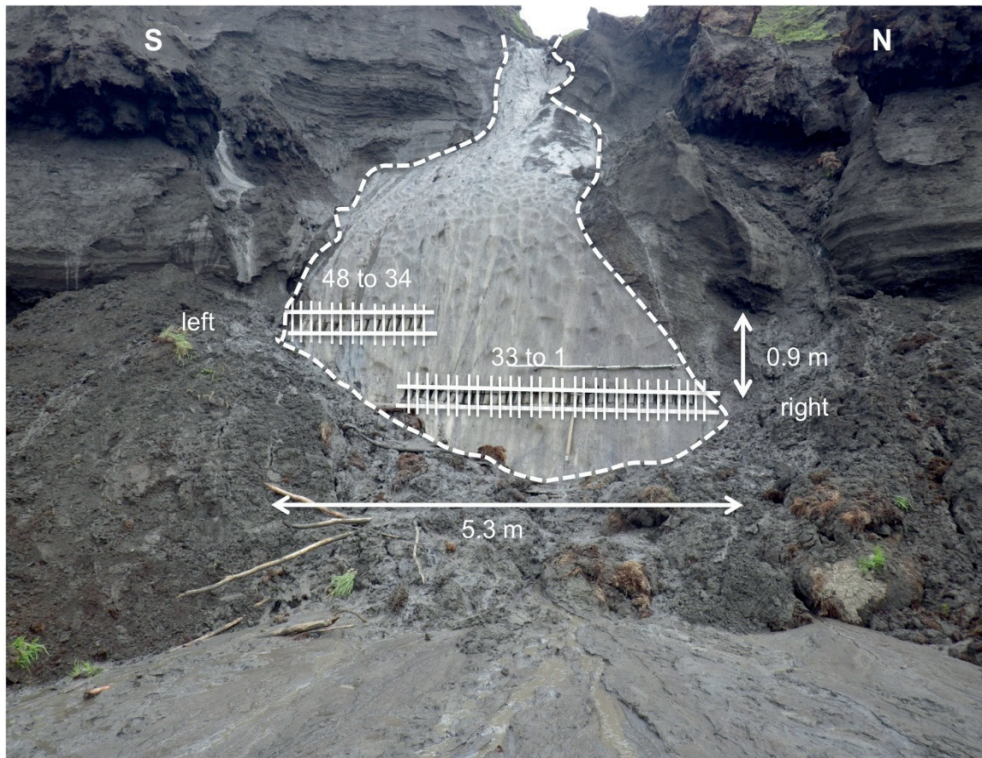


Figure 4-12 Ice wedge MUO12-IW7.

4.5.4 Ice wedges MUO12-IW8 and -IW9 (N 71°36'38.9", E 129°57'10.9")

Ice wedge MUO12-IW8 is an about 5 m wide Ice Complex ice wedge visible in the outcrop between 4 and 9 m a.s.l. and was sampled in an altitude of about 7.5 m a.s.l (Figure 4-13). This is the second oldest ice wedge transect sampled during this field campaign (first ice wedge generation).

The ice wedge is surrounded by ice-rich grayish-brownish, sometimes greenish sandy silt with lens-like to layered cryostructure. The contact of the ice wedge to the lateral deposits is often unclear. These are interrupted by several distinct peat horizons. (1) a 0.1-0.2 m thick organic layer at ca. 5 m a.s.l., (2) an about 0.5 m thick peat horizon at 8 to 8.5 m a.s.l. and (3) an a 0.1-0.2 m thick organic layer at ca. 10 m a.s.l., thus 1 m above the top of IW8. Between the peat at 10 m a.s.l. and the top of IW8, more coarse-grained, sandy to gravelly material has been deposited (sediment sample SS-7). The ice wedge has been sampled from left to right in a horizontal profile in 10 cm intervals (samples 1 to 38). IW8 was cut perpendicular to its long axis.

The wedge ice of IW8 is similar to that of IW7 with turbid yellowish-greyish colour and rich in spherical bubbles reaching up to 1 mm. It exhibits very clear structures such as single ice veins of 5-6 mm width. The content in sediments and organic matter in wedge ice is low to middle.

4.5 Studies of Late Pleistocene ice wedges

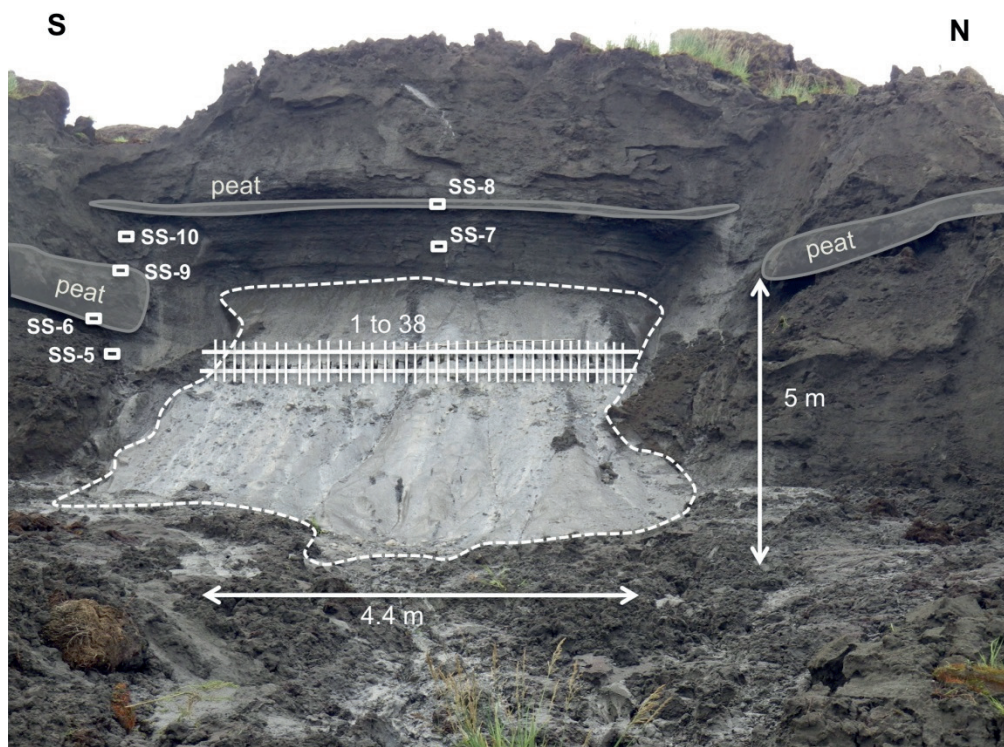


Figure 4-13 Ice wedge MUO12-IW8 and sampling transect. The surrounding sediments have been sampled (SS-5 to SS-10).

A second ice wedge IW9 has been sampled closed to IW8 (not displayed in Figure 4-13). IW9 is a 5 cm wide ice wedge, which has been sampled by hammer and axe at about 6.0 m (sample 9-1) and 6.5 (sample 9-2) m a.s.l.

4.6 STUDIES OF SOILS AND FLORA OF MUOSTAKH ISLAND

Irina Yakshina

Fieldwork period: August 07 to August 26, 2012; Muostakh Island

During the 2012 field season, the research was focussed on Muostakh Island in the Buor Khaya Gulf. This research seeks to characterize the soil cover, flora and vegetation of the island, which is located in an ecological subzone of typical tundras.

Seventeen basic soil profiles were described, including full geobotanical descriptions of each pit. Soil pits were excavated and prepared following generally accepted methods (see e.g. Desyatkin et al., 2009, Afanasjeva et al., 1979). Fifty soil samples were taken from the pits for standard chemical analysis (Table 4-3). The samples will be processed in Germany. Based on the results of this work, a soil map of the study area is in preparation.

For classifying soils we used the classification of Yelovskaya (1987).

The main soil types and subtypes of the island are:

Section: Gley

Order: Humus-Gley

Type: Permafrost Turfness-Gley

Subtype: Permafrost Turfness-Gley Typical

TG

Type: Permafrost Peat-Gley

Subtype: Permafrost Peat-Gley

PG

Subtype: Permafrost Peatish-Gley

PshG

In addition to soil and geobotanical research, the following work was made:

1. Measurement of thaw depth (active layer depth) – 335 points along whole island from N to S. The highest thaw depth was found in sands without vegetation cover (more than 100 cm), and the lowest depth was in peat under sphagnum (about 20 cm).
2. Photographing panoramas of shore scarps around the whole island – 315 panoramas with 7 or more frames each one, about 13.5 km.
3. Drawing up list of vascular plants of the Island.
4. Making photo herbarium.
5. Bird watching.

4.6 Soil and vegetation studies

Expected outcome

1. Classification and systematic description of the types of Muostakh Island soils.
2. Characteristics of the chemical composition of investigated soils.
3. Mapping of soil cover of Muostakh Island.
4. Drawing up more complete list of vascular plants of the Island.

Table 4-3 List of soil samples

№	# cut	Coordinates,		Sample Depth, cm (T = peat)
		°N	°E	
1	01Mou09.08.2012	71°33,658	130°01,452	4-10
2				11-21
3				23-33
4				40-50
5				60-64
6	02Mou09.08.2012	71°34,059	130°01,304	5-12
7				13-21
8				23-32
9	03Mou11.08.2012	71°34,332	130°00,930	10-20T
10	04Mou11.08.2012	71°34,658	130°00,864	5-15T
11	05Mou11.08.2012	5 m W of 04Mou		1-5
12				6-12
13				14-24
14				30-40
15				50-60
16	06Mou11.08.2012	71°35,134	130°00,153	3-10T
17				12-22

4.6 Studies of soils and flora

	07Mou11.08.2012	71°35,164	130°00,119	without samples
18	08Mou12.08.2012	71°35,282	130°00,032	5-13T
19				14-24T
20				30-40T
21	09Mou12.08.2012	7 m N of 08Muo		5-15
22				20-30
23				40-50
24				65-75
25	10Mou12.08.2012	71°35,458	129°59,484	3-8
26				8-12
27				12-20
28				25-35
29	11Mou17.08.2012	71°36,674	129°56,646	1-6T
30				20-30
31				45-55
32	12Mou17.08.2012	71°36,398	129°57,741	8-18T
33				25-35T
34	13Mou17.08.2012	71°36,184	129°58,055	4-14
35				17-27
36				45-55
37				60-70
38	14Mou17.08.2012	71°35,967	129°58,268	5-15
39				30-40
40				60-70
41				100-110T

4.6 Soil and vegetation studies

42	15Mou17.08.2012	71°35,705	129°58,831	8-18
43				30-40
44	16Mou20.08.2012	71°35,619	129°59,189	7-15T
45				20-30
46				47-57
47	17Mou23.08.2012	71°35,541	129°59,225	2-12T
48				20-30
49				40-50
50				60-70

References

Afanasjeva, T.V., Vasilenko, V.I., Tereshina, T.V., Sheremet, B.V. (1979) Soils of the USSR. Moscow, Mysl', 15-18 (In Russian).

Desyatkin, R.V., Okoneshnikova, M.V. Desyatkin, A.R. (2009) Soils of Yakutia, Bichik, Yakutsk, 9-10 (In Russian).

Yelovskaya, L.G. (1987) Classification and diagnostics of permafrost soils of Yakutia. Yakutsk. 172 pp. (In Russian).

4.7 STUDIES OF DISSOLVED ORGANIC MATTER

Ivan Dubinenkov

Fieldwork period: August 07 to August 26, 2012; Muostakh Island

4.7.1 Introduction

Muostakh Island is formed by the organic-rich Ice Complex. Organic carbon pool stored in the Ice Complex (coastal and inland) is estimated to contain ~400 Pg of carbon (Zimov et al., 2006, Tarnocai et al., 2009) worldwide. This pool is approximately half of the terrestrial organic carbon (~1000 Pg C) pool stored in the permafrost in tundra and taiga (Tarnocai et al., 2009). Organic-rich permafrost is one of the major and vulnerable (Engelhaupt, 2008) sources of organic matter (OM) in the Arctic. The degradation and mobilization of this carbon pool will have critical implications for primary production and carbon cycling in the Arctic and in the Arctic Ocean Basin interior (Schuur et al., 2008, Frey and McClelland, 2009). Studies on dissolved organic matter (DOM) as the most mobile phase of organic matter are of great importance, especially in application to climate change studies and vulnerable ecosystems. DOM is a complex mixture of organic compounds of different nature and plays an important role in a wide range of biogeochemical processes. Although there were several attempts to estimate the quantity of permafrost OM, there is still the gap in the quality of DOM studies in the Arctic ecosystems.

The aim of this research was the identification of trends in molecular composition (signatures) of emitted DOM and DOM stored in the Ice Complex and the correlation of these trends with other biogeochemical parameters. Objectives of this research were the comparison of two permafrost degradation processes in view of DOM chemistry: intensive (coastal erosion and formation of mud streams) degradation and degradation stabilized by several factors (e.g. vegetation cover). Also one of the objectives of research was to understand OM conservation and mineralization processes on a long time scale (thousands of years) – by sampling sediment samples in different depths and further correlations of molecular information of OM with the age of organic matter. Previously was demonstrated that DOM molecular composition achieved by Fourier Transform Ion Cyclotron Resonance Mass Spectrometry (FT ICR MS) can carry degradation state and age information (Flerus et al., 2011).

Advanced understanding of the chemical composition of Ice Complex DOM will noticeably broaden knowledge and understanding of Ice Complex formation, evolution of OM in Ice Complex and possible future climatic changes due to degradation of this carbon source.

4.7.2 Methodology

Sample preparation and extraction were provided in the field lab which was constructed in the camp on Muostakh Island. Water sources of Muostakh Island were sampled for DOC analysis and nutrients. Water was passed through pre-combusted 0.45µm GF/F filters, placed to the vials and frozen for further transportation. For solid phase extraction (SPE)

4.7 Studies of dissolved organic matter

of DOM we used PPL sorbent pre-packed cartridges as described in (Dittmar et al., 2008). Filtered water was acidified and passed through the columns, enriched with DOM cartridges and then stored at -20°C in the dark. Sediment and soil samples were placed to coolers directly after sampling and then transported to the field lab freezer. Elution, further analysis of DOM and sediment material processing will be provided in the labs of AWI Bremerhaven after freight arrival.

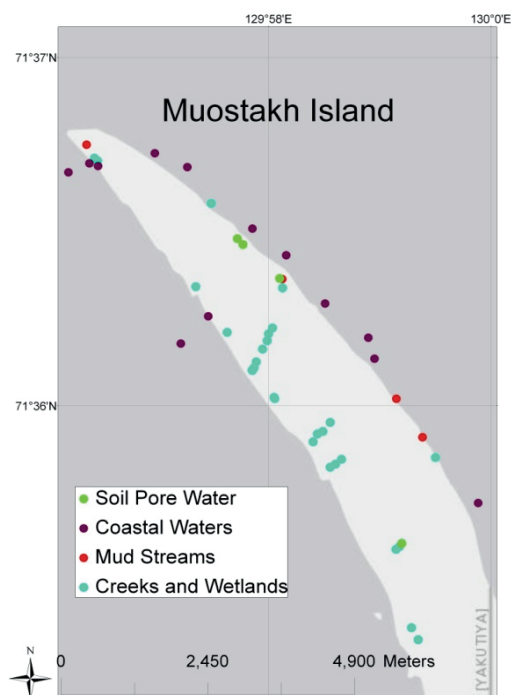


Figure 4-14 Sampling points on Muostakh Island. Different DOM sources indicated are with colors according to the legend.

4.7.3 Expected results

During the field campaign different OM sources of Muostakh Island and surrounding waters of the Buor-Khaya Bay were sampled including melt water creeks, wetlands, and coastal waters around the island, soil pore water and thawed permafrost mud streams. Sediments and soil were sampled in the exposures on the north-east side of the Island. Additionally, also DOM from the Lena River main channels, Samoylov Island creeks and lakes was sampled for previous data set extension (expeditions of 2009 and 2010). 70 SPE DOM samples were prepared. 100 samples were prepared for DOC and nutrients analyses. 28 sediment and 12 active layer soil samples were sampled.

Figure 4-14 shows sampling points on Muostakh Island. The north-east side of the island is highly affected by the wave action and coastal erosion processes occur there. The south-west side of the Island is not highly affected by the wave action and the coast is stabilized by vegetation cover which causes the formation of melt water creek valleys. For further understanding and comparison of these two processes DOM was sampled in the different locations and origins of the Island as indicated on the map.

After the transportation of samples to Germany we plan to analyze DOM samples by a range of chemical techniques including DOC analysis, total nitrogen, nutrients and FT ICR MS with its extremely detailed molecular information. General characterization of samples and detailed sampling site descriptions (in cooperation with Hanno Meyer, Thomas Opel and Alexander Dereviagin) are of great importance here because we plan to find which environmental factors act as drivers and control the molecular composition of organic matter.

References

- Dittmar, T., Koch, B.P., Hertkorn, N., Kattner, G. (2008) A simple and efficient method for the solid-phase extraction of dissolved organic matter (SPE-DOM) from seawater. *Limnology and Oceanography: Methods* 6, 230-235.
- Engelhaupt, E. (2008) Don't be fooled by seemingly "permanent" permafrost. *Environmental Science & Technology* 42, 8623-8624.
- Flerus, R., Koch, B.P., Lechtenfeld, O.J., McCallister, S.L., Schmitt-Kopplin, P., Kaiser, K., Kattner G. (2011) A molecular perspective on the ageing of marine dissolved organic matter. *Biogeosciences Discussions* 8, 11453-11488.
- Frey, K. E., McClelland, J.W. (2009) Impacts of permafrost degradation on arctic river biogeochemistry. *Hydrological Processes* 23, 169-182.
- Schuur, E.A.G., Bockheim, J. Canadell, J.G., Euskirchen, E. (2008) Vulnerability of Permafrost Carbon to Climate Change: Implications for the Global Carbon Cycle. *BioScience* 58(8), 701-715.
- Tarnocai, C., Canadell, J.G. Schuur, E.A.G., Kuhry, P., Mazhitova, G., Zimov, S. (2009) Soil organic carbon pools in the northern circumpolar permafrost region. *Global Biogeochemical Cycles* 23, GB2023.
- Zimov, S.A., Schuur, E.A.G. Chapin, F.S. (2006) Permafrost and the global carbon budget. *Science* 312(5780), 1612-1613.

4.8 REPEATED TACHEOMETRIC SURVEY OF ICE COMPLEX COAST

Thomas Opel, Hanno Meyer, Mikhail Grigoriev, and Frank Günther

Fieldwork period: August 07 to August 26, 2012; Muostakh Island

Muostakh features constant high coastal retreat rates and serves as a natural laboratory for studying the processes driving erosion along ice-rich permafrost coasts in the Arctic. In order to continue the regular stationary monitoring time series on Muostakh by Grigoriev et al. (2009), on-site measurements were conducted at the northern cape of the island. As a backup for this time-series, new reference points were marked next to the northern cape and measured within a tacheometric survey. The survey has been carried out not only in the area around the northern tip, but also along the cliff top of the northeast-facing coast. The aim of the survey was the collection of topographic reference measurements and ground truth data for remote sensing applications and especially the repeat measurement of a survey campaign that was done in August 2011 by Günther et al. (2013) along the coasts on Muostakh consisting of Ice Complex deposits. The exact time span of one year between the two surveys provides a new benchmark of current coastal erosion. This snapshot in time will serve as basis for validation of seasonal and inter-annual thermo-denudation rates along the cliff top line obtained from dense time series of very high-resolution satellite imagery.

We used a ZEISS ELTA C30 tacheometer for distance and height measurements with a work setup similar to Günther et al. (2013). In order to perform stationing and orientation of the instrument, we used the existing marked backside points on the edoma upland and the associated local coordinate system that was established in 2011. From three different instrument positions (Table 4-4), we measured 689 points in total at both, the western and eastern coast around the northern cape of Muostakh Island, but in particular along the cliff top line of the east-facing coast, which is equivalent to 3,460 m of coastline respectively almost a quarter of the islands perimeter (Figure 4-15). Since thermo-abrasion at the cliff bottom of the northwestern coast seemed to have been reactivated during the last years, we concentrated cliff bottom reference measurements on this coastline section. Frequently overhanging blocks of ground ice and frozen sediment in combination with thermo-niches made it almost impossible to perform cliff bottom measurements also along the east-facing coast.

4.8 Repeated tacheometric survey of Ice Complex coast

Table 4-4 Summary of topographic survey on Muostakh Island divided into campaigns of different tacheometer stations.

Date	№ of backside points used for stationing	№ of measurement points	xy stationing accuracy [m]
10.08.2012	5	233	0.015
17.08.1012	3	253	0.14
24.08.2012	3	203	0.16

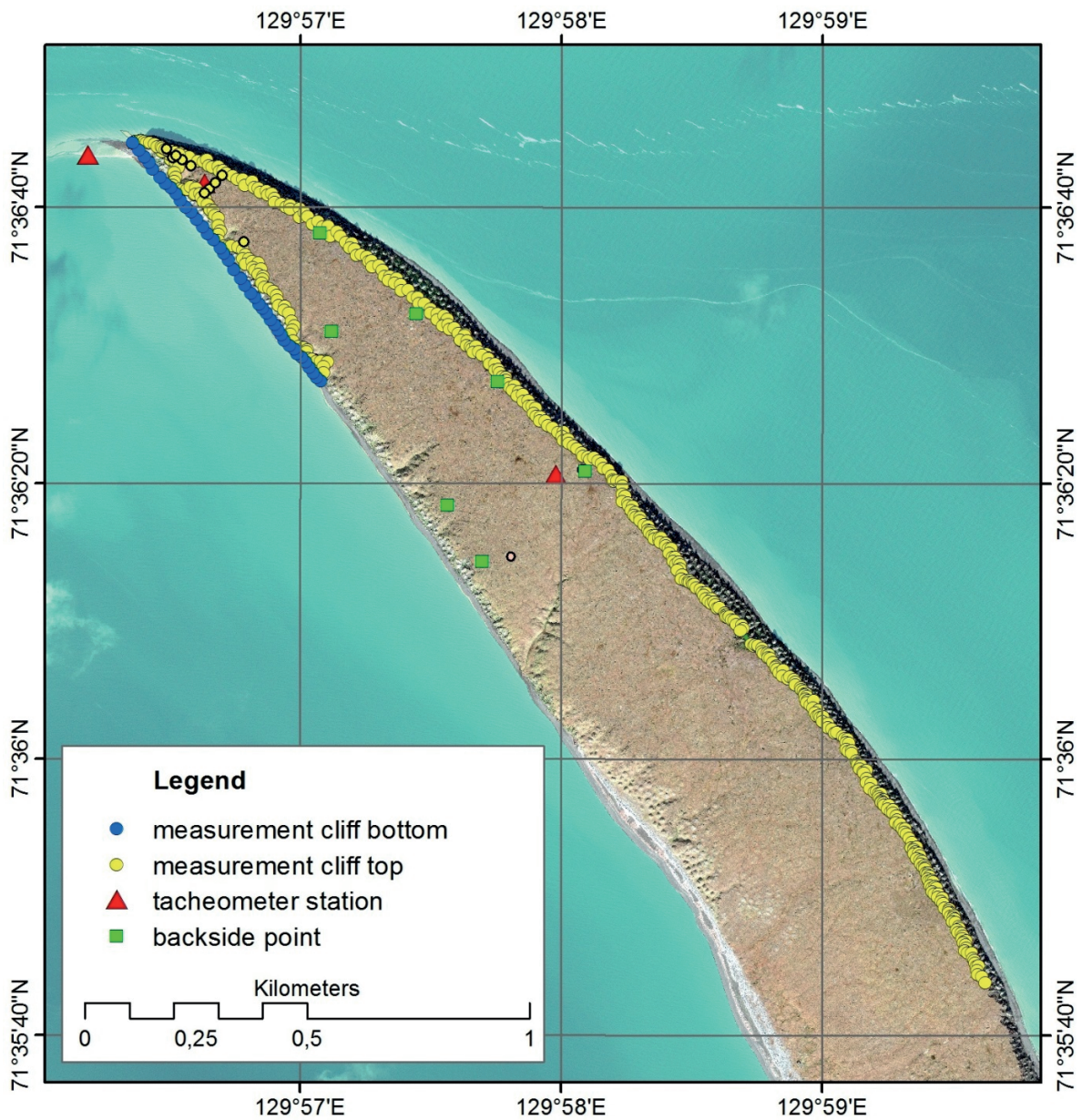


Figure 4-15 Map of the northern half of Muostakh showing tacheometry set-up of August 2012 and point measurements. Background: PanSharpened GeoEye satellite image, acquired on 7 September 2012.

4.8 Repeated tacheometric survey of Ice Complex coast

In order to ensure comparability of the 2011 and 2012 surveys and because of the irregular shape of the cliff top line, point measurements were made on average at a dense interval every 8.5 m. Using all backside points of the repeat survey, the transformation of the entire point cloud from a local to UTM 52N coordinate system was done with an RMSE of 1.43 m. Subsequent digitization of the August 2012 cliff top line along the east-facing coast and calculation of the eroded area compared to the previous survey in August 2011, revealed 7,293 m² of areal land loss along the cliff top of about 2.8 km coastline length during the 2011-2012 period. Dividing the coast into 50m long segments, this was equivalent to an average thermo-denudation rate of $-2.7 \pm 1.9 \text{ m a}^{-1}$, while for example the northern cape changed its position by -39 m during the observation period. However, when examined over a single 50 m segment, during 2011 to 2012 the northern cape retreated at -12 m a^{-1} (Figure 4-16).

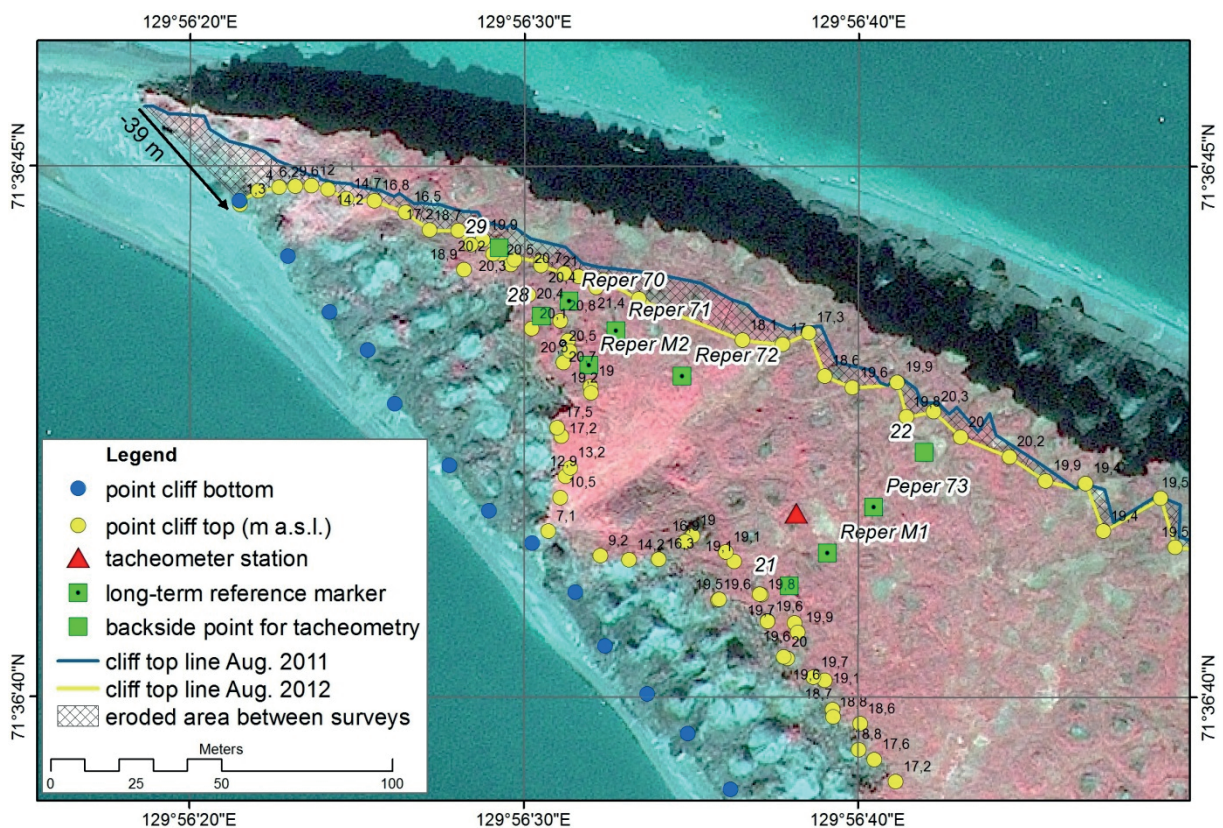


Figure 4-16 Map detail of the northern cape area on Muostakh Island showing tacheometry set-up of 2012 and digitized cliff top lines of August 2011 and August 2012. Thermo-denudation within six 50 m coastline segments along this 300 m section was -7.2 m a^{-1} on average. Background: Pansharpended GeoEye satellite image, acquired 13 July 2010.

References

Grigoriev, M.N., Kunitsky, V.V., Chzhan, R.V., and Shepelev, V.V. (2009) On the variation in geocryological, landscape and hydrological conditions in the Arctic zone of East Siberia in connection with climate warming. *Geography and Natural Resources* 30, 101–106.

4.8 Repeated tacheometric survey of Ice Complex coast

Günther, F., Sandakov, A., Baranskaya, A., and Overduin, P. (2013) Topographic survey of Ice Complex coasts, in: Günther, F. et al. (Eds.) The Expeditions Laptev Sea Mamontov Klyk 2011 & Buor Khaya 2012. Berichte zur Polar- und Meeresforschung/Reports on Polar and Marine Research 664, 16–54.

Die **Berichte zur Polar- und Meeresforschung** (ISSN 1866-3192) werden beginnend mit dem Band 569 (2008) als Open-Access-Publikation herausgegeben. Ein Verzeichnis aller Bände einschließlich der Druckausgaben (ISSN 1618-3193, Band 377-568, von 2000 bis 2008) sowie der früheren **Berichte zur Polarforschung** (ISSN 0176-5027, Band 1-376, von 1981 bis 2000) befindet sich im electronic Publication Information Center (**ePIC**) des Alfred-Wegener-Instituts, Helmholtz-Zentrum für Polar- und Meeresforschung (AWI); see <http://epic.awi.de>. Durch Auswahl "Reports on Polar- and Marine Research" (via "browse"/"type") wird eine Liste der Publikationen, sortiert nach Bandnummer, innerhalb der absteigenden chronologischen Reihenfolge der Jahrgänge mit Verweis auf das jeweilige pdf-Symbol zum Herunterladen angezeigt.

The **Reports on Polar and Marine Research** (ISSN 1866-3192) are available as open access publications since 2008. A table of all volumes including the printed issues (ISSN 1618-3193, Vol. 1-376, from 2000 until 2008), as well as the earlier **Reports on Polar Research** (ISSN 0176-5027, Vol. 1-376, from 1981 until 2000) is provided by the electronic Publication Information Center (**ePIC**) of the Alfred Wegener Institute, Helmholtz Centre for Polar and Marine Research (AWI); see URL <http://epic.awi.de>. To generate a list of all Reports, use the URL <http://epic.awi.de> and select "browse"/ "type" to browse "Reports on Polar and Marine Research". A chronological list in declining order will be presented, and pdf icons displayed for downloading.

Zuletzt erschienene Ausgaben:

684 (2015) Russian-German Cooperation SYSTEM LAPTEV SEA: The Expedition Lena 2012, edited by Thomas Opel

683 (2014) The Expedition PS83 of the Research Vessel POLARSTERN to the Atlantic Ocean in 2014, edited by Hartwig Deneke

682 (2014) Handschriftliche Bemerkungen in Alfred Wegeners Exemplar von: Die Entstehung der Kontinente und Ozeane, 1. Auflage 1915, herausgegeben von Reinhard A. Krause

681 (2014) Und sie bewegen sich doch ...Alfred Wegener (1880 – 1930): 100 Jahre Theorie der Kontinentverschiebung – eine Reflexion, von Reinhard A. Krause

680 (2014) The Expedition PS82 of the Research Vessel POLARSTERN to the southern Weddell Sea in 2013/2014, edited by Rainer Knust and Michael Schröder

679 (2014) The Expedition of the Research Vessel 'Polarstern' to the Antarctic in 2013 (ANT-XXIX/6), edited by Peter Lemke

678 (2014) Effects of cold glacier ice crystal anisotropy on seismic data, by Anja Diez

677 (2014) The Expedition of the Research Vessel "Sonne" to the Mozambique Ridge in 2014 (SO232), edited by Gabriele Uenzelmann-Neben

676 (2014) The Expedition of the Research Vessel "Sonne" to the Mozambique Basin in 2014 (SO230), edited by Wilfried Jokat

675 (2014) Polarforschung und Wissenschaftsutopien: Dargestellt und kommentiert am Beispiel von zehn Romanen aus der Zeit von 1831 bis 1934, von Reinhard A. Krause

674 (2014) The Expedition of the Research Vessel 'Polarstern' to the Antarctic in 2013 (ANT-XXIX/7), edited by Bettina Meyer and Lutz Auerswald

Recently published issues:



ALFRED-WEGENER-INSTITUT
HELMHOLTZ-ZENTRUM FÜR POLAR-
UND MEERESFORSCHUNG

BREMERHAVEN

Am Handelshafen 12
27570 Bremerhaven
Telefon 0471 4831-0
Telefax 0471 4831-1149
www.awi.de

